AD-A135 545 SINGLE TRIAL BRAIN ELECTRICAL PATTERNS OF AN AUDITORY AND VISUAL PERCEPTU..(U) EEG SYSTEMS LAB SAN FRANCISCO CA A S GEVINS ET AL. JUN 83 AFOSR-TR-83-1014 1/1

UNCLASSIFIED F49620-82-K-0006 F/G 6/16 NL

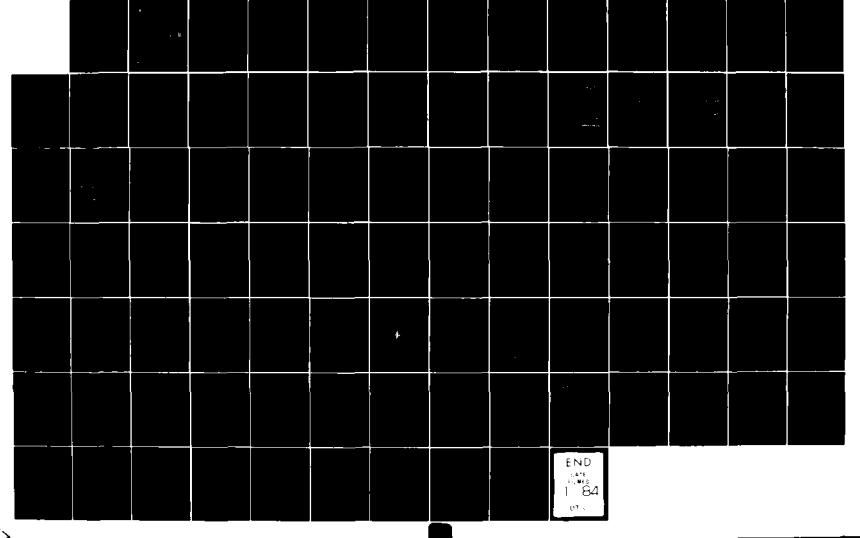

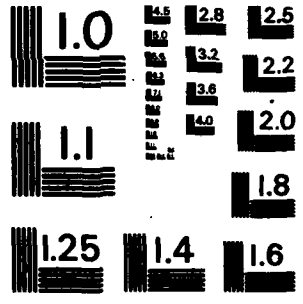

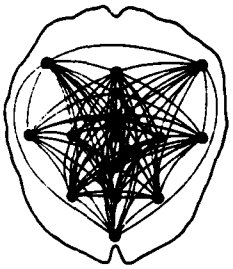

AFOSR-TR- 83-1014

(4)

EEG SYSTEMS LABORATORY

1855 FOLSOM ST.
SAN FRANCISCO CA 94103
(415) 621-8343

INTERIM PROGRESS REPORT: 22 FEB 82 to 1 JUN 83

AFOSR contract: F49620-82-K-0006

A. Fregly, Scientific Officer

AD-A135745

Title - "Single Trial Brain Electrical Patterns of an Auditory and Visual Perceptuomotor Task"

A. Gevins, Director

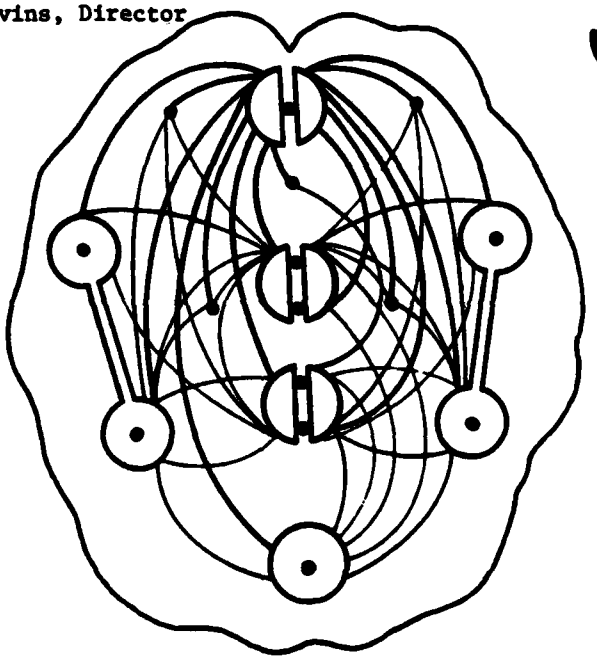

Approved for public release; distribution unlimited.

Unclassified

SECURITY CLASSIFICATION OF THIS PAGE (When Data Entered)

REPORT DOCUMENTATION PAGE	READ INSTRUCTIONS BEFORE COMPLETING FORM
1. REPORT NUMBER: AFOSR-TR-83-1014 / 2. GOVT ACCESSION NO: A135 375	3. RECIPIENT'S CATALOG NUMBER
4. TITLE (and Subtitle): SINGLE TRIAL BRAIN ELECTRICAL PATTERNS OF AN AUDITORY AND VISUAL PERCEPTUOMTOR TASK	5. TYPE OF REPORT & PERIOD COVERED: Interim Progress Report: 22 FEB 82 to 1 JUN 83
	6. PERFORMING ORG. REPORT NUMBER
7. AUTHOR(s): Alan S. Gevins, Steven L. Bressler, Brian A. Cutillo, Joseph C. Doyle Robert S. Tannehill, & Gerald M. Zeitlin	8. CONTRACT OR GRANT NUMBER(s): F49620-82-K-0006
9. PERFORMING ORGANIZATION NAME AND ADDRESS: EEG Systems Laboratory, 1855 Folsom, San Francisco CA 94103	10. PROGRAM ELEMENT, PROJECT, TASK AREA & WORK UNIT NUMBERS: 2313 A4, 61102 F
11. CONTROLLING OFFICE NAME AND ADDRESS: Directorate of Life Sciences, AFOSR/NL, Building 410, Bolling AFB DC 20332	12. REPORT DATE: JUNE 1983
	13. NUMBER OF PAGES: 86
14. MONITORING AGENCY NAME & ADDRESS(if different from Controlling Office)	15. SECURITY CLASS. (of this report): unclassified
	15a. DECLASSIFICATION/DOWNGRADING SCHEDULE
16. DISTRIBUTION STATEMENT (of this Report): Approved for public release; distribution unlimited	Accession For: NTIS GRA&I ☑, DTIC TAB ☐, Unannounced ☐, Justification, By, Distribution/, Availability Codes, Dist | Avail and/or Special, A-1
17. DISTRIBUTION STATEMENT (of the abstract entered in Block 20, if different from Report)	
18. SUPPLEMENTARY NOTES: DTIC COPY FURNISHED TO	
19. KEY WORDS (Continue on reverse side if necessary and identify by block number): perceptuomotor, auditory, visual, brain potentials, event related potentials, evoked correlations, single trial, digital signal processing, mathematical pattern recognition	

20. ABSTRACT (Continue on reverse side if necessary and identify by block number)

This past year the proposed auditory-visual perceptuomotor paradigm was designed and implemented, and 12 twenty-one channel pilot recordings were conducted. The objective was to compare spatiotemporal brain-potential patterns associated with: (1) the preparation to receive auditory or visual numeric stimuli, and (2) the processing of auditory and visual numeric stimuli. A bimodal paradigm sufficiently controlled for the application of a 49 channel Neurocognitive Pattern (NCP) Analysis has been finalized

(cont. next page)

DD FORM 1 JAN 73 1473 EDITION OF 1 NOV 65 IS OBSOLETE

Unclassified

SECURITY CLASSIFICATION OF THIS PAGE (When Data Entered)

(cont. Block #20)

and participant screening sessions have begun. Sections III and IV of this Interim Progress Report are comprised of published (Science, 220:97-99, 1983) and in preparation papers describing our recent visuospatial move/no-move study. The results of further signal processing studies on that data are described in Sections V and VI. The research described in sections (III-VI) was also sponsored by the Office of Naval Research and the Air Force School of Aerospace Medicine.

The research described in Sections I.D.4 through I.E.2 and Sections III to VI is also sponsored by the Office of Naval Research and the Air Force School of Aerospace Medicine.

I. OVERVIEW

A. Senior Scientific Personnel of the EEG Systems Laboratory

Steven L. Bressler, Neurophysiologist
Brian A. Cutillo, Cognitive Scientist
Joseph C. Doyle, Neurophysicist
Alan S. Gevins, Director
Ronald K. Stone, Neuropsychiatrist
Robert S. Tannehill, Programmer
Gerald M. Zeitlin, Systems Engineer

B. 1983 Papers

1. Gevins, A.S., Schaffer, R.E., Doyle, J.C., Cutillo, B.A., Tannehill, R.L. and Bressler, S.L. Shadows of thoughts: Rapidly changing, asymmetric, brain potential patterns of a brief visuomotor task. Science, 1983, 220, 97-99.

2. Gevins, A.S. Brain potentials and mental functions: methodological requirements. In I. Alter (Ed.), The Limits of Functional Localization, Raven Press, 1983, In press.

3. Gevins, A.S. Brain potential evidence for lateralization of higher cognitive functions. In J.B. Hellige (Ed.), Cerebral Hemisphere Asymmetry: Method, Theory and Application. Praeger Press, 1983, In press.

4. Gevins, A.S. Brain Potentials and Human Higher Cognitive Functions: Methods, research and future directions. In J. H. Hannay (Ed.), Handbook of Neuropsychology. Oxford Press, 1983, In press.

C. Major Presentations, 1982-1983, A. Gevins

1. Symposium Chairman, American Association for the Advancement of Science,
Washington, D.C., 1982.

2. Symposium Chairman, Winter Conference on Brain Research, Steamboat Springs, 1982.

3. Special Invited Lecturer, Int. Conf. Neuropsychology, Pittsburg, 1982.

4. Invited Speaker, Society for Biological Psychiatry, New York, 1983.

5. Symposium Chairman, IEEE Computer Des., New York, 1983.

6. Invited Lecturer, Third European EEG Conference, Basle, 1983.

D. Experiments

The EEGSL is in the process of developing the method of Neurocognitive Pattern (NCP) Analysis for measuring aspects of mass neural processes related to perceptuomotor and cognitive activities. Several generations of NCP Analysis have been used to study both complex and simple tasks, and a number of findings have emerged. Taken together, these results suggest that neither strictly localizationist nor equipotentialist views of neurocognitive functioning are realistic. Since even simple tasks are associated with a rapidly shifting mosaic of focal scalp-recorded patterns, neurocognitive functioning might be better modeled as a network in which the activity of many specialized local processing elements is periodically integrated. Our research is directed toward developing methods for measuring these processes more precisely and modeling them more explicitly.

N.B. It must be understood that scalp-recorded potentials, even unaveraged timeseries, are not necessarily cortical in origin. Until this issue is settled, it is essential not to interpret scalp designations, which conventionally refer to underlying cortical areas, as implying measurement of the activity of cortical sources. For convenience, we use the convential scalp designations subject to this caveat.

Specific findings include:

1. Complex perceptuomotor and cognitive activities such as reading and writing have unique, spatially differentiated scalp EEG spectral patterns. These patterns had sufficient specificity to identify the type of task from the EEG (EEG Clin. Neurophysiol. 47:693-703, 1979). The results were in accord with previous reports of hemispheric lateralization of 'spatial' and 'linguistic' processing.

2. When tasks are controlled for stimulus, response and performance-related factors, complex cognitive activities such as arithmetic, letter substitution and mental block rotation have identical, spatially diffuse EEG spectral scalp distributions. Compared with staring at a dot, such tasks had approximately 10% reductions in alpha and beta band spectral intensities (EEG Clin. Neurophysiol. 47: 704-710, 1979; Science 203:665-668, 1979). This reduction may be an index of their task workload. Since no patterns of hemispheric lateralization were found, this study suggested that previous reports of EEG hemispheric lateralization may have confounded EEG patterns related to limb and eye movements and arousal with those of mental activity per se (Science 207:1005-1008, 1980).

3. Split-second visuomotor tasks, controlled so that only the type of judgment varied, are associated with complex, rapidly shifting patterns of single-trial, evoked inter-electrode correlation of brain potential timeseries. Differences between spatial and numeric

judgments were evident in the task-cued prestimulus interval. Complex and often lateralized patterns of difference shifted with split-second rapidity from stimulus onset to just prior to response, at which time there was no difference between spatial and numeric tasks (Science 213:918-922, 1981). This suggested that once task-specific differential perceptual and cognitive processing was completed, a motor program common to both tasks was executed, regardless of differences in the stimuli or type of judgment.

4. Rapidly shifting, focal brain potential patterns, representing the maximal difference between similar split-second tasks, can be extracted with NCP analysis. The move and no-move variants of a split-second visuospatial judgment task, which differed slightly in expectation, differed in type of judgment, and differed greatly in response, were associated with distinct differences in the patterns of single-trial evoked correlation between scalp-recorded channels (Science 220:97-99, 1983; see Sections III and IV). These patterns of difference increased in magnitude in each successive analysis interval. In the prestimulus interval, correlation of the midline frontal electrode distinguished the tasks ($p<.01$). In the interval spanning the N1, P2 and N2 event-related potential (ERP) peaks, the between-task evoked correlation contrast was focused at the midline parietal electrode ($p<.001$). In the interval centered on the P3a ERP peak, the focus of correlation difference was at the right parietal electrode and involved higher correlation of the right parietal with occipital and midline precentral electrodes in the no-move task, and with the right central electrode in the move task ($p<5 \times 10^{-5}$). In an interval centered 135 msec after the P3a ERP peak, which included right-handed response preparation and initiation, the focus of contrast shifted to the left central electrode, involving higher correlation with midline frontal and occipital electrodes in the move task and with the midline parietal electrode in the no-move task ($p<5 \times 10^{-6}$). These results concur with neuropsychological models of these tasks derived from clinical observations. They suggest that although simple perceptuomotor tasks are associated with a complex, dynamic mosaic of brain electrical patterns, it is possible to isolate foci of maximal differences between tasks. It is clear that without a split-second temporal resolution it is not possible to isolate the rapid shift in lateralization which presumably is associated with perceptual-cognitive and efferent processing stages.

5. The focal patterns of evoked correlation derived by NCP analysis significantly distinguished the single-trial data of 7 of the 9 people in the above study. This suggested that similar neurocognitive mechanisms were being measured across the majority of participants (see Section IV).

6. Behaviorally identical trials of the move and no-move visuospatial tasks in the above study were found to be associated with distinctly different brain potential patterns (Section VI). This suggests that appropriate brain potential measures may provide a tool for more detailed examination of previously unmeasured neurocognitive processes.

E. Analytic Methods

Neurocognitive Pattern (NCP) analysis currently consists of the application of an adaptive-network, nonlinear mathematical pattern classification algorithm to extract task-related signals from sets of data. The analysis is applied to single-trial timeseries in brief time windows (100 to 175 msec) for up to 49 scalp electrodes (using power measures) and up to 1176 electrode pairings (using crosscorrelation or crosscovariance measures). The data windows are determined for each person from the peaks of their averaged ERPs as well as from stimulus and response times, but measures are made on single trials.

1. Similarities and Differences Between NCP Analysis and Conventional ERP Analysis

NCP analysis is grounded on the vast body of information gained from ERP methods and has the same underlying goal, namely to resolve spatially and temporally overlapping, task-related mass neural processes. However, it departs in several ways from the currently popular approach of extracting independent features from averaged ERPs by principal components analysis (PCA) followed by hypothesis testing with ANOVA. First, NCP analysis is concerned with spatiotemporal task-related activity recorded by many electrodes in a number of time intervals from before the stimulus through the response. It quantifies neurocognitive activity in terms of a variety of parameters, rather than amplitude and latency of ERP components. Thus, it is possible that the increased dimensionality of parametrization may facilitate the measurement of subtler aspects of neurocognitive processes. Second, the questionable assumption of a multivariate normal distribution of brain potentials is not made in NCP analysis. Third, brain-potential feature extraction and hypothesis testing are performed as a single process which determines features which are maximally different between the conditions of an experiment, rather than those which meet possibly irrelevant criteria such as statistical independence. Fourth, task-related patterns of consistency are extracted from sets of single-trial data. Significant results may be obtained as long as there is a pattern of consistent difference between tasks, even though the means of the two data sets do not differ significantly.

Taken together, these aspects of NCP analysis may enable it to resolve small task-related signals from the obscuring background 'noise' of the brain, revealing useful spatiotemporal information about mass neural processes. However, this is not without its costs. NCP analysis requires several orders of magnitude more computing than PCA and ANOVA, and larger data sets than conventional ERP studies. Also, because of its sensitivity, highly controlled experimental paradigms are required to assure that the results are truly related to the hypothesis and not to spurious or idiosyncratic factors. (The process of developing one such task is described in Section II of this report.) This requires a greater allocation of effort and resources to experimental design, recording and analysis than is needed for most

ERP experiments.

Although we have obtained several promising results with NCP analysis, the latest of which is described in Sections III and IV, we must caution that 'the jury is still out'. Additional basic studies are needed to determine whether NCP analysis is really worthwhile. If so, it should be possible to optimize, standardize and simplify it for use in other laboratories.

2. Evoked Correlations Between Scalp Electrodes

For the past few years we have concentrated on a measure of the degree of waveshape similarity (crosscorrelation) between timeseries from pairs of electrodes. Measures of single channel power are also being used and will be reported later this year. The crosscorrelation approach is based on the (unproven) hypothesis that when areas of the brain are functionally related there is a consistent pattern of waveshape similarity between them. There are a number of considerations in interpreting the correlation patterns of scalp recordings, such as volume conduction from subcortical sources and driving by distant sources. Some of the ambiguities may be mitigated by careful experimental design, but the neurophysiological interpretation of correlation patterns is an unsettled issue.

Besides the scientific value of studying the neural activity associated with preparation to receive and the subsequent processing of numeric information in two sense modalities, the auditory-visual experiment described in this Interim Progress Report is designed to provide a data base for refining the NCP analysis and investigating some aspects of the neurophysiological interpretation of correlation patterns. In addition to inter-channel, zero-lag correlation, NCP analysis can employ other measures such as multi-lagged correlation and covariance, and single channel power, all in specific frequency bands. Preliminary studies described in this report (Section V) have revealed significant information with such measures. A major goal during the coming year is to explore and resolve some of these issues.

II. PILOTING OF AN AUDITORY-VISUAL PERCEPTUOMOTOR TASK

A. Design Considerations

A number of issues had to be addressed in designing a bimodal paradigm sufficiently controlled to reveal NCPs which might distinguish auditory and visual perceptuomotor tasks during the modality-cued prestimulus and post-stimulus intervals.

1. Cognitive Considerations

Two hypotheses are being tested. First, NCPs should show neuroanatomically interpretable differences between the processing of auditory and visual numeric stimuli in post-stimulus intervals when feature extraction is thought to occur in sensory and related cortical areas. There should be minimal differences after sense-specific

processing is completed. Second, NCPs should differ in the modality-cued prestimulus interval as a function of the preparation to receive either visual or auditory stimuli. The second hypothesis requires complete equivalence of cue properties and performance-related factors between auditory and visual conditions, and also a strong inference that a modality-specific expectancy set exists in the cued prestimulus interval.

2. Experimental Control

The first hypothesis (ie. post-stimulus processing) requires control of stimulus, response and performance-related factors across conditions so that the major difference between conditions is stimulus modality. Visual and auditory modalities have fundamental differences. Input for the former is parallel (for brief foveally presented stimuli), while for the latter it is serial. Inherent differences in auditory and visual processing latencies can be compensated for by centering several analysis windows on the average ERP peak latencies in each person for auditory and visual conditions separately. Differences in ERP amplitudes can be explicitly measured by NCP analysis of single-channel signal power. With regard to the second hypothesis (ie. prestimulus attentional set), the modality-cued paradigm elicits a contingent negative variation (CNV) between cue and stimulus, with consequent resolution after stimulus presentation. NCP analysis will be applied to measure pre- and post-stimulus modality differences. The results may shed some light on the interface between preparatory activity and post-stimulus processes.

3. Montage

A 21 electrode scalp montage suitable for recording activity over auditory, visual, motor, parietal and dorsolateral prefrontal cortices was used during these pilot recordings. Four additional channels recorded vertical and horizontal EOG, EMG and the response. The final design will expand this to 49 brain potential channels to allow a resolution of approximately 6 square centimeters (see section II.C.). The investigation and conclusions concerning these issues during the developmental program of 12 pilot recordings is reported in the following section.

B. Task development and pilot recordings

1. Phase one (P's #1-8): (Respond to miscues)

a. Rationale. The existence of a modality-specific prestimulus attentional set was investigated with the 'miscueing' technique (Posner, 1978). In this method a randomly ordered 20% of the modality cues (a visually presented letter in both conditions) are incorrect. The lengthening of mean response time in these miscued trials is considered the 'cost' incurred by the expectation of a stimulus in a specific modality, and is used to infer the existence of a modality-specific preparatory set.

b. Task. Stimulus presentation and response measurement

were performed by the real time subsystem of the ADIEEG system, which also digitized the 25 channels of physiological signals at 256 samples/sec. The participant (P) was instructed to fixate a point at the center of the CRT screen of an AED II graphics terminal and await a visually presented modality cue (V for visual; A for auditory; duration 375 msec) 1.5 sec later the stimulus was presented. Auditory stimuli consisted of the numbers 1 to 9 generated by a Votrax speech synthesizer and presented through two speakers about 2 ft. above the participant's head. Duration varied from 245 to 430 msec (the number 7 was generated as "SEVN"). Visual stimuli were single digit numbers presented on the CRT, subtending a visual angle of under one degree. Their duration was equated to that of their corresponding auditory numeric stimuli.

The participant was instructed to attend the modality cue and "focus his attention" on the speakers or screen as indicated by the cue, while maintaining his gaze on the screen. He was to respond to the stimulus without hesitation with a ballistic contraction of his right hand index finger on a modified Grass force transducer with a pressure corresponding to the stimulus number on a linear scale of 1 to 9. Feedback indicating the exact pressure applied was presented as a 2 digit number on the CRT screen (duration 375 msec) 1 second after completion of response as determined by the program.

If the response was sufficiently accurate, the feedback number was underlined, signifying a "win". The error tolerance for a "win" was continually adjusted throughout the session as a moving average of the accuracy of the preceeding five correctly cued trials in visual and auditory modalities separately.

A random 18% of the trials were miscued (ie. the stimulus arrived in the wrong modality). The participant was to respond to these just like the correctly cued trials. Correctly cued and miscued auditory and visual trials were presented in randomly ordered blocks of 17 trials, self-initiated by the participant.

c. Recordings. Eight normal, right-handed adult male participants were recorded in pilot sessions consisting of about 350 to 700 trials each. Three were personel of the EEGSL and 5 were naive paid participants. Details were settled during the first 6 recordings, and technically acceptable recordings were obtained from the last 2 people. The electrode montage was Fz, F7, F8, aF1, aF2, Cz, C3, C4, C5, C6, Pz, P3, P4, T3, T4, T5, T6, Oz, aO1 and aO2, referenced to linked mastoids (modified expanded 10-20 system nomenclature; Picton, et al, 1978). For P#8 several placements were changed (see section B.2). Vertical and horizontal eye movements, response muscle activity, and force transducer output were also recorded. All signals were amplified by a 64-channel Bioelectric Systems Model AS-64P amplifier with .10 to 100 Hz passband, continuously digitized to 11 bits at 256 samples/sec and stored on digital tape. Signals were also recorded on three 8 channel polygraphs to monitor the session and for off-line artifact editing. Average response times (RT) and error rate (proportion of "lose" trials) were computed for behavioral evidence of a "cost" due to a

prestimulus attentional set in a total data set of 3735 trials.

d. Results and Discussion. For correctly cued trials, the mean response times were quicker for visual stimuli for all but two people. Average RT across P's was 675 msec for visual stimuli and 711 msec for auditory. The longer RT for auditory stimuli, which is opposite to the findings in simpler bimodal paradigms, may be due to the nature of the verbally presented number stimuli. All information needed for visual stimulus decoding appeared on the screen within 33 msec, while auditory information was not completed for up to several hundred msec. The longer RT for the auditory stimuli may also be due to the use of synthesized speech stimuli.

In the miscued trials a lengthening of RT and increase in error rate was observed in almost every case (Tables 1 and 2). For miscued auditory stimuli the average increase in RT was 47 msec and the average increase in error rate (proportion of 'lose' trials) was 9%. For misuced visual stimuli the 'costs' of miscueing were slightly greater (increase in RT = 65 msec; increase in error rate = 10%). There was a small (18 msec) asymmetry in RT effect. That is, miscueing a visual stimulus caused a greater increase in RT than miscueing an auditory stimulus. This asymmetry and the magnitude of the RT lengthening in miscued trials is in agreement with previous studies using simpler tasks (Posner, 1978). Further, the standard deviations for all cued and miscued conditions were similar within persons, indicating that the RT 'costs' due to miscueing were based on a consistent effect rather than greater variability in a smaller sample (about 4 to 1 ratio of correctly vs. incorrectly cued trials.) Thus it was verified that there was a 'cost' in the miscued trials indicative of an attentional committment to a particular modality in the prestimulus interval.

The ERPs for one person (P#7) are illustrated in Figure 1. In the auditory condition (Figures 1a and b) the N1 peak occurred at 120 msec in correctly cued trials and 136 msec in miscued trials. Its amplitude was maximal at midline fronto-central sites. The P2 peak at 208 msec was maximal at midline fronto-central sites, and was well represented at midline parietal sites. In miscued auditory trials (Figure 1b) a P3 peak was apparent at 314 msec, maximal at the midline. parietal derivation, and extending to fronto-central, lateral central and lateral parietal electrodes.

The visual stimuli elicited an N1 peak at 150 msec in both correctly cued and miscued conditions (Figures 1c and d). Although in this person the N1 peak was clearly seen at the midline occipital electrode, it was larger over left anterior occipital and posterior temporal sites (a01 and T5). The P2 peak was maximal at Pz, where its latency was 215 msec, but at midline fronto-central sites the first positive peak occurred at 179 msec. This earlier positive peak at anterior sites (which was also observed in P#8) was actually the resolution of the prestimulus CNV, which in the auditory condition was masked by the fronto-central N1 peak. In the miscued visual trials (Figure 1d) a P3 peak was present at 300 msec in P#7 and 330 msec in P#8. It was slightly larger at Cz than Pz, and was also prominent at

midline frontal and lateral central and parietal electrodes. The P3 peak was of larger amplitude, broader, and more anteriorly distributed in the visual miscued trials than in the auditory miscued trials.

The pre-stimulus CNV is evident as a fronto-central negative displacement of the prestimulus baseline in both conditions and its resolution could occur at different latencies after visual and verbal stimuli. Also, the information content of the verbal stimuli occurred at various latencies (as in "six" and "seven", or "four" and "five", as compared to the other numbers). What effect this may have upon the latencies of endogenous ERP components is not known, but it is likely that greater variability of the P3 latency in the auditory condition may account for the smaller, lower amplitude peak. These issues will be addressed in analyses of later, more controlled data sets.

A negative going slow potential shift was observed to commence at the P2 latency in all but the miscued visual trials, where it may have been obscured by the robust P3 peak. It was maximal at Cz, and larger over the left central (C3) than the right central (C4) electrode. This lateralization began well before the average response times in each condition.

2. Phase two (P's #9-12): (No response to miscues)

a. Rationale.

The behavioral results of phase one confirmed the existence of a prestimulus attentional set, and the respond-to-miscues design was modified for the formal recordings to a move/no-move design in which the "response" to a miscued stimulus was to make no movement. This was done so that there would be a behavioral confirmation of attention to the cue in each trial, and so that post-stimulus processing could be examined in each modality separately by a within-modality, move vs no-move NCP analysis. The within-modality analyses will serve as standards to aid in interpreting the results of the between-modality analyses.

b. Task. The task was the same as before, except that the participant was instructed to make no response on miscued trials (random 20%). A monetary incentive was added by rewarding accurate (win) move trials as a function of the accuracy attained (about 5 cents for each win). The accrued monetary bonus was displayed at the end of each block of 17 trials, as well as the average error tolerance for that block (as a performance index) for auditory and visual conditions separately. The cue-to-stimulus intervals were 2.5 sec for P's #9-11, and 1 sec for P#12. For P#12 a separate run was recorded at the 2.5 sec interval for the visual modality only.

c. Recordings. Four normal, right-handed adult males participated in sessions consisting of about 100 practice and 400 test trials. The 21 channel montage consisted of Fz, F7, F8, aF1, aF2, aCz, Cz, C3, C4, C5, C6, Pz, P3, P4, aP5, aP6, T5, T6, Oz, a01 and a02, referenced to linked mastoids. Tin scalp electrodes were attached using a stretchable nylon cap (Electrocap International).

Vertical and horizontal eye movements (electrode at outer canthi) and response muscle potentials (EMG from flexor digitorum) were recorded with Ag-AgCl cup electrodes. Other aspects of the recording procedure were the same as in Phase one.

Trials were visually inspected off-line to eliminate artifacted trials and no-move trials where muscle activity was present on the EMG channel. Average stimulus-registered ERPs were computed for all scalp channels, as well as averages of vertical and horizontal EOG and EMG. Cue-registered averages were also computed for P#12 for the cue-to-stimulus interval (1. sec for this P); the averaging epoch extended from 250 msec before the cue to 250 msec after the stimulus.

d. Results and Discussion. Response time, error rate (proportion of "lose" trials), and average error tolerance in the move trials for the 4 participants are shown in Table 3. Average response times and error rates were similar across move conditions, but the adaptive error tolerance (inversely related to skill level) tended to be larger for the auditory condition, indicating that performance was slightly better for visual stimuli. We will attempt to eliminate this difference in the formal recordings by providing more practice at the auditory task.

At the 2.5 sec cue-to-stimulus interval (P's #9-11), there was a high rate of data attrition (about 25%) in the no-move (miscued) trials due to mistaken overt responses. This may have been due to a decay of the attentional set. At the 1 sec interval (P#12) there was no attrition due to response movements. Since the no-move trials are infrequent, the attrition rate must be very low to collect sufficient data for the within-modality move vs no-move NCP analysis. Thus the 1 second interval seems more desirable.

The stimulus-registered ERPs for the move trials (Fig. 2a and c) were similar to the correctly cued trials of Phase one. In the visual condition the N1 peak was poorly represented at the midline occipital electrode, and in P#12 at the lateral occipital placements also (Fig. 2c). In all P's (including those in Phase one) the N1 peak to visual stimuli was largest at the lateral posterior temporal sites (T5 and T6). This may have been due to the small visual angle (under 1 degree) subtended by the foveal stimuli.

In P's #9, 10 and 12 the no-move (miscued) trials elicited an augmentation of the P3 peak. The P3 peak amplitude in both move and no-move averages was maximal at midline fronto-central sites. Examination of vertical and horizontal EOG channels revealed no eye movement which would account for this anterior distribution; thus it was most likely due to the resolution of a prestimulus CNV, an issue to be addressed in the formal study.

A frontally-dominant negative displacement of the pre-stimulus baseline (CNV) was seen in all participants. In a cued paradigm such as this a CNV may well be concomitant to the expectancy set we wish to study (reviewed by Tecce, 1972). The cue-registered averages for the 1 sec interval (P#12) revealed the time-course of the prestimulus CNV

to correctly cued auditory and visual stimuli. The negativity was largest at the midline fronto-central electrodes, but did not seem to differ between modalities. NCP analysis of the cue-to-stimulus interval in the formal study may shed more light on the modality-specificity of the anatomical distribution of CNV-related activity, which has not been thoroughly examined (Ritter, et al, 1980).

C. Final Paradigm Screening of Participants

As of 1 JUN 83, one full recording has been made. 1000 trials were recorded from a well-practiced participant using the paradigm, electrode montage, and recording procedure described above. The cue-to-stimulus interval was 1 sec, the visual stimuli were thickened and increased in size to just under a 2 degree visual angle, and the proportion of miscued (no-go) trials was increased to 22%. ERPs from this recording were quite satisfactory in most respects.

This paradigm, and a 49 channel scalp montage (Figure 3) will be used in the formal experiment. A common average reference will be computed, and the passband will be .1 to 50 Hz with digitization at 128 Hz. A recent study of trimodal attentional set using the regional cerebral blood flow technique (Roland, 1982) has revealed that the spatial patterns of focal neural processes related to attention and modality processing are complex even when viewed with a 30 sec temporal resolution. In order to adequately sample brain potentials which may correspond to these regions of focal activation, denser coverage of dorsolateral prefrontal areas, superior and inferior posterior parietal and superior and posterior temporal areas is required.

A screening program is being conducted to select and train candidate participants. During screening sessions EEGs are recorded from Fz, Cz, Pz, aO1 and aO2 (to examine the ERP waveform), and T1 and T2 (to assess potentials from temporalis muscles). Vertical and horizontal eye-movements are recorded by a single pair of diagonally placed electrodes. Behavioral records are examined to assess the quality of task performance, polygraphs are inspected to determine the amount of data attrition due to artifact, and average ERPs are computed to verify the presence of expected peaks. Participants for the formal study will be drawn from these candidates. To date (1 JUN 83) 17 candidates have been screened in this manner, 6-8 of whom will be recalled for the formal experiment.

D. Bibliography

Picton, T., Woods, D., Stuss, D. and Campbell, K. Methodology and meaning of human evoked potential scalp distributed studies. Proc. 4th Intl. Cong. on Event Related Potentials of the Brain Hendersonville, N.C., EPA-60019-77-043, 1978, 515-522.

Posner, M. Chronometric Explorations of Mind. Lawrence Erlbaum Assoc., N.J., 1978.

Ritter, W., Rotkin, L. and Vaughan, H. The modality specificity of the slow negative wave. Psychophys., 1980, 17:3;222-227.

Roland, P. Cortical regulation of selective attention in man. J. Neurophys., 1982, 48:5, 1059-1078.

Tecce. J. Contingent negative variation (CNV) and psychological processes in man. Psych. Bull., 1972, 77:2;73-108.

Table 1 - Average response time (in msec) and standard deviation for correctly cued and miscued auditory and visual trials for the 8 participants recorded in phase one of task development. (Miscues total 18% of trials; 9% of each type).

		Auditory		Visual		Increase	Increase
		correctly cued (S.D.)	mis-cued (S.D.)	Correctly cued (S.D.)	mis-cued (S.D.)	in R.T. miscued auditory	in R.T miscued visual
#1	318	830 (198)	803 (171)	710 (213)	757 (221)	-27 msec.	+47 msec
#2	368	702 (112)	803 (124)	648 (120)	796. (116)	+101	+148
#3	406	574 (81)	632 (89)	473 (93)	539 (93)	+58	+66
#4	609	687 (140)	718 (198)	578 (140)	652 (120)	+31	+74
#5	606	850 (136)	865 (124)	722 (140)	737 (116)	+15	+15
#6 (39)	668 (54)	528 (**54)	625 (39)	603 (54)	664 (54)	+97	+61
#7	372	892 (43)	978 (58)	1052 (58)	1106 (19)	+86	+54
#8	388	626 (95)	636 (81)	609 (110)	667 (80)	+10	+58
X (S.D across persons)		711 (106)	758 (111)	675 (116)	740 (103)	+47 msec	+65 msec
Total trials	3735	1560	302	1565	308		

Table 2 - Error rate (% of 'lose' trials) in correctly cued and miscued auditory and visual conditions in phase one of task development. (Miscued trials = 18%).

P#	Trials	Auditory Lose %		Visual Lose %		Auditory increase in lose %	Visual increase in lose %
		correct cued	mis-cued	correct cued	miscued		
#1	318	57	53	45	80	-4	+35
#2	368	53	57	48	69	+4	+21
#3	406	50	63	55	53	+13	-2
#4	609	51	69	59	65	+18	+6
#5	606	52	61	54	58	+9	+4
#6	668	49	58	54	53	+9	-1
#7	372	47	66	49	59	+19	+10
#8	388	51	53	53	59	+2	+6
X	3735 (Total)	51%	60%	52%	62%	+9	+10

Table 3 Response times, error rate (% lose trials) and error tolerance (inversely related to skill level) for phase two (P's #9-12), move/no-move design.

P#	Trials	Average RT in msec (S.D.)		Error rate		Average error tolerance (S.D.)	
		audi-tory	visual	auditory	visual	audi-tory	visual
#9	374	844 (218)	846 (219)	52%	50%	10.6 (4.0)	6.4 (2.1)
#10	370	795 (190)	797 (182)	53%	47%	6.7 (2.4)	5.8 (2.5)
#11	340	1008 (225)	957 (279)	55%	59%	8.2 (3.1)	7.5 (3.1)
#12	410	636 (85)	651 (62)	54%	51%	6.2 (2.4)	5.6 (3.8)
(Total) 1494							
X (S.D.) across persons		821 (180)	813 (186)	53.5%	51.8%	7.9 (3.0)	6.3 (2.9)

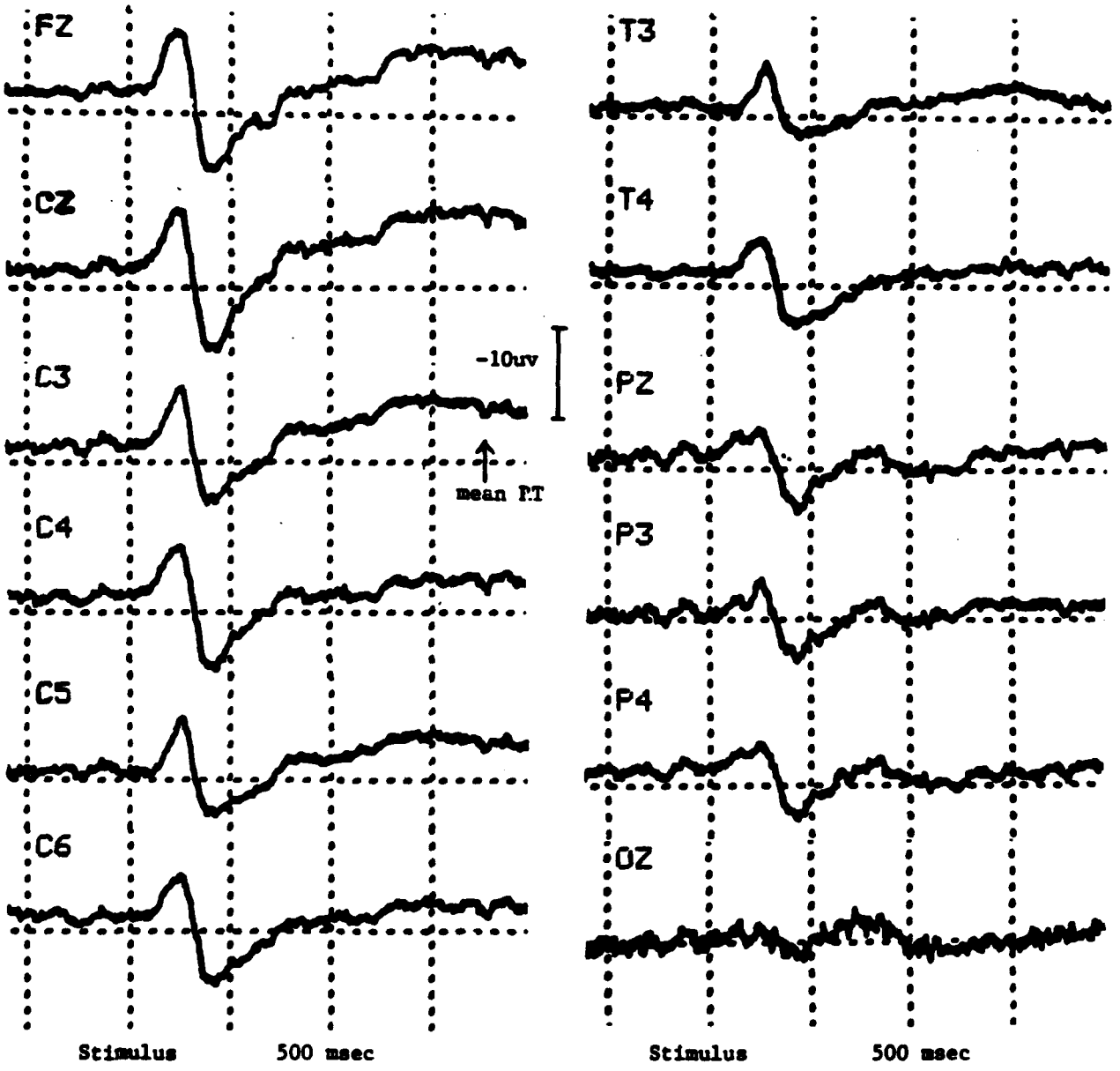

Figure 1a - Auditory correctly cued condition; average event-related potentials for selected channels for p#7. (91 trials, .1 to 100 Hz passband)

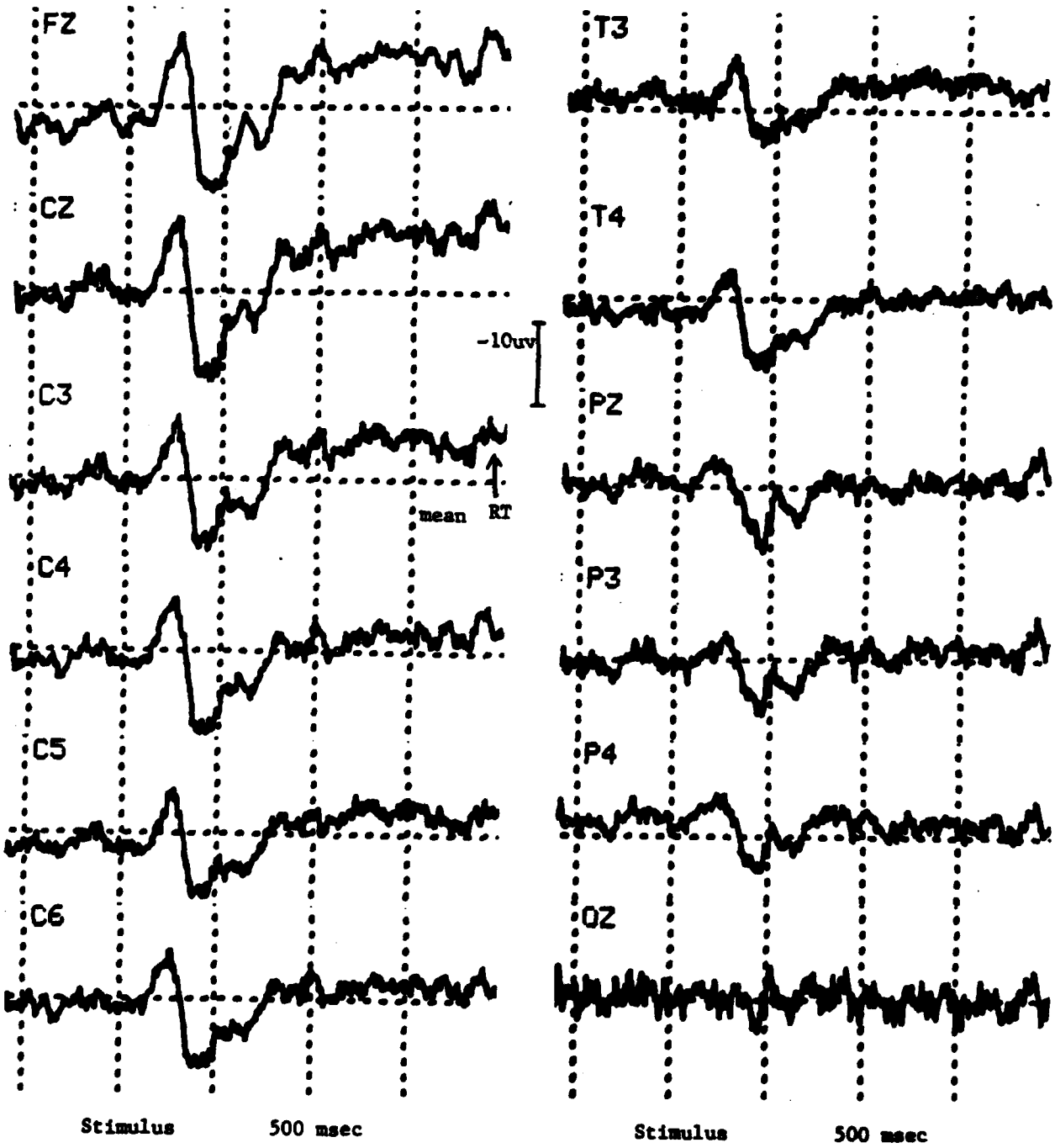

Figure 1b - Auditory miscued condition with response (p#7, 27 trials)

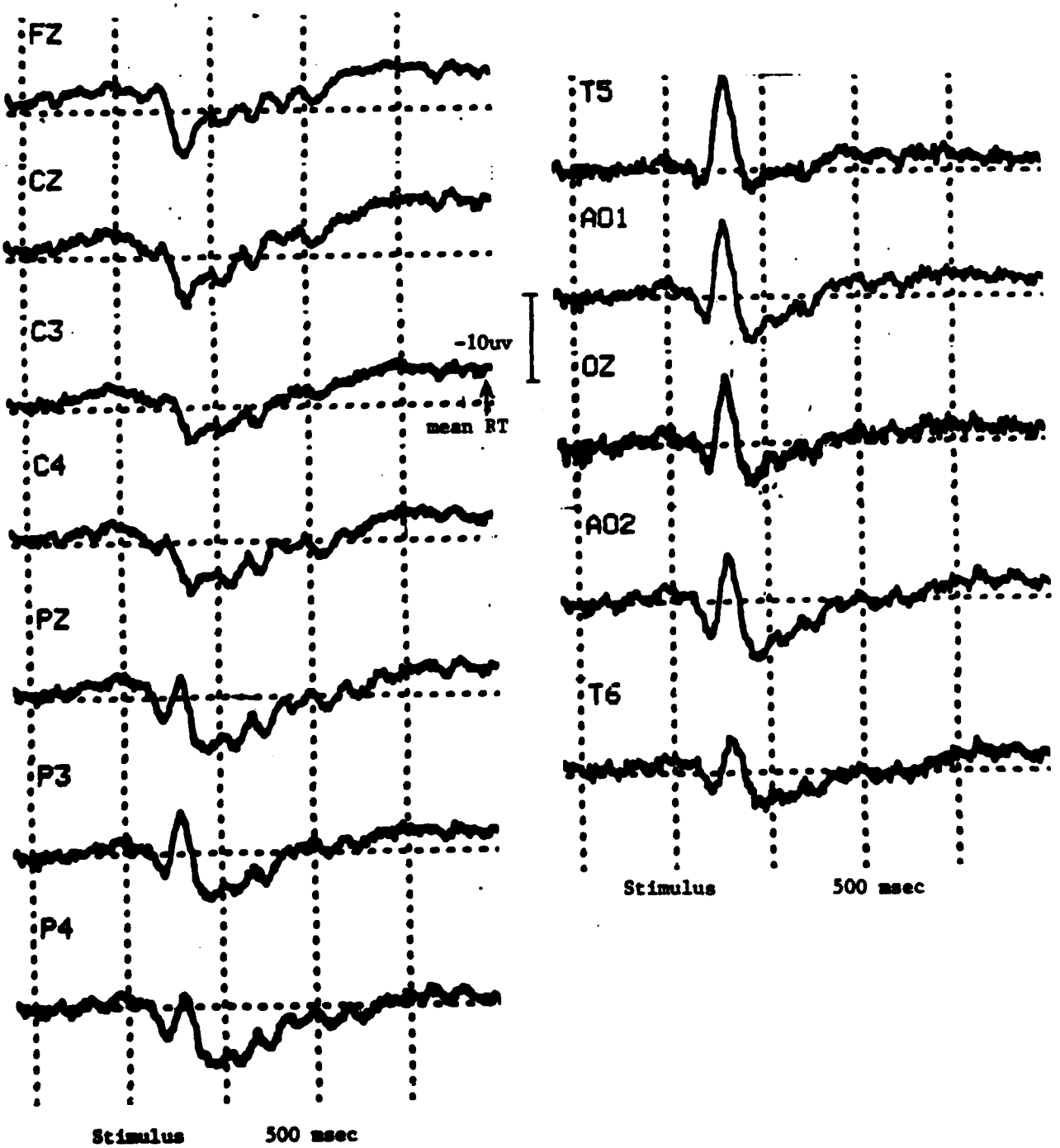

Figure 1c - Visual correctly cued condition, selected channels (p#7, 96 trials)

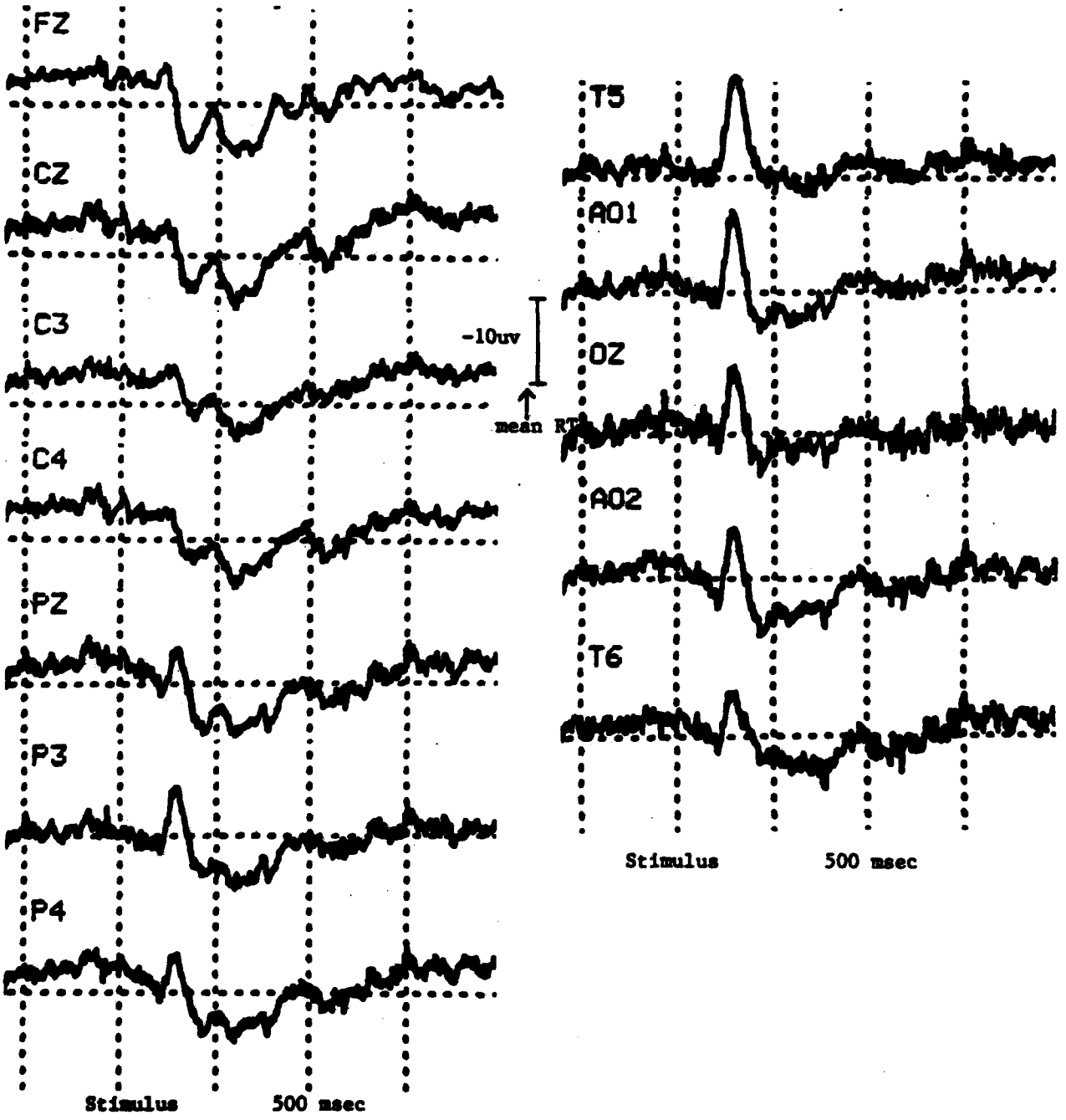

Figure 1d - Visual miscued condition with response (p#7, 31 trials)

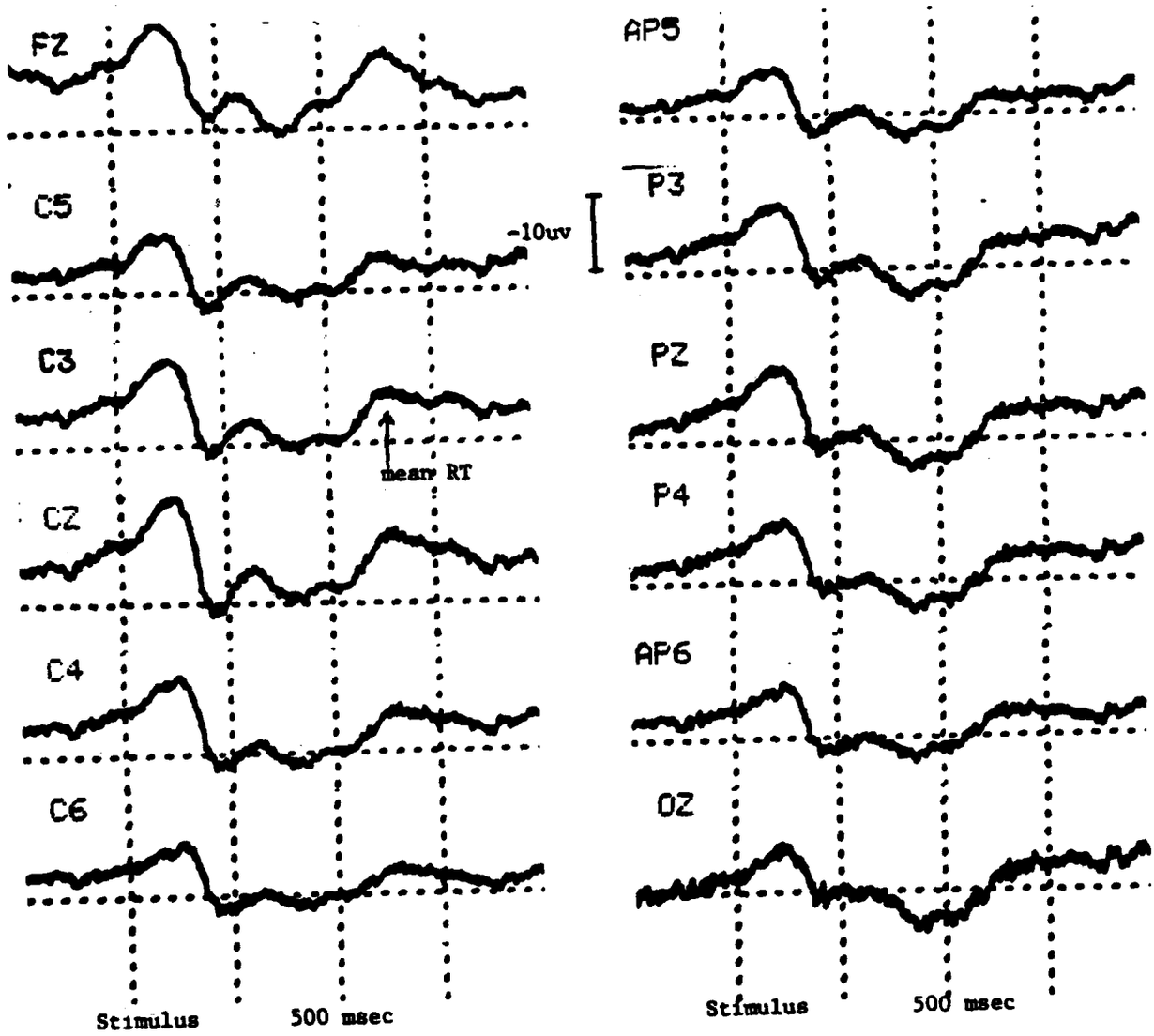

Figure 2a - Auditory correctly cued (move) condition. Average event-related potentials from selected channels from p#12 (103 trials, .1 to 100 Hz passband).

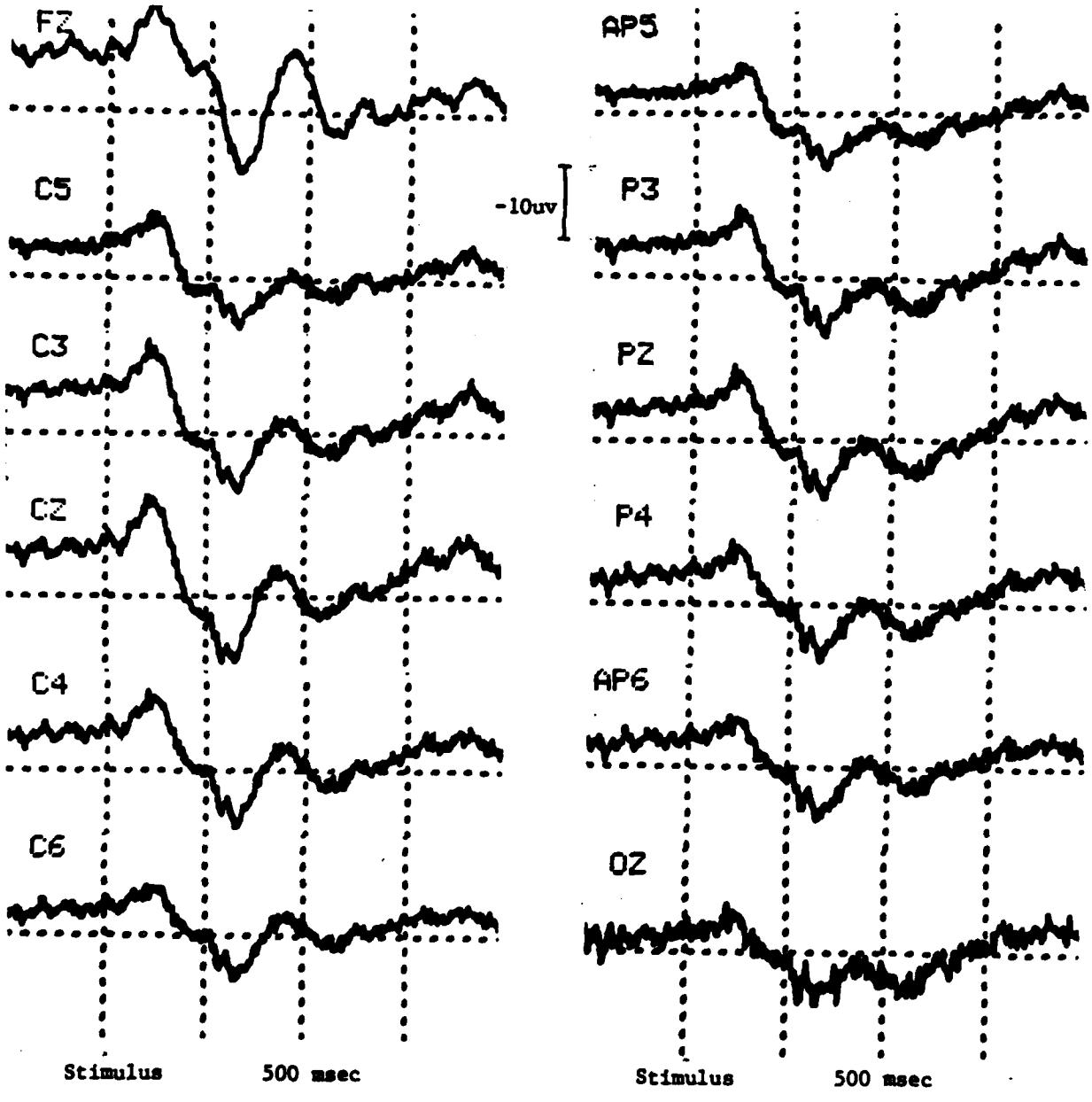

Figure 2b - Auditory miscued (no-move) condition. (p#12, 36 trials).

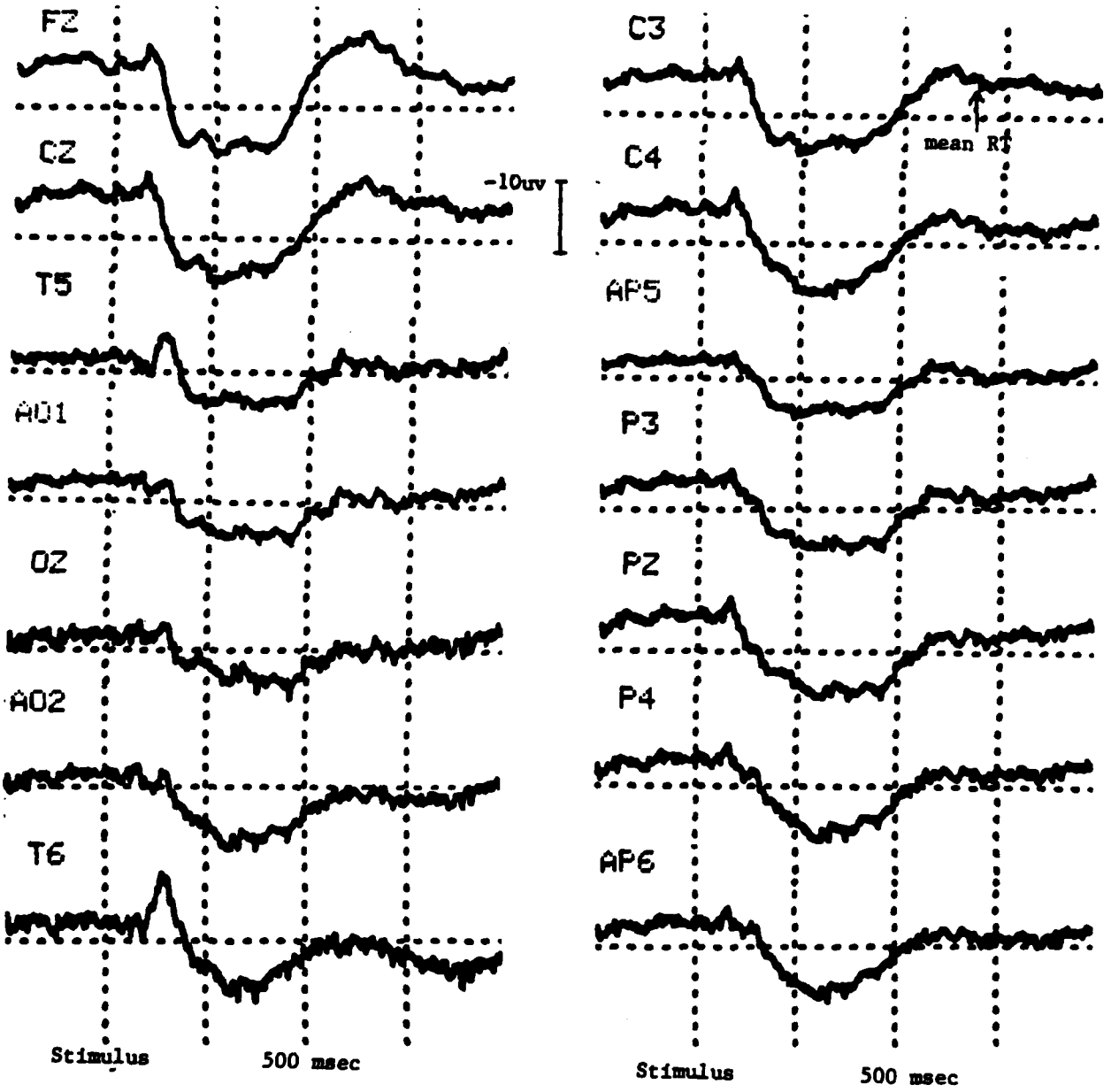

Figure 2 c- Visual correctly cued (move) condition. (p#12, 98 trials).

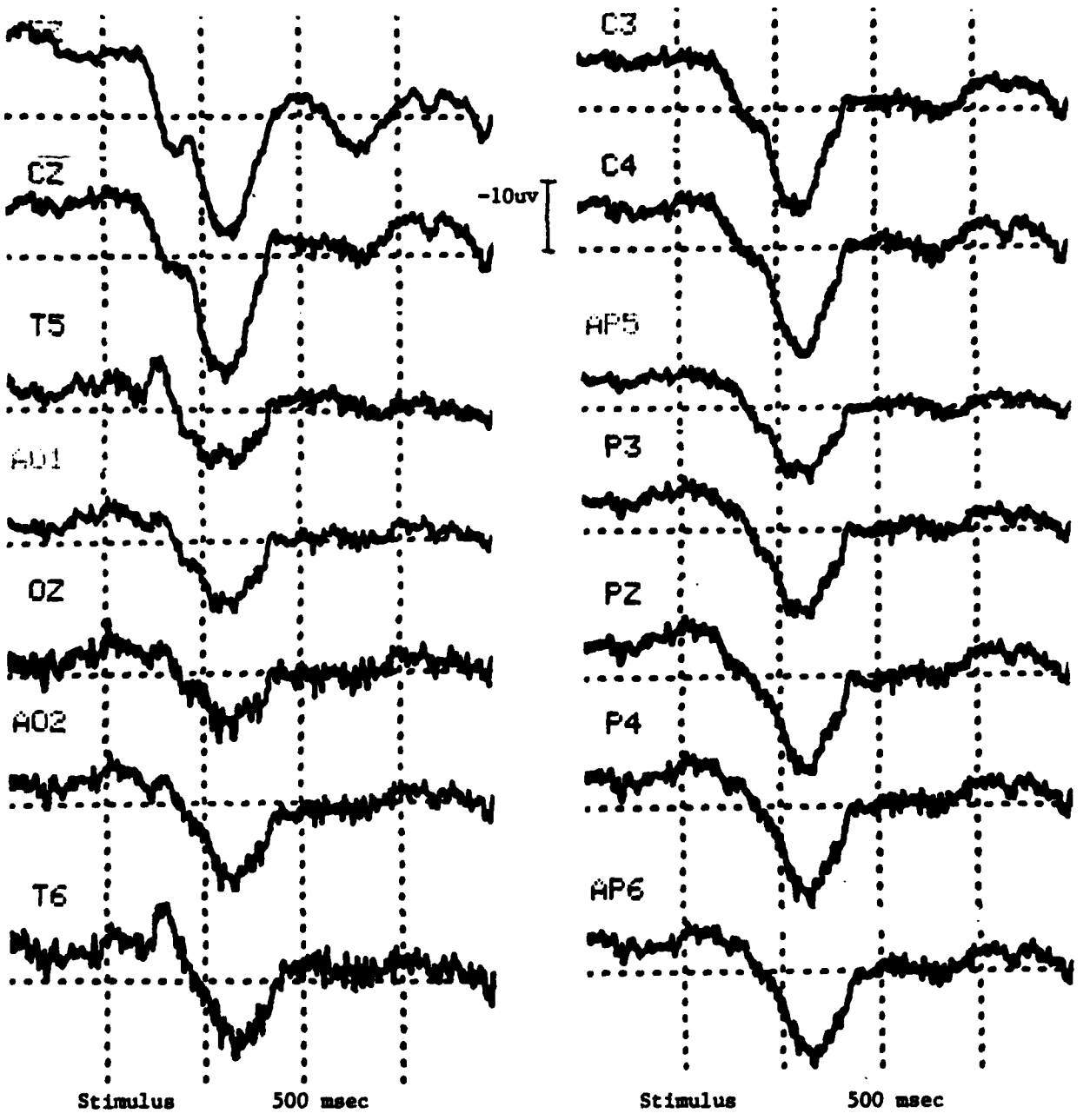

Figure 2d - Visual miscued (no-move) conditions. (p#12, 33 trials).

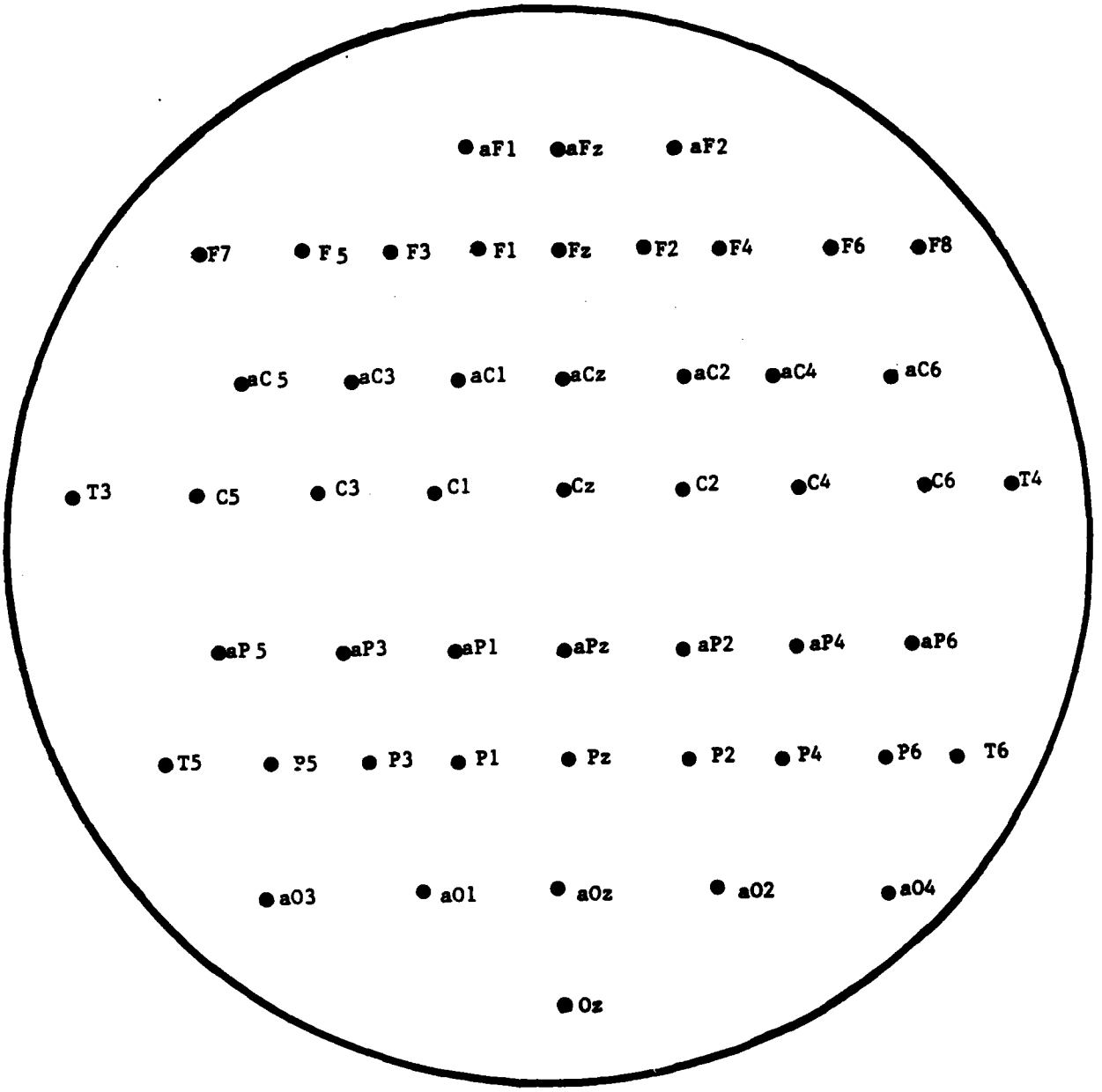

Figure 3 - 49 channel recording montage

SECTION III

Reprint Series
1 April 1983, Volume 220, pp. 97–99

SCIENCE

Shadows of Thought: Shifting Lateralization of Human Brain Electrical Patterns During Brief Visuomotor Task

Alan S. Gevins, Robert E. Schaffer, Joseph C. Doyle, Brian A. Cutillo, Robert S. Tannehill, and Steven L. Bressler

Shadows of Thought: Shifting Lateralization of Human Brain Electrical Patterns During Brief Visuomotor Task

Abstract. *Dynamic spatial patterns of correlation of electrical potentials recorded from the human brain were shown in diagrams generated by mathematical pattern recognition. The patterns for "move" and "no-move" variants of a brief visuospatial task were compared. In the interval spanning the P300 peak of the evoked potential, higher correlations of the right parietal electrode with occipital and central electrodes distinguished the no-move task from the move task. In the next interval, spanning the readiness potential in the move task, higher correlations of the left central electrode with occipital and frontal electrodes characterized the move task. These results conform to neuropsychological expectations of localized processing and their temporal sequence. The rapid change in the side and site of localized processes may account for conflicting reports of lateralization in studies which lacked adequate spatial and temporal resolution.*

Many investigators have reported that brain activity is lateralized during cognitive tasks. Advanced radiological methods reveal relative localization and lateralization, but cannot resolve temporal sequencing because of the long time required for observation. Studies of ongoing, background electrical activity do not reveal split-second changes in neurocognitive patterns, and those that have reported lateralization of neurocognitive activity have been questioned on methodological grounds (*1–6*). Although the components of averaged event-related potentials (ERP's) may indicate the sequencing of some neurocognitive processes, they have not revealed consistent, robust signs of lateralization, even for language (*7*). Conclusions derived from patients with focal brain lesions or with "split-brains," cannot be directly extended to normal subjects. Lateralized processes inferred from reaction time differences to hemifield or dichotic stimulation have also been questioned on methodological grounds (*8*). These factors have undoubtedly contributed to conflicting reports of lateralization of brain activity.

To observe the spatial patterns and sequencing of neurocognitive activity, we have developed a new method called neurocognitive pattern (NCP) analysis. In NCP analysis the average ERP's of each person are used to determine the time intervals of task-related neural processes. Within these intervals the similarity of brain-potential waveshapes over the scalp is measured on a single-trial basis by computing the cross-correlation coefficient between paired combinations of electrodes. Although the neuroanatomic origin and neurophysiological significance of these correlations is not known, it has been suggested that cognitive activity may be associated with characteristic scalp correlation patterns (*9*). However, task-related electrical signals from the brain are spatially smeared in transmission to the scalp and are embedded in background activity. Since linear statistical methods were not effective in dealing with these obstacles, we used a more powerful analysis called trainable classification-network mathematical pattern recognition (*2, 3, 10–13*). For this method, artificial intelligence algorithms are used to extract patterns of correlation that differ between two conditions with no assumptions about the distribution of correlation values. The algorithm is first applied to a labeled subset of the experimental data called the training set, and the invariant patterns (classification functions) found are then verified on a separate unlabeled subset of data called the test set. If the classification functions can significantly separate the test set into the two conditions, the extracted patterns have intrinsic validity.

Previously we reported the existence of complex, rapidly changing patterns of brain-potential correlation involving many areas of both hemispheres that distinguished numeric and spatial judgments in a visuomotor task (*13*). Since the sequencing of neurocognitive differences between numeric and spatial processing is not definitely known, the complex patterns were difficult to interpret. The present experiment was designed to clarify this situation by highlighting presumably localized neural processes. In comparing two types of spatial judgment, the common activity of brain areas should cancel, revealing differences in the right parietal area presumed to mediate spatial judgments. The right-handed finger response in one task was designed to elicit lateralized activity of the left central motor area.

In this study a person estimated the distance a "target" should be moved to intersect a displayed arrow's trajectory. The "move" task required pressure of the right index finger on a transducer with a force proportional to that distance (*14*). In the "no-move" task the arrow pointed directly at the target, and no pressing was required (pseudorandom 20 percent of trials). Thus, the spatial judgment and response differed between tasks, while gross stimulus characteristics were the same.

Nine right-handed, healthy adults (eight males, one female) participated in the study. The average response initiation (muscle potential onset) time for the move trials was 0.59 second (standard deviation, 0.19; mean of standard deviations within persons, 0.24). Brain potentials were recorded from 15 scalp electrodes and referenced to linked mastoids (Fig. 1A) (*15*). Vertical and horizontal eye movements, muscle potentials from the responding finger, and the output of the force transducer were also recorded. The data were edited to remove trials with artifacts, and a set of 1612 correct, representative trials (839 move, 773 no-move) was formed. Averaged ERP's were computed for all electrodes (Fig. 1B), and *t*-tests and analyses of variance (ANOVA's) were performed (*16*, *17*).

Cross-correlations were computed between 91 paired combinations of the 15 electrodes for each trial in each of three 175-msec intervals (Fig. 1B). Two intervals spanned the N100–P200 and P300 ERP peaks, and the third (RP) interval spanned most of the readiness potential (in the move task). The centerpoint of each interval was determined for each person (*18*). The correlations were standardized within persons, within electrode pairs (mean, 0; standard deviation, 1), and then grouped across people. The *t*-tests and ANOVA's of single-trial correlations did not distinguish meaningful differences in between-task spatiotemporal patterns.

Mathematical pattern classification was then applied to the single-trial correlations of all nine people to search for subtle between-task differences in each interval. To make the results anatomically interpretable, we performed the search separately on each of 15 sets of electrode pairs. Each set consisted of the correlations of a particular electrode with ten other electrodes (Fig. 1C). For each interval, the electrode set that distinguished conditions on the test set with the highest significance level (*19*), and the most prominent correlations for that electrode set (*20*), were diagramed.

In the N100–P200 interval, correlations of the midline parietal electrode distinguished the tasks ($P < .001$) (Fig. 2A). In the P300 interval, correlations of the right parietal electrode with the midline occipital and precentral electrodes were greater in the no-move task, while correlations of the right parietal with the right central electrode were greater in the move task ($P < 5 \times 10^{-5}$) (Fig. 2B). In the RP interval, correlations of the left central electrode with the midline frontal and occipital electrodes were greater in the move task, while correlations of the left central electrode with the midline parietal electrode were greater in the no-move task ($P < 5 \times 10^{-6}$) (Fig. 2C).

The right parietal locus of between-task difference in the P300 interval may reflect a lateralization of activity distinguishing the two types of spatial judgment (*21*) or the difference between movement estimation in the move task and the cancellation of response in the no-move task. The left central focus of difference in the RP interval 135 msec later may reflect the preparation and initiation of the movement of the right index finger. In contrast, the pattern of difference in the N100–P200 interval was not lateralized.

These results may help explain conflicting reports of brain-potential lateralization. In many studies, various "verbal-analytic" and "spatial" tasks 1 minute or more in duration have been associated with relative left and right hemisphere EEG activity (*1*–*6*). However, it

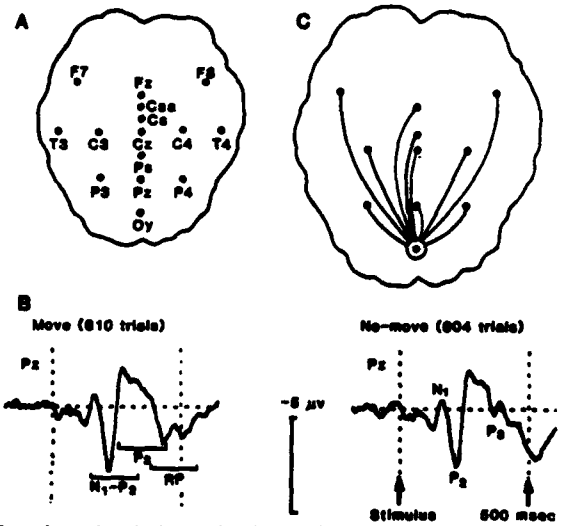

Fig. 1. (A) Montage of 15 electrodes. Nonstandard placements are intended to overlie cortical areas of particular interest: anterior occipital (*Oy*), anterior parietal (*Ps*), midline precentral (superior edge-*Cs*), and midline premotor (*Csa*) areas. (B) Composite average event-related potentials (ERP's) from four persons (75 percent of the total data from nine persons) for the Pz electrode, showing the major ERP peaks and corresponding single trial correlation analysis intervals. The P300 ERP peak is larger in the infrequent no-move trials. (C) One of the 15 sets of ten electrode pairs into which the 91 paired correlations were grouped. The anterior occipital (*Oy*) set is shown. In Fig. 2 the principal electrodes of differing sets are circled and the most prominent correlations are indicated as solid and dotted lines.

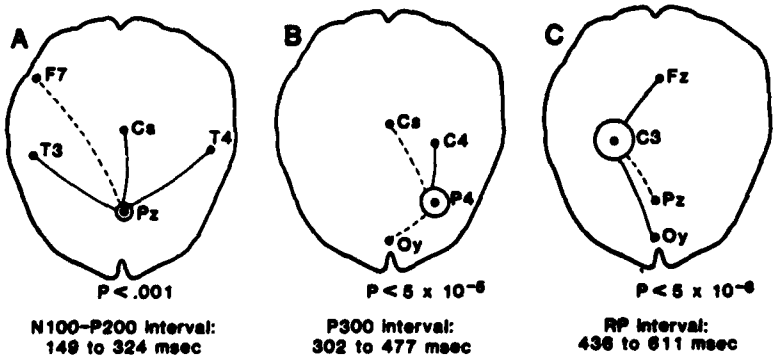

Fig. 2. Diagrams of between-task differences in the (A) N100–P200, (B) P300, and (C) RP intervals generated by neurocognitive pattern (NCP) analysis. The most significantly differing electrode sets, their significance level, and the most prominent correlations within the set are shown. A solid line between two electrodes indicates that the correlations were higher in the move task, while a dotted line indicates higher no-move task correlations.

is not clear whether this activity is associated with mental aspects of tasks or with sensorimotor components, or with artifacts. In a previous study we found no topographic differences in EEG spectra between 15-second arithmetic, block rotation and letter substitution tasks after rigorously controlling other-than-cognitive factors (*2–4*). However, such heterogeneous tasks cannot be resolved into serial components reflecting different neurocognitive processes. We therefore refined our approach by using short (less than 1 second) tasks, using time references based on person-specific average ERP measurements, computing correlations between channels on a single-trial basis, and using mathematical pattern classification to reveal split-second sequential processing. This yielded a sequence of clear-cut between-task difference patterns involving split-second changes in the localization and lateralization of mass neural activity. Appropriate studies of neurocognitive functions should take into account this rapidly shifting network of localized and lateralized processes.

ALAN S. GEVINS
ROBERT E. SCHAFFER
JOSEPH C. DOYLE
BRIAN A. CUTILLO
ROBERT S. TANNEHILL
STEVEN L. BRESSLER

EEG Systems Laboratory,
1855 Folsom Street,
San Francisco, California 94103

References and Notes

1. E. Donchin, M. Kutas, G. McCarthy, in *Lateralization in the Nervous System*, S. Harnard *et al.*, Eds. (Academic Press, New York, 1977), pp. 339–384.
2. A. Gevins, G. Zeitlin, C. Yingling, J. Doyle, M. Dedon, R. Schaffer, J. Roumasset, C. Yeager, *Electroencephalog. Clin. Neurophysiol.* **47**, 693 (1979).
3. A. S. Gevins, G. M. Zeitlin, J. C. Doyle, C. D. Yingling, R. E. Schaffer, E. Callaway, C. L. Yeager, *Science* **203**, 665 (1979).
4. A. Gevins and R. Schaffer, *CRC Crit. Rev. Bioeng.* **1980**, 113 (1980).
5. A. S. Gevins, J. C. Doyle, R. E. Schaffer, E. Callaway, C. Yeager, *Science* **207**, 1006 (1980).
6. A. Gevins, in *Cerebral Hemisphere Asymmetry: Method, Theory and Application*, J. Hellige, Ed. (Praeger, New York, in press).
7. D. Friedman, R. Simpson, W. Ritter, I. Rapin, *Electroencephalog. Clin. Neurophysiol.* **38**, 13 (1975); C. Wood, *J. Exp. Psychol. Hum. Percep.* **104** (No. 1), 3 (1975); J. Marsh and W. Brown, *Prog. Clin. Neurophysiol.* **3**, 60 (1977); R. Thatcher, *Behav. Biol.* **19**, 1 (1977).
8. J. Hellige, Ed., *Cerebral Hemisphere Asymmetry: Method, Theory and Application* (Praeger, New York, in press).
9. M. Livanov, *Spatial Organization of Cerebral Processes* (Wiley, New York, 1977); J. Busk and G. Galbraith, *Electroencephalog. Clin. Neurophysiol.* **38**, 415 (1975); E. Callaway and P. R. Harris, *Science* **183**, 873 (1974).
10. A. Gevins, *IEEE Trans. Patt. Anal. Machine Intell.* **2**, 383 (1980); S. Viglione, in *Adaptive Learning and Pattern Recognition Systems*, J. Mendel and K. Fu, Eds. (Academic Press, New York, 1970), pp. 115–163.
11. The two-layered, nonlinear, distribution-independent trainable classification-network algorithm used in this study is described in A. Gevins, J. Doyle, R. Schaffer, B. Cutillo, R. Tannehill, S. Bressler, *Electroencephalog. Clin. Neurophysiol.*, in preparation; and Gevins *et al.* (*12*).
12. A. Gevins, J. Doyle, G. Zeitlin, S. Bressler, *IEEE Trans. Patt. Anal. Machine Intell.*, in preparation.
13. A. S. Gevins, J. C. Doyle, B. A. Cutillo, R. E. Schaffer, R. S. Tannehill, J. H. Ghannam, V. A. Gilcrease, C. L. Yeager, *Science* **213**, 918 (1981). In the key for figure 3 of that report, $P < .005$ should have been next to the blank circle, while $P < .5 \times 10^{-3}$ should have been next to the hatched circle.
14. The stimulus subtended a visual angle of less than 2 degrees. The vertical position and side of screen of the target changed randomly across trials for both tasks, as did the horizontal angle and direction of the arrow. Response was made on a Grass isometric force transducer and varied randomly across trials from 0.1 to 1 kg. An individual trial consisted of a neutral warning that was followed after 2 seconds by the stimulus. One second after its completion the response was displayed.
15. Brain potentials were amplified with a Bioelectric Systems model AS-64P and Beckman Accutrace with a passband of about 0.1 to 50 Hz. Electrooculogram and muscle potentials were amplified by a Grass model 6 with similar filter settings. All signals were digitized to 11 bits at 128 samples per second, and a 12-Hz, 15-point nonrecursive digital low-pass filter was applied.
16. A task-by-electrode-by-person analysis of variance of the P300 peak voltage revealed a significant task effect [$F(1, 8) = 29.0$, $P < .001$] and task-by-electrode interaction [$F(13, 104) = 2.9$, $P < .005$]. Correlated *t*-tests revealed P300 voltage enhancements in the no-move task for all but the lateral temporal electrodes: the most significant difference ($P < .0005$) was at the anterior midline parietal electrode. When corrected for multiple comparisons by the Bonferroni method only the right central, anterior, and posterior midline parietal electrodes reached significance ($P < .05$). P300 ERP peak amplitude increases have been associated with similar go versus no-go decisions [R. Simson, H. Vaughan, W. Ritter, *Electroencephalog. Clin. Neurophysiol* **43**, 864 (1977)] and with the perception of a novel or relevant stimulus. This study differs from typical P300 studies in that a difficult motor response is required to the more frequent stimulus.
17. A task-by-electrode-by-person analysis of variance of the slope of a straight line fitted to the slow-potential shift across the RP interval revealed a significant task effect [$F(1, 8) = 5.6$, $P < .05$], electrode effect [$F(14, 112) = 1.9$, $P < .05$], and task-by-electrode interaction [$F(14, 112) = 2.7$, $P < .005$]. Correlated *t*-tests showed larger move task slopes for nine electrodes; the most significant difference ($P < .005$) was at the left central electrode. When Bonferroni-corrected, no electrode reached significance at $P < .05$.
18. The N100–P200 and P300 centerpoints in milliseconds for each of the volunteers were: V1 (218, 452); V2 (200, 388); V3 (228, 482); V4 (210, 462); V5 (208, 390); V6 (208, 298); V7 (212, 368); V8 (181, 318); and V9 (203, 358). The RP interval was centered 135 msec after the P300 centerpoint.
19. The functions were derived from two-thirds of the data and were tested on the remaining one-third. This was repeated three times and the average test-set classification accuracy was computed. A test-set classification accuracy of 55 percent corresponds to $P < 5 \times 10^{-7}$. This is more than 3.8 standard deviations above the mean classification accuracy of 48 classifications using 1612 randomly labeled move and no-move trials. Mean accuracy on the randomly labeled data was 50.6 percent, with a standard deviation of 1.1 percent, an accuracy that could have occurred by chance with $P = .32$ according to the binomial distribution. High classification accuracy was not the objective. Rather, the relative classification accuracy of each electrode set was used as an indicator of anatomic and temporal localization of task-related patterns. The classification accuracy of the P300 and RP intervals assessed on each individual was at the chance level for only two of the nine people. Their data comprised only 9 percent of the total data set. When the entire analysis was performed on the data of one person (V7) in the P300 interval, the P4 electrode set again achieved the highest classification accuracy.
20. To select the most prominent correlations from significant classification functions, the pattern recognition analysis was applied recursively on the highest weighted correlations. Test-set classification accuracy based on the final three or four correlations was significant at $P < .001$ or better in each interval.
21. The P300 ERP peak has not been found to vary in lateralization specifically as a function of cognitive task (*1*). J. Desmedt [*Proc. Natl. Acad. Sci. U.S.A.* **74**, 4037 (1977)] reported a qualitative change in the ERP over the right hemisphere in a somatosensory-motor task, but the effect was general and was not present in the P300 peak.
22. We thank the late Gobind B. Lal for the "shadows of thought" metaphor; H. Currens for manuscript preparation and artwork; G. Gilcrease and J. Ghannam for assistance with recordings and analysis; R. Adey, M. Aminoff, P. Bach-y-Rita, F. Benson, E. Callaway, J. Engel, B. Geroutte, W. Gorsch, R. Halliday, E. Roy John, B. Libet, J. Mazziotta, M. Mesulam, K. Pribram, J. Roumasset, A. Selamy, C. Skinner, J. Spire, H. Vaughan, D. O. Walter, C. Woods, and J. Vidal for valuable comments; J. Miller (Air Force School of Aerospace Medicine), D. Woodward (Office of Naval Research), A. Pregly (Air Force Office of Scientific Research), J. Fetzer, and M. Bachman-Hoffman for research support.

19 November 1982; revised 1 February 1983

NOTE 18a. The average ERP waveforms (Figure 1B) contain several late positive peaks. P391 and P530 are larger in amplitude in the infrequent no-move trials, while P425 is larger in the frequent move tirals. The P300 analysis interval was centered on P391, the earliest positive peak to show a significant between-task difference maximal at the anterior midline parietal electrode ($p<.0005$). Since P391 and P530 were larger in the infrequent no move trials, and P391 followed a negative difference ERP peak (N2) at 240 msec, P391 and P530 could be designated P3a and P3b according to the convention of Squires, et al (Electroencph. Clin. Neurophysiol. 38;387-401, 1975). The P300 interval might then be specified as the "P3a interval", as in our previous study of similar tasks (Gevins, et al, Science, 213:918-922, 1981). The response preparation (RP) interval, centered 135 msec after the P300 interval, also spans the P530 peak of the no-move trials.

Section IV

NEUROCOGNITIVE PATTERN ANALYSIS OF A VISUOMOTOR TASK: LOW-FREQUENCY EVOKED CORRELATIONS

Alan S. Gevins, Joseph C. Doyle, Brian A. Cutillo, Robert E. Schaffer, Robert S. Tannehill, Steven L. Bressler,

EEG SYSTEMS LABORATORY
1855 Folsom
San Francisco, CA 94103
415-621-8343

Note to colleagues: This manuscript will shortly be submitted for publication. We would appreciate receiving your cricital comments and suggestions. Thanks.

ABSTRACT

Spatial patterns of single-trial evoked correlations of human scalp-recorded brain potentials were determined by applying Neurocognitive Pattern (NCP) analysis to data from nine adults performing a visuospatial task. Mathematical pattern recognition was used to determine the differences in the spatial patterns of correlation of "move" and "no-move" trials in successive 175-msec intervals. The magnitude of the patterns of difference between tasks increased in each successive interval. In the prestimulus interval, correlation of the midline frontal electrode with lateral central and left temporal electrodes was greater for the no-move task, while its correlation with the left parietal electrode was greater for the move task ($p<.01$). In the interval spanning the N1, P2 and N2 event-related potential (ERP) peaks, the between-task contrast was focused at the midline parietal electrode and involved higher correlation of that electrode with lateral temporal and midline precentral electrodes in the move task, and with the left frontal (F7) electrode in the no-move task ($p<.001$). In the interval centered on the P3a peak, the focus of correlation difference was at the right parietal electrode and involved higher correlation of the right parietal with occipital and midline precentral electrodes in the no-move task, and with the right central electrode in the move task ($p<5\times10^{-5}$). In the interval centered 135 msec after the P3a ERP peak, and which included the right-handed response preparation and initiation, the major focus of contrast shifted to the left central electrode, involving higher correlation of that electrode with midline frontal and occipital electrodes in the move task, and with the midline parietal electrode in the no-move task ($p<5\times10^{-6}$). In seven of the nine participants, the group equations significantly distinguished the tasks. Move and no-move trials which were behaviorally correct, but which were misclassified by the algorithm showed high prestimulus alpha activity in the averages, and had post-stimulus waveform morphologies intermediate between correctly classified move and no-move types. Although the neurophysiological significance of these patterns of evoked correlation is unknown, the results are consistent with the observation in humans and primates that simple visuospatial tasks involve the integration of spatially-distributed activity in many neural areas.

INTRODUCTION

Neurocognitive Pattern (NCP) analysis is a method of measuring the functional topography of human scalp-recorded brain potentials during goal directed activity. It involves application of mathematical pattern recognition to measures of inter-electrode correlations of single-trial evoked brain potentials. Here we report the measurement of rapidly shifting, focal patterns of correlation which distinguish two variants of a brief 'move/no-move' visuospatial task.

It has been proposed that task-specific neural processes manifest patterns of waveshape similarity (crosscorrelation) of low-frequency macropotentials (Dumenko, 1970; Livanov, 1977). A number of studies have approached this issue with scalp-recorded EEGs (Walter and Shipton, 1951; Brazier and Casby, 1952; Callaway and Harris, 1974; Busk and Galbraith, 1975; Livanov, 1977), but this hypothesis remains unproven due to problems of experimental design and lack of methodology for precise measurement of task-related correlation patterns at the scalp.

Any test of the hypothesis that waveshape similarity among scalp-recorded brain potentials reflects task-related processing in underlying neural populations must meet several methodological criteria. First, the functional relationships of specific areas must be explicitly manipulated. Well established 'landmarks' such as sensory, 'association' and motor areas must be used as anatomic reference points in the experimental design, and the scalp projections of the presumed generators must be considered. Second, the experiment must be rigorously controlled for stimulus, cognitive, performance and response-related factors to allow unambiguous association of experimental manipulations with spatiotemporal electrical patterns. Third, a high degree of temporal resolution is required, since the neural processes involved in brief cognitive tasks last only a fraction of a second. Fourth, measures must be made on single-trial EEG timeseries rather than averages, since the exact timing of neurocognitive processes may vary from trial to trial. Fifth, the analytic method must be able to extract small task-related signals from the obscuring effects of background activity and volume conduction.

Our first study employing NCP analysis (Gevins, et al, 1981) revealed complex, rapidly changing patterns of evoked correlation which involved many areas of both hemispheres which differed between numeric and spatial judgments performed on equivalent stimuli. However, the complex patterns were difficult to interpret since the sequencing of neurocognitive activity in numeric and spatial judgments is not definitively known. The present study was designed to clarify this situation by highlighting presumably localized neural processes. In comparing the move and no-move variants of a spatial judgment task the common activity of brain areas should cancel, revealing focal differences in visual and parietal areas presumed to mediate visual discrimination and spatial judgments. The

right-handed response in the "move" task should elicit lateralized activity of the left central motor area.

METHODS

Tasks and Protocol

The participant (P) was seated in an acoustically dampened recording chamber with right-hand index finger resting on a force transducer. Stimuli were presented on a Tektronix graphics terminal and subtended a visual angle of less than 2 degrees horizontally and vertically. They consisted of an arrow originating at center screen and a vertical line segment (the "target") to one side (Fig. 1). The target's vertical position and side of screen changed randomly across both move and no-move trials, as did the angle and direction of the arrow. The arrow's angle varied from 0 to 30 degrees from the horizontal, and target size ranged from 2 to 36 mm (see below). Stimuli remained on the screen until feedback was presented. On move trials the participant was to estimate the distance the target must be moved so that the arrow's trajectory would intersect its center, and apply a pressure proportional to that distance with a ballistic contraction of the right index finger. Responses were made on a Grass isometric force transducer with maximum 1mm travel at a force rate of 1 kg/mm. The required force varied randomly from .1 to 1 kg. On "no-move" trials the arrow and target were oriented so that the arrow's trajectory would intersect the center of the target, and no movement was to be made (Fig. 1).

Trials occurred in blocks of 13 or 17. The blocks were self-initiated by the participant and lasted about 1.5 min. The no-move trials constituted 20% of the total number of trials and were presented in semi-random order such that the first two trials of a block were always move trials, and a no-move trial was always followed by a move trial. Each trial consisted of a warning symbol followed after 2 sec by the stimulus. One second after completion of response in the move task, feedback indicating the response pressure was presented for 1 sec. Feedback for no-move trials was presented 3.5 sec. post-stimulus. The inter-trial interval was 1.8 sec.

Two factors were included to reduce the automatization of task performance. First, at the start of each block of trials the gain of the response transducer was switched between 2 levels of sensitivity, requiring the participant to adjust his responses between 2 pressure/distance scales. Second, the target automatically shrank or lengthened (from 2 to 36 mm) for both move and no-move trials as an on-line function of accuracy in the previous 5 move trials. Thus task difficulty was continually adjusted to match each person's current performance level.

Recordings

Nine right-handed adults (8M, 1F) were recorded. The first five were healthy students and professionals, ages 20 to 35, who received about

50 practice trials before performing the tasks during 2.5 hour recording sessions. The last four were highly skilled aircraft pilots who had several hundred practice trials and who performed a large number of trials in 6 hour recording sessions.

Brain potentials were recorded from 15 scalp electrodes and referenced to linked mastoids (Fig. 2a). The montage included several non-standard midline placements intended to overlie cortical areas of particular interest: 'aOz' (anterior occipital), 'aPz' (anterior parietal), 'aCz' (precentral), and 'pFz' (anterior motor). The first five Ps' brain potentials were amplified by two Beckman Accutraces with .16 to 50 Hz passband; for the other four a Bioelectric Systems Model AS-64P amplifier with .10 to 50 Hz passband was used. Vertical and horizontal eye-movement potentials (electrodes at outer canthi and above and below one orbit), response-muscle potentials (flexor digitorum), and response transducer output were amplified by a Grass Model 6 with .30 to 70 Hz passband. All signals were low-pass filtered at 50 Hz (40 dB/octave rolloff) and digitized to 11 bits at 128 samples/sec.

Software System

The ADIEEG, integrated software system, was used for all aspects of the experiment (Gevins and Yeager, 1972; Gevins, et al, 1975, 1979a, 1981, 1983b). This system performs real-time control of experiments and behavioral and physiological data collection; allows automatic on-line modification of experimental parameters as a function of task performance; has a flexible database structure and integrated data path for the recording and analysis of up to 56 physiological channels; allows selection and control of the stimulus, response and performance-related variables used to aggregate trials into data sets; performs digital filtering and timeseries analysis of EEGs and ERPs; and tests hypotheses with linear univariate and multivariate analyses and mathematical pattern recognition.

Formation of Data Sets

Polygraph records were edited off-line to eliminate trials with evidence of eye movement in the EOG channels, or muscle or instrumental artifacts in the EEG channels, from 0.5 sec before the stimulus to 0.5 sec after response initiation. The total set of 1612 trials (839 move, 773 no-move) submitted to analysis consisted of 69 to 350 behaviorally correct trials from each of the 9 participants (Table 1). Correct move trials were those in which the participant's response was ballistic, was completed by 1.5 sec after stimulus onset, and was not greatly 'off target'. Correct no-move trials were those in which no EMG was evident in response to the 'no-move' stimulus configurations. There was no difference between the two data sets in the stimulus parameters of arrow angle and side of screen of the arrow and target, since these parameters were randomized by the program. Target size was balanced between move and no-move trials. The set of move trials had representative distributions of response variables including response initiation time, accuracy, pressure, duration, and velocity. Response initiation was determined by the

beginning of the average EMG burst of the right index finger's flexor digitorum. Thus move and no-move tasks differed slightly in expectancy and stimulus configuration, differed in the decision based on spatial judgment, and differed greatly in type and difficulty of response.

Average ERPs

Average ERPs for all channels were computed for each person in order to determine centerpoints of time intervals for NCP analysis. Amplitudes of the major ERP peaks were measured from a 500-msec prestimulus baseline. N1 was the first major negative deflection, maximal posteriorly. P2 was the immediately succeeding positive deflection, maximal at the anterior parietal electrode. P3a and P3b were the first and second positive peaks enhanced in the infrequent no-move task and maximal at parietal electrodes. The immediately succeeding negative potential shift (in the move trials) was measured as the slope of a straight line fitted to the ERP in the 175-msec interval centered 135 msec after the P3a peak.

Single Evoked Trial Correlations

After applying a phase-preserving, nonrecursive digital lowpass filter (3 dB amplitude point at 12 Hz) to the single-trial timeseries, crosscorrelations between pairs of electrodes were computed according to the formula:

$$\frac{\sum_{N} XY - \frac{\sum_{N} X \sum_{N} Y}{N}}{N^2 \, s_x \, s_y}$$

where X and Y are the sampled voltages of channels x and y at N time points, and s_x, s_y their standard deviations. A Fisher's z' transformation was then applied to each correlation value. Correlations were computed for each of the 1612 trials in each of 4 analysis intervals for 91 of the 105 possible pairwise combinations of electrodes (Fig. 2b). 14 pairs which were non-homologous or closely spaced were excluded due to computational limitations.

Since the major ERP peaks indicate the average latencies of distinct task-related processes, the centerpoint locations of three of the four 175 msec analysis intervals were determined from the peak latencies of the average ERP (Fig. 3). This was done separately for each person to account for individual variations. The first interval was the 175 msec epoch preceding the stimulus. The second interval straddled each person's N1-P2 peak complex, and the third was centered on the P3a peak, which was the first positive peak to show a between task difference. The fourth interval was centered 135 msec after the P3a peak and spanned a portion of the response preparation (RP) in the move trials and the P3b peak in the no-move trials. (An NCP analysis synchronized to the movement onset will be reported elsewhere).

To equalize the scale of correlation values across people, the Fisher z'-transformed correlations were converted to standard scores within each person's data in each interval (x=0, s=1) and then grouped across people. ANOVAs and t-tests were performed on the single-trial correlations to determine task-related differences observable by linear statistical methods.

Use of Mathematical Pattern Recognition for Spatiotemporal Analysis

The analysis of between-task differences in spatial patterns of evoked correlation was performed with nonlinear, distribution-independent, trainable classification-network mathematical pattern recognition (Viglione, 1970; Gevins, 1980; Gevins, et al, 1979a, 1981, 1983ab). This method is similar in purpose to stepwise discriminant analysis, but uses a more sophisticated algorithm to search for combinations of variables which distinguish the data of two conditions of an experiment. The search is conducted on a task-labeled portion of the data, called the training set, and then the extracted patterns of difference (classification equations) are verified on the remaining unlabeled data, called the test set. If these classification equations can significantly divide the test set into the two conditions, the extracted patterns can be said to have intrinsic validity.

To avoid spurious results, the sensitivity of this method requires that the experimental conditions be highly balanced for all factors not related to the intended manipulations (Gevins and Schaffer, 1980; Gevins, et al, 1980, 1983b; Gevins 1980; 1983ab), and that the ratio of observations to variables be on the order of 20 to 1 or more. The variables submitted to analysis should be grouped (constrained) according to neuroanatomical and neurophysiological criteria so that interpretable results may be obtained (Gevins, et al, 1979ac, 1981, 1983ab; Gevins 1980). In this study temporal constraints consisted of locating the analysis intervals according to the major peaks of each person's average ERP. Anatomical constraints were applied by forming sets consisting of the correlations of each of the 15 scalp electrodes (called a principal electrode) with 10 other electrodes (Fig. 2c). (To reduce the amount of computation, 4 of the 14 possible pairings were excluded from each set. These involved electrodes adjacent to the principal electrode, or pairings nearly redundant with others.) Midline sets were symmetrical, and lateral sets were mirror images of each other.

Classification equations. A separate classification equation was computed for each of the 15 electrode sets in each analysis interval for each task-labeled training set. Each classification equation consisted of a linear combination of the binary decisions of 1 to 6 discriminant functions. Each discriminant function consisted of a linear combination of 6 correlations selected by the algorithm from the 10 electrode-pair correlations of an electrode set.

A recursive procedure was used to develop each classification equation. First, 15 discriminant functions were computed (this number was set by computer limitations), and the best was retained as a binary output (move or no-move) times a coefficient weighted for optimum classification performance by minimization of an exponential loss function. This process was repeated 6 times; the best discriminant function from each new set of 15 was added to the evolving classification equation, and the weights assigned to each were updated. After each pass, the training data were re-weighted inversely to the classification effectiveness of the classification equation, so that the next pass would concentrate on the incorrectly classified data. In this way a classification equation which optimally partitioned the training data set into move and no-move tasks was formed.

Training and testing (validation) data sets. The data set of 1612 trials was partitioned into 3 non-overlapping test (validation) sets. For each test set, the remaining two-thirds of the data served as its training set. This rotation of training and testing sets reduced sampling error due to test-set selection.

A separate classification equation was formed using each of the 3 training sets. Then the classification accuracy of each of the 3 equations for each interval was measured on its corresponding test set, and the average test-set classification accuracy was determined.

Significance levels of classification. Since our aim was to determine task-related spatiotemporal patterns, rather than to predict behavior, the analysis was constrained to facilitate a neuroanatomically and neurophysiologically meaningful interpretation. Thus classification accuracies were not as high as they would have been without constraints. To determine the significance levels of the classification accuracies it was necessary to determine a baseline significance level and safeguard against a Type 1 error. To do this, equations were formed from sets of randomly task-labeled data for each analysis interval. The average classification accuracy of 48 such random-labeled studies was 50.6%, with a standard deviation of 1.1%. This could have occurred by chance with $p=.32$, according to the normal-curve approximation to the binomial distribution. Actual test-set classification accuracies of 52.9%, 53.9%, 54.9% and 55.5% correspond to $p<.01$, $p<.001$, $p<5 \times 10^{-5}$ and $p<5 \times 10^{-8}$, respectively. These significance levels were used as an index of the relative consistency of differences between move and no-move tasks.

Diagrams of classification equations. In order to illustrate the strongest between-task differences, diagrams were drawn showing the principal electrode and the electrode pairings which contributed most to the classification function for the most significant electrode set in each interval. These 'prominent' evoked correlations were determined by applying the pattern recognition procedure recursively to the most significant electrode set. Each discriminant function (combination of correlations) whose weight was more than 0.1 times that of the maximum weighted function was retained on each pass.

Within the selected discriminant functions, those correlations whose weight was more than .25 times the highest weighted correlation were retained. The selected correlations were weighted by the number of discriminant functions remaining in the classification equation, and summed over the 3 test sets. The 5 highest weighted correlations were then input to the pattern classifier. If 'test-set' classification for a given interval was still significant at $p<.01$, the entire procedure was repeated with the least significant correlation removed until a classification function incorporating a minimum set of 3 or 4 'prominent correlations' was produced.

RESULTS

Average ERP Description

The average ERP waveforms from Ps #6-9 (Fig. 4) consisted of a posteriorly maximum negative peak (N163) and a centro-parietally maximum positive peak (P230) in both tasks. In the move task there were parietally maximum positive peaks at 425 and 500 msec, followed by a centrally maximum, left-lateralized negative-going slow potential shift. In the no-move task a positive peak was observed at 391 msec, maximal at the anterior parietal electrode (aPz), another at 425 msec and a third at 530 msec, both maximal at the midline parietal electrode (Pz). Subtraction ERPs (Fig. 5) showed that the P391 peak in the infrequent no-move task immediately follows a negative peak (N2) at 240 msec, and thus may be the probability sensitive P3a peak (Squires, et al, 1977). The larger amplitude of P425 in the move task may be due to the atypical experimental paradigm, in which a difficult response is required to the frequent task-related stimuli. P530 in the infrequent no-move task may correspond to the P3b peak observed in go/no-go paradigms and to infrequent task-related stimuli. Peak latencies, the corresponding NCP analysis intervals, and response initiation times for each person are given in Table 1.

ANOVAs and t-tests were performed for the P391 (P3a) peak amplitude and the slope of the immediately succeeding slow negative potential shift. For the P391 peak, a task x electrode x person ANOVA revealed a significant task effect ($F(1,8) = 29.0$, $p<<.001$) and task x electrode interaction ($F(13,104) = 2.9$, $p<.005$), but no electrode effect ($F(13,104) = 1.2$, N.S.). Correlated t-tests revealed significant voltage enhancements in the no-move task for all but the lateral temporal electrodes, the most significant effect being at the midline anterior parietal electrode (aPz) ($p<.0005$) (Table 2). When Bonferroni-corrected for multiple comparisons, only the aPz, Pz and C4 electrodes remained significant ($t = 4.35$ for $p<.05$). Mean amplitudes across persons at aPz were .1 uV and 2.3 uV for move and no-move tasks, respectively.

A task x electrode x person ANOVA of the slope of a straight line fitted to the slow potential shift in the response preparation (RP) interval revealed a significant task effect ($F(1,8) = 5.6$, $p<.05$), electrode effect ($F(14,112) = 1.9$, $p<.05$), and task x electrode

interaction ($F(14, 112) = 2.7$, $p<.005$). Correlated t-tests showed significantly larger move-task slopes for 9 electrodes (Table 3). The most significant difference ($p<.005$) was at the C3 electrode, where the mean slope values were .24 and -.50 for move and no-move tasks, respectively. When Bonferroni-corrected for multiple comparisons, no electrode remained significant ($t = 4.35$ for $p<.05$).

Linear Analysis of Evoked Correlations

Mean evoked correlation values over persons and electrode pairs were, for the move trials: prestimulus interval = .64, N1-P2 interval = .65, P3a interval = .65, RP interval = .65; and for the no-move trials: prestimulus = .65, N1-P2 = .65, P3a = .65, and RP = .64. t-tests of differences in single-trial correlations between tasks were performed for the 91 electrode-pair correlations (Table 4). When Bonferroni-corrected for multiple comparisons only the F7-T3 and F8-Pz pairs in the RP interval reached significance ($t = 3.58$ for $p<.05$). Without Bonferroni correction, correlations significant at $p<.05$ or better were found in every interval. In the prestimulus interval 5 of the 9 significant electrode pairs included the Fz electrode. In the N1-P2 interval the 4 significant pairs all included parietal sites. In the P3a interval the 6 significant pairs were fronto-central, with the exception of the P4-C4 pair. In the RP interval the 25 significant pairs were widely distributed, but 8 included Fz, 9 included F8, and 5 included C3.

Pattern Recognition Analysis of Single-Trial Evoked Correlations

Pattern recognition analysis revealed patterns of difference in evoked correlation which increased in magnitude in each successive interval. The principal electrode and prominent correlations of the most significant electrode set in each interval are shown in Figure 6. In the prestimulus interval there was a weak between-task difference of the Fz electrode set ($p<.01$), involving higher prominent correlations of Fz with P3 in the move task and higher correlations of Fz with T3, C3 and C4 in the no-move task.

In the N1-P2 interval the distinguishing significant difference was in the Pz electrode set ($p<.001$), with higher correlations of Pz with aCz, T3 and T4 in the move task, and higher correlations of Pz with F7 in the no-move task.

In the P3a interval the most significant difference was in the P4 electrode set ($p<5 \times 10^{-3}$), with higher correlations of P4 with C4 in the move task, and higher correlations of P4 with aCz and aOz in the no-move task. At the $p<.001$ level the aOz electrode set also distinguished the tasks.

In the RP interval the most significant difference was in the C3 electrode set ($p<5 \times 10^{-8}$), with higher correlations of C3 with Fz and aOz in the move task, and higher correlations of C3 with Pz in the no-move task. Four other electrode sets distinguished the tasks at lower significance levels: C4 ($p<1 \times 10^{-3}$), F7 and T3 ($p<5 \times 10^{-4}$), and Pz ($p<.001$).

For the prestimulus and N1-P2 intervals the reduced classification functions required 4 "prominent correlations" to achieve significant classification, while in the P3a and RP intervals only 3 were needed. Further, significant classification ($p<.05$) could be achieved with just the first term (discriminant function) of the reduced classification equation (Table 5).

To test the interperson validity of the results, the classification accuracies of the classification equations for the P4 electrode set in the P3a interval and the C3 set in the RP interval were assessed on the data of each person individually, and compared with the overall classification accuracy (Table 6). The group equations were valid for 7 of the 9 people. As a further test, the entire analysis was performed on the data of one person (255 trials from P #7) for the P3a interval. The P4 electrode set again achieved the highest classification accuracy (59.4%; $p<5 \times 10^{-3}$).

DISCUSSION

Neurophysiological Significance of Task-Related Evoked Correlations

In theory, a task-related difference in evoked correlation between two scalp electrodes could be due to one or more possible causes: 1) functional coordination of two distinct cortical populations, 2) driving by a third cortical or subcortical neural area, and 3) volume conducted activity from a distant generator. While it is if the task-related patterns of evoked correlation determined by Neurocognitive Pattern (NCP) analysis reflect functional coordination between cortical (and possibly subcortical) areas, their anatomical and temporal specificity suggests that significant aspects of task-related neural processes are being measured. (A preliminary NCP Analysis of single channel signal power determined significant, but weaker, between-task patterns of difference. Some of the significant electrodes corresponded to those found with correlation measures. These results will be reported elsewhere.) However, the significance of waveshape similarity in scalp-recorded brain potentials will not be understood until further studies are completed.

NCP Analysis, ERPs and Neuropsychology

In this section the main NCP results will be discussed in light of previous neuropsychological and electrophysiological (ERP) findings, showing how they concur with and elaborate the information obtainable by those methods. Psychological interpretation of these results must be considered speculative, since the processing stages involved in the task are not definitively known.

The magnitude of between-task difference increased from interval to interval. The presence of a small significant effect in the prestimulus interval might be the result of a weak task-specific preparatory set generated in the course of the session by the ordering of move and no-move trials. The locus of this difference in the Fz electrode set is consistent with neuropsychological and

electrophysiological (CNV) findings suggesting involvement of prefrontal cortex in preparatory activity (Teuber, 1964; Walter, 1967; Fuster, 1980). A previous NCP study (Gevins, et al, 1981) also revealed evidence of a task-specific preparatory set in the task-cued prestimulus interval preceding numeric and spatial judgments. The prominent correlations of Fz with T3, C3, C4 and P3 in the present study suggest that this preparatory activity extends beyond prefrontal areas.

In the N1-P2 interval, correlations of the Pz electrode set distinguished move and no-move tasks at $p<.001$. Subtraction ERPs revealed an enhancement of the N2 peak no-move trials in 6 of the 9 participants (79% of the total data set) (Fig. 5). Its mean latency of 240 msec. placed it near the center of the N1-P2 analysis interval, and its amplitude was maximal (1.7 uv) at Pz. Thus the between-task correlation differences in this interval may be related to N2. Although an amplitude increase in the N2 peak in no-go trials of a go/no-go paradigm with equiprobable conditions has been reported (Simson, et al, 1977), N2 has usually been reported to be sensitive to infrequent changes in gross stimulus properties or patterns (Naatanen, et al, 1980). However, in the present study, stimuli were equivalent between conditions in all respects, save that in no-move trials the arrow pointed directly at the target in various randomly-ordered configurations. The N2 effect at 240 msec suggests that a no-move configuration has been identified by that time, and that N2 may reflect a more subtle process than the detection of a gross "mismatch" in stimulus characteristics, as indicated by other recent studies (Ritter, et al, 1982). The prominent correlations of Pz with T3, F7, aCz, and T4 suggest that these processes are not confined to the parietal area.

In the P3a interval (which was centered on the P3a peak and overlapped a portion of the P3b peak), the right parietal (P4) locus of correlation differences ($p<5 \times 10^{-5}$) provides novel evidence for the lateralization of neural processes related to these late positive ERP peaks. Although on the basis of lesion evidence, the right parietal cortex is known to be necessary for such spatial judgments, the late positive ERP peaks have not been found to vary in lateralization according to type of cognitive task (Donchin, et al, 1977). J. Desmedt (1977) reported a relative right-sided lateralization in the ERP in a spatial somatosensory-motor task, but the effect was general and was not present in the P3 peak, nor was its scalp distribution determined. A previous NCP study (Gevins, et al, 1981) demonstrated lateralized temporo-parietal evoked correlation differences between numeric and spatial judgments in the interval centered on the P3a peak at 340 msec., but the interval centered on the P3b peak at 450 msec. exhibited bilateral between-task differences from frontal, central, and parietal electrodes. In the present study, the between-task differences in correlations of the right parietal electrode with central and occipital electrodes is in accord with neuropsychological expectations, as is the somewhat weaker effect in the aOz electrode set. The lateralized NCP finding is in contrast with the anterior midline parietal (aPz) locus of maximal amplitude difference of the

P3a ERP peak.

In the response preparation (RP) interval, centered 135 msec after the P3a interval centerpoint, the focus of between-task difference shifted to the left central (C3) electrode set ($p<5 \times 10^{-6}$), involving higher correlations of C3 with Fz and aOz in the move task and with Pz in the no-move task. Since the RP interval overlapped EMG onset in a portion of the set of move trials (average response time = 590 msec, mean S.D. within persons = 240 msec.), the RP interval results may also include a contribution from the output activity of motor cortex. The C4, F7, and T3 electrode sets, which differed at lower significance levels, may also reflect movement preparation and initiation, since the presumed generators of voluntary finger movements are buried in the lateral bank of the central sulcus and their scalp projection may be diffuse. The less significant difference in the Pz electrode set may reflect concurrent processes related to P3b.

Rapidly Shifting Lateralization

The rapid (135 msec) shift in side and site of lateralization from the P3a to the RP interval may help clarify the controversy surrounding the existence of lateralization of brain potentials in different types of cognitive activity. Although various 'verbal-analytic' and 'spatial' tasks lasting one minute or more have been associated with relative left and right hemisphere activity, it is not clear whether this is due to cognitive activity, or to stimulus, motor, or arousal-related aspects of the tasks (Donchin, et al, 1977; Gevins and Schaffer, 1980; Gevins, et al, 1980; Gevins, 1983ab). In an earlier study (Gevins, et al, 1979abc), we first found prominent spatial differences, including lateralized patterning of EEG spectra, between one minute linguistic and spatial tasks (reading and writing, Koh's Block Design and mental cube reconstruction). However, no spatial differences in EEG spectra were found between similar 15 second tasks which were more controlled for other-than-cognitive factors. Since heterogeneous tasks composed of many component operations cannot be clearly resolved into serial processes, our subsequent study (Gevins, et al, 1981) refined the approach. It used short (less than 1 second) visuomotor tasks differing only in type of judgment (numeric and spatial), employed 175-msec analysis intervals based on person-specific ERP measurements, and used measures of between-channel correlations in single trials as features for NCP Analysis. That study revealed that even split-second judgments involve a complex, rapidly shifting mosaic of task-related evoked correlation patterns involving many electrodes over both hemispheres. Thus, simplistic views of neurocognitive processing may be the result of inadequate temporal resolution of rapidly changing neural activity.

The present study confirmed this by comparing move and no-move variants of the same spatial task. The results suggest that the tasks involve split-second changes in the relative localization and

lateralization of neural activity. A dramatic switching of the foci of patterns of evoked correlations is seen as the stimulus is anticipated, perceived, judged, and a response executed. These rapidly shifting patterns are consistent with network models of higher cognitive functions (Luria, 1977; Arbib and Caplan, 1979; Zurif 1980; Mesulam, 1981; and Gevins, 1981, 1983b). It should be understood that the simplicity of the patterns reported (Figure 6) is due to the fact that only the most significant results were diagrammed. The inclusion of results at lower significance levels would create more complex patterns, particularly in the RP interval. Further, in a separate within-task analysis, where each post-stimulus interval was compared with its prestimulus interval, it was evident that within-task differences were complex and increased in magnitude and anatomic distribution from interval to interval. This is consistent with a within-task interlatency analysis reported previously (Gevins, et al, 1981).

Individual Differences

Although the classification accuracies of the overall (multiperson) classification equations assessed on the data of the individual participants varied appreciably (Table 6), the existence of some invariant task-related patterns in 7 of the 9 persons was confirmed. The fact that the significant difference between tasks was also found at the P4 electrode set in the P3a interval when the data of one-person was subjected to NCP analysis also supports the inference of patterns which are invariant across people. Moreover, a nonparametric randomization test performed on the individual classification accuracies of the two groups of P's (#1-5 and #6-9) confirmed that the classification equations did not significantly differ between the two groups.

Is NCP Analysis Useful?

Analytic methodology is a critical factor in determining the precision and relevance of results in brain potential studies. NCP analysis uses modern signal processing and pattern recognition technologies to distinguish spatially and temporally overlapping task-related brain potential patterns. It builds on the vast body of ERP research by using the average ERP to determine person-specific time intervals during which successive stages of task-related processing may be assumed to occur. It then searches the single-trial, multichannel brain potential data with a mathematical pattern classification algorithm to extract spatial patterns which distinguish the two conditions of an experiment. As with other advanced approaches (reviewed in McGillem, et al, 1981 and Gevins 1980), it has the potential to reveal information not obtainable from averaged waveforms. Further studies will determine whether NCP analysis produces results meaningful enough to justify the large amount of computation required.

A full comparison of NCP analysis with linear multivariate methods is beyond the scope of this paper. Two linear tests were performed to give some indication of the differences between methods: post-hoc task x electrode-pair ANOVAs on selected variables, and the Bonferroni-corrected t-tests on the full set of single-trial correlations. The ANOVAs were limited to the 10 correlations of the most significant electrode sets determined NCP analysis: the P4 set in the P3a interval and the C3 set in the RP interval. Only the electrode-pair effect reached significance ($F(14,72) = 57.9$, $p<<.001$ and $F(14,72) = 48.6$, $p<<.001$, respectively). There was no significant task main effect or task x electrode-pair interaction. This result and the results of the t-tests (Table 4) suggest that the variable subset selection and the nonlinear, distribution-independent properties of the NCP Analysis were both important. This is consistent with two previous studies where this type of mathematical pattern recognition proved more effective than ANOVA and stepwise linear discriminant analysis (Gevins, et al, 1979a; Lieb, et al, 1981). Although the Bonferroni-corrected t-tests were significant for only two electrode pairs in one interval, at uncorrected significance levels ($p<.05$ or better), the significant electrode pairs did show a slight similarity to the NCP results. Of the significant Fz pairs in the prestimulus interval, 3 are identical to the prominent correlations determined by NCP Analysis (Fz-C3, Fz-C4 and Fz-T3), and the frontal distribution of significant pairs accords with the distinguishing Fz electrode set in the NCP results. For the N1-P2 and P3a intervals, however, only the T4-Pz electrode pair in the former interval and the P4-C4 pair in the latter correspond to prominent evoked correlations of the NCP analysis. In the RP interval the t-tests were focused on the frontal areas and included only two significant pairs from the NCP results (C3-Fz and C3-Pz).

In its present form, NCP Analysis seems able to extract patterns of task-related evoked differences from the obscuring effects of volume conduction and background EEG. Further research is being conducted using measures of interchannel timing and single channel power in paradigms involving manipulation of modality and responding hand. These studies may help elucidate the significance of inter-electrode evoked correlations accompanying neurocognitive processes.

ACKNOWLEDGEMENTS

H. Currens for manuscript preparation and artwork. H. Vaughan, D.O. Walter and C. Woods for critical reviews. E. Callaway of the Langley Porter Institute, D. Woodward of the Office of Naval Research, A. Fregly of the Air Force Office of Scientific Research, J. Miller of the Air Force School of Aerospace Medicine, and M. Brachman-Hoffman for research support.

BIBLIOGRAPHY

Arbib, M. and Caplan, D. Neurolinguistics must be computational. Behavioral and Brain Sciences, 1979, 2, 449-483.

Brazier, M. and Casby, J. Crosscorrelation and autocorrelation studies of electroencephalographic potentials. Electroencephalography & Clinical Neurophysiology, 1952, 4, 201-211.

Busk, J. and Galbraith, G. EEG correlates of visual-motor practice in man. Electroencephalography & Clinical Neurophysiology, 1975, 38, 415-425.

Callaway, E. and Harris, P. Coupling between cortical potentials from different areas. Science, 1974, 183, 873-875.

Desmedt, J. Active touch exploration of extrapersonal space. Proc. National Academy of Science, 1977, 74(9), 4037-4040.

Donchin, E., Kutas, M., and McCarthy, G. Electrocortical indices of hemispheric utilization. In S. Harnad et al. (Eds.), Lateralization in the Human Nervous System. New York, NY: Academic Press, 1977. Pp. 339-384.

Dumenko, V. Electroencephalographic investigation of cortical relationships in dogs during formation of a conditioned reflex stereotype. In Rusinov, V. (Ed.), Electrophysiology of the Central Nervous System, New York:Plenum Press, 1970.

Friedman, D., Vaughan, H. and Erlenmeyer-Kimling, L. Stimulus and response related components of the late positive complex in visual discrimination tasks. Electroencephalography & Clinical Neurophysiology, 1978, 45, 319-330.

Fuster, J. The Prefrontal Cortex. New York:Raven Press, 1980.

Gevins, A. and Yeager, C. EEG spectral analysis in real time. OECUS Proceeding, Maynard, Mass:Spring, 1972. Pp. 71-80.

Gevins, A., Yeager, C., Diamond, S., Spire, J., Zeitlin, G., and Gevins, G. Automated analysis of the electrical activity of the human brain (EEG): a progress report. IEEE Proceedings, 1975, 63(10), 1382-1399.

Gevins, A., Zeitlin, G., Yingling, C., Doyle, J., Dedon, M., Henderson, J., Schaffer, R., Roumasset, J. and Yeager, C. EEG patterns during cognitive tasks: I. Methodology and analysis of complex behaviors. Electroencephalography & Clinical. Neurophysiology, 1979(a), 47, 693-703.

Gevins, A., Zeitlin, G., Doyle, J., Schaffer, R. and Callaway, E. EEG
patterns during cognitive tasks, II. Analysis of controlled tasks. Electroencephalography & Clinical Neurophysiology, 1979(b), 47, 704-710.

Gevins, A., Zeitlin, G., Doyle, J., Schaffer, R., Yingling, C., Yeager, C. and Callaway E. EEG Correlates of higher cortical functions. Science, 1979(c), 203, 665-668.

Gevins, A. and Schaffer, R. Critical review of research on EEG correlates of higher cortical functions. CRC Reviews in Bioengineering, CRC Press, October 1980. Pp. 113-164.

Gevins, A., Doyle, J., Schaffer, R., Callaway, E. and Yeager, C. Lateralized cognitive processes and the electroencephalogram. Science, 1980, 207, 1005-1008.

Gevins, A. Pattern recognition of human brain electrical potentials. IEEE Transactions on Pattern Analysis and Machine Intelligence, 1980, PAMI-2(5), 383-404.

Gevins, A., Doyle, J., Cutillo, B., Schaffer, R., Tannehill, R., Ghannam, J., Gilcrease, V. & Yeager, C. New method reveals dynamic patterns of correlation of human brain electrical potentials during cognition. Science, 1981, 213, 918-922.

Gevins, A. Dynamic brain electrical patterns of cognition, in Third IEEE Conf. Eng. Med. Biol, New York:IEEE Press, 1981.

Gevins, A. Brain potentials and mental function: methodological requirements. In I. Alter (Ed.), The Limits of Functional Localization, New York:Raven Press, 1983a, In press.

Gevins, A. Brain potential evidence for lateralization of higher cognitive functions. In Cerebral Hemisphere Asymmetry: Method, Theory and Application. J. B. Hellige (Ed.), Praeger Press, 1983b, In press.

Gevins, A., Schaffer, R., Doyle, J., Cutillo, B., Tannehill, R. and Bressler, S. Shadows of thought: Shifting lateralization of human brain electrical patterns during a brief visuomotor task. Science, 1983(a), 220, 97-99.

Gevins, A., Doyle, J., Zeitlin, G., Bressler, S. A trainable classification network algorithm for studying brain potential patterns of higher cognitive functions. IEEE Transactions on Pattern Analysis and Machine Intelligence, 1983(b), In Prep.

Lieb, J., Engel, J., Gevins, A., and Crandall, P. Surface and depth EEG correlates of epileptic foci and surgical outcome in temporal lobe epilepsy. Epilepsia, 1981, 22, 515-538.

Livanov, M. Spatial Organization of Cerebral Processes. New

York:Halsted (Wiley), 1977.

Luria, A. Higher Cortical Functions in Man. New York:Basic Books, 1977.

McGillem, C., Aunon, J. and Childers, D. Signal processing in evoked potential research. CRC Review in Bioengineering, 1981, 6(3), 225-265.

Mesulam, M. A cortical network for directed attention and unilateral neglect. Ann. Neurol. 1981, 10(4), 309-325.

Naatanen, R., Hukkanen, S. and Jarvilehto. Magnitude of stimulus deviance and brain potentials. In H. Kornhuber and L. Deeke, (Eds.) Motivation, Motor and Sensory Processes of the Brain: Electric Potentials, Behavior and Clinical Use, Amsterdam:Elsevier, 1980.

Renault, B., Ragot, R., Lesevre, N. and Remond, A. Onset and offset of brain events as indices of mental chronometry. Science, 1982, 215, 1413-1415.

Ritter, W., Vaughan, H. and Simson, R. On relating event-related potential components to stages of information processing. In Gaillard, A. and Ritter, W. (Eds.), Tutorials in Event-Related Brain Research, Amsterdam:Elsevier, 1983.

Simson, R., Vaughan, H., and Ritter, W. Scalp topography of potentials in auditory and visual go/no-go tasks. Electroencephalography & Clinical Neurophysiology, 1977, 43, 864-875.

Squires, K., Donchin, E., Herning, R., and McCarthy, G. On the influence of task relevance and stimulus probability on event-related potential components. Electroencephalography & Clinical Neurophysiology, 1977, 42, 1-14.

Teuber, H. The riddle of frontal lobe function in man. In M. Warren and K. Abert (Eds.), Frontal Granular Cortex and Behavior, New York:McGraw-Hill, 1964. Pp. 410-477.

Viglione, S. Applications of pattern recognition technology. In J. Mendel and k. Fu (Eds.), Adaptive Learning and Pattern Recognition Systems. New York:Academic Press, 1970. Pp. 115-161.

Walter, W. Slow potential changes in the human brain associated with expectancy, decision and intention. Electroencephalography & Clinical Neurophysiology (Suppl.), 1967, 26, 123-130.

Walter, W. and Shipton, H. A new toposcopic display system. Electroencephalography & Clinical Neurophysiology, 1951, 3, 281-292.

Zurif, E. Language mechanisms: A neuropsychological perspective. American Scientist, 1980, 68, 305-310.

LEGENDS

Figure 1 - Examples of stimuli for move and no-move trials. Arrow originated at center screen; its direction and the location of the target changed randomly across trials. The labels "Move" and "No-Move" did not appear in the actual stimuli.

Figure 2A - Electrode montage.

Figure 2B - 91 pairwise correlations were computed between the 15 electrodes.

Figure 2C - Anatomical constraints. The correlations of a principal electrode was measured with 10 other electrodes. The aOz electrode set is shown.

Figure 3 - The major peaks of the average event-related potential (ERP) and Neurocognitive Pattern (NCP) Analysis intervals determined from them. This illustration is an average of the data from the last four persons in the study; in practice, the peaks and analysis intervals were determined separately for each person.

Figure 4a - ERPs for Move trials (610 trials from P's #6-9).

Figure 4b - ERPs for No-Move trials (604 trials from P's #6-9).

Figure 5 - Subtraction ERP's (No-Move minus Move, 6 P's) showing the negative (N2) peak at 240 msec.

Figure 6 - Between-task NCP results obtained from single trial evoked correlations. The most significantly differing electrode set and its prominent correlations are shown in each interval.

Figure 7a - Average right parietal ERP of those Move trials correctly classified by the NCP analysis in both the P3a and RP intervals using correlation measures (195 trials from 4 people).

Figure 7b - Average ERP of correctly classified No-Move trials. P391 (P3a) and P530 (P3b) peaks are larger in the correctly classified No-Move trials (193 trials from 4 people).

Figure 7c - Average ERP of incorrectly classified, but behaviorally correct, Move trials (122 trials from 4 people).

Figure 7d - Average ERP of incorrectly classified, but behaviorally correct, No-Move trials. P3a is absent and P3b is smaller, thus resembling the correct Move ERP (121 trials from 4 people).

Table 1 - Number of trials, ERP peak latencies, centerpoints of the NCP single trial correlation analysis intervals, and average response

initiation latency (EMG onset) for each of the 9 participants.

Table 2 - Averaged P3a peak amplitude (in micro-volts) and correlated t-tests (df = 9).

Table 3 - Response Preparation (RP) interval: averaged slope of a straight line fitted to slow negative potential shift and correlated t-tests (df=9).

Table 4 - t-tests of correlations for the nine participants (1612 trials: 839 Move, 773 No-Move). Only those channel pairs showing a significant uncorrected t-value are listed. ($p<.05$ = 1.96, $p<.01$ = 2.57, $p<.001$ = 3.29. *Bonferroni-corrected t-value of 3.58 = $p<.05$.)

Table 5 - Simplified, single discriminant function classification equation. G(f) =1 for f>0, else G(f) =0; (X/Y) is the standardized, Fisher's z' transformed correlation value of the X-Y electrode pair. Individual trials whose classification function G(f) = 1 were assigned to the no-move class; those whose G(f) = 0 to the move class.

Table 6 - Classification accuracy for the P3a and RP intervals for each of the 9 participants using the equations derived from the whole group.

P	# Trials		ERP peaks (msec)			Analysis intervals centerpoint			EMG onset (msec)
	Move	No Move	N_1	P_2	No-Go P_{3a}	N_1-P_2	P_{3a}	RP	
1	42	33	164	236	452	218	452	587	971
2	36	36	164	236	388	200	388	523	913
3	39	30	176	243	482	228	482	617	791
4	42	39	164	236	462	210	462	597	1128
5	42	39	164	241	398	203	398	533	638
6	156	144	172	222	298	208	298	433	434
7	132	123	164	225	368	212	368	503	570
8	182	167	143	214	318	181	318	453	500
9	168	162	157	214	358	203	358	493	507
[illegible]	(Total) 839	773	163	230	391	207	391	526	$\bar{x}$=590 SD.=190

Table 1

Psych. 83 —June 7

	Average P3a Amplitude (μv)		Correlated $\underline{t}$	Uncorrected P<
	Move	No Move		
F_z	1.3	2.90	-2.95	.01
aCz	-.26	1.69	-2.91	.01
C_z	-.80	1.53	-3.16	.01
aPz	.14	2.30	-5.34*	$5x10^{-4}$
P_z	.49	2.32	-4.77*	.005
aO_z	-.94	0.34	-2.28	.05
C_3	-.62	1.82	-3.82	.005
C_4	-.17	2.12	-4.44 *	.005
P_3	-.39	1.94	-2.97	.01
P_4	-.80	1.11	-3.05	.01

* Bonferroni $\underline{t}$ (15 comparisons, df = 7, $p<.05$ = 4.35

Table 2

	Average Slope RP Interval		Correlated t	Uncorrected P<
	Move	No Move		
Fz	.24	-.18	1.09	N.S.
aCz	.17	-.48	2.80	.05
Cz	.07	-.82	2.30	.05
aPz	.00	-.51	2.14	.05
Pz	-.03	-.69	2.10	.05
aOz	-.17	-.35	1.9	.05
C3	.24	-.50	3.5	.005
C4	.62	-.54	3.0	.01
P3	-.01	-.58	2.8	.05
P4	-.11	-.69	2.2	.05

* Bonferroni t (15 comparisons, df = 7) $p < .05 = 4.35$

Table 3

Correlation Electrode Pair	t Prestimulus Interval	t N_1 - P_2 Interval	t P_{3a} Interval	t RP Interval
F_z - F_7				2.24
F_z - F_8			2.88	
F_z - T_3	2.38			
F_z - C_3	3.12			2.42
F_z - C_4	2.60			2.08
F_z - P_3				2.16
F_z - pFz				2.58
F_z - aCz	2.38			
F_z - C_z	2.35			2.43
F_z - aPz				2.38
F_z -aOz				2.46
F_8 -aCz	2.08		2.37	2.70
F_8 - P_z				3.13
F_8 - P_3				3.30
F_8 - P_4				3.16
T_4 - P_z		2.11		
P_4 - C_4		2.47	2.94	
aCz - C_3	2.60			
T_4 - T_3	2.29			
C_4 - C_3	2.17			
F_7 - C_3				3.20
F_7 - T_3				3.72*
F_8 - aFz			2.58	2.63
F_8 - C_z			2.50	3.34
F_8 - aPz				3.82*
F_8 -aOz				3.29
F_8 - C_4				3.56
aCz - C_z			2.09	
aPz - C_3				2.80
P_z - C_3				3.01
P_3 - T_4		2.22		
P_4 - C_3				2.51
T_4 - aPz		2.13		2.38
T_4 - C_4				2.70
T_4 - P_4				2.17

Table 4

*Bonferroni-corrected t; (100 comparisons, df = 120, $p < .05 = 3.58$)

Interval	Classification Equation
Prestimulus	G[-.089(Fz/T3)-.183(Fz/C4)+.355(Fz/P3)-.438(C3)]
N1 — P2	G[.336(Pz/T3)-.471(Pz/F7)+.233(PzT4)-.130(Pz/aCz)
$P3_a$	G[-.323(P4/aOz)+.573(P4/C4)-.270(P4/aCz)
RP	G[-.697(C3/Pz)+.319(C3/Fz)+.480(C3/aOz)]

Table 5

Interval \ P	1	2	3	4	5	6	7	8	9	whole group
P_{3a}	64.4	55.0	53.2	51.7	55.1	52.5	58.7	51.5	54.4	55.1
RP	62.8	64.6	47.0	43.9	64.2	58.7	52.0	58.8	60.2	55.6

Table 6

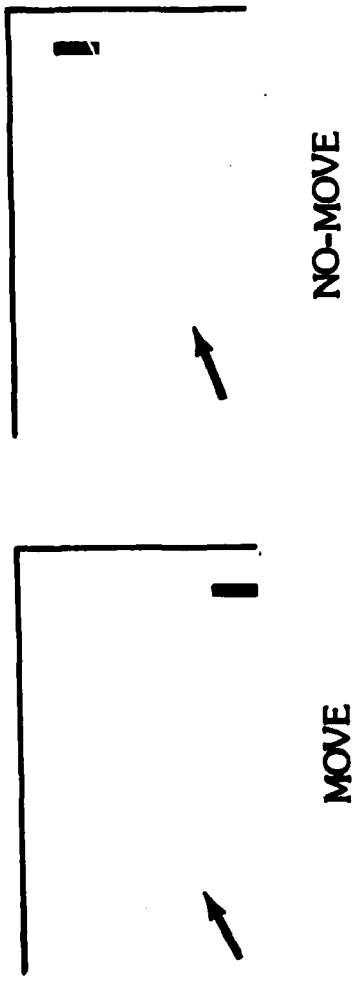

Fig. 1

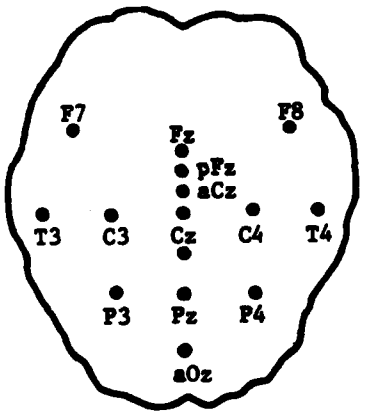

Fig. 2A

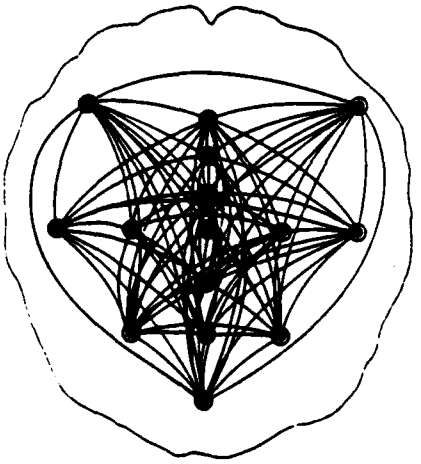

Fig. 2B

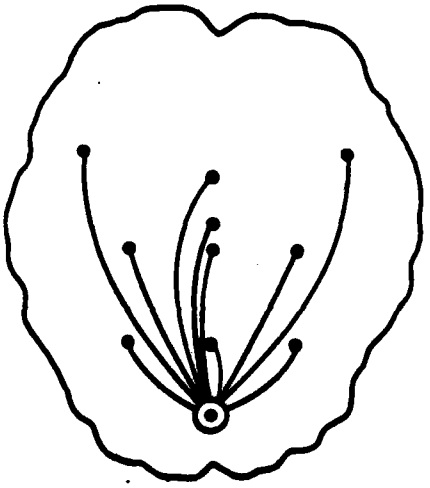

Fig. 2C

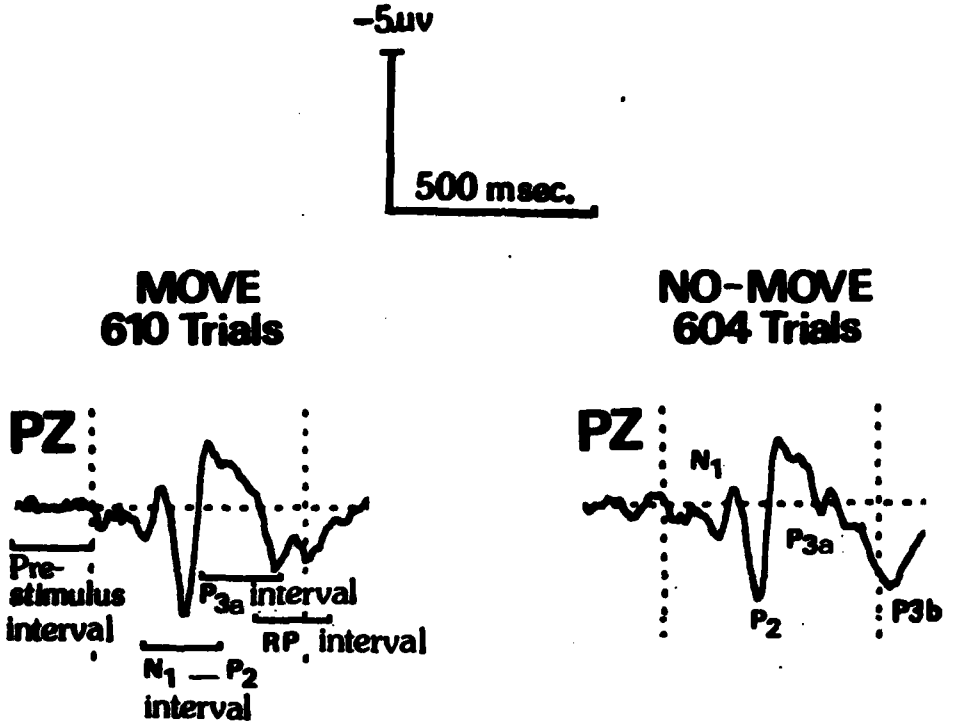
-5uv
500 msec.
MOVE
610 Trials
NO-MOVE
604 Trials
PZ
Pre-
stimulus
interval
P3a interval
RP interval
N1 — P2
interval
PZ
N1
P3a
P2
P3b

Fig. 3

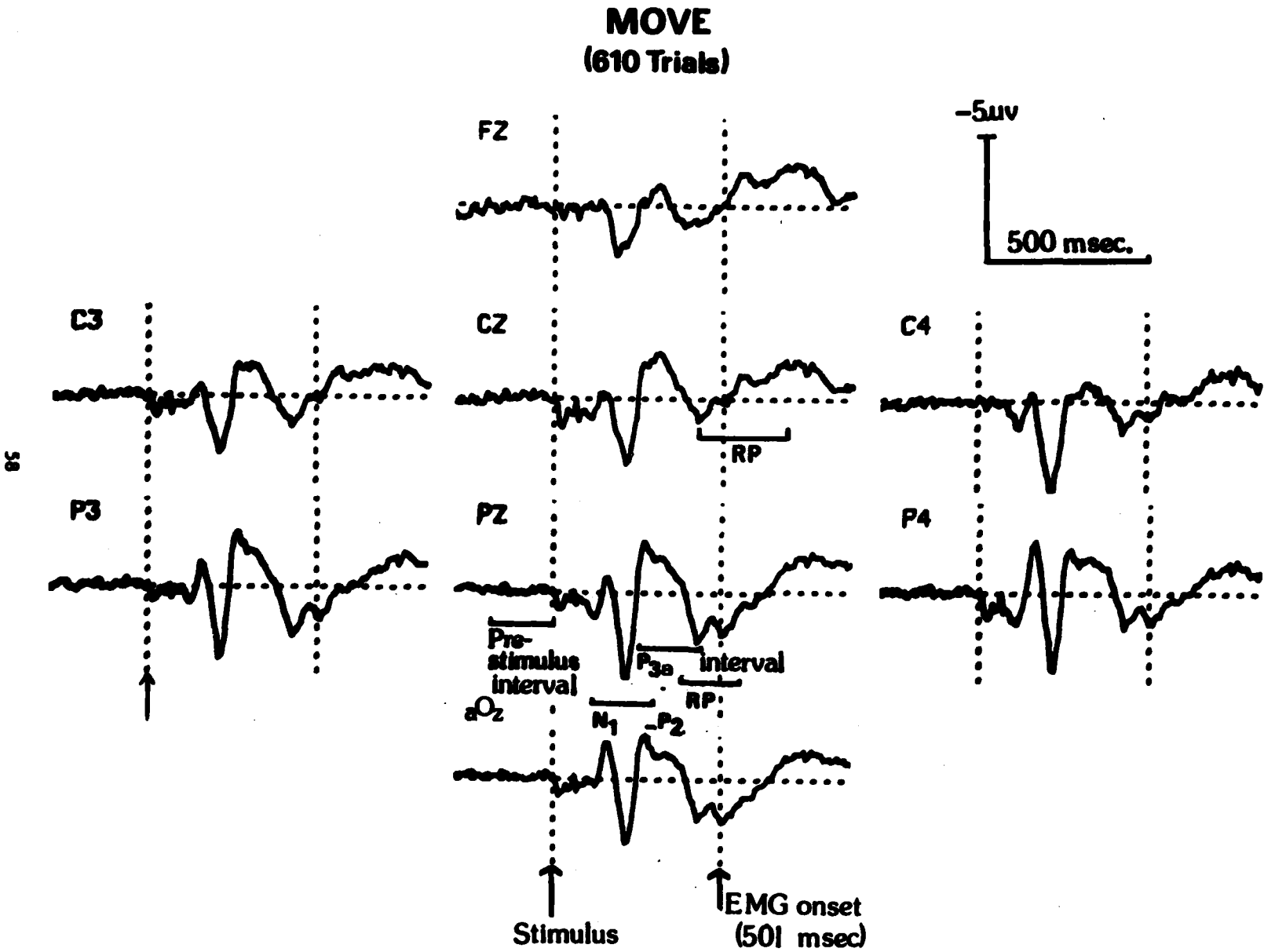
MOVE
(610 Trials)
FZ
-5μv
500 msec.
C3
CZ
C4
RP
SS
P3
PZ
P4
Pre-
stimulus
interval
P3a
interval
RP
EOG
N1
P2
Stimulus
EMG onset
(501 msec)

Figure 4a

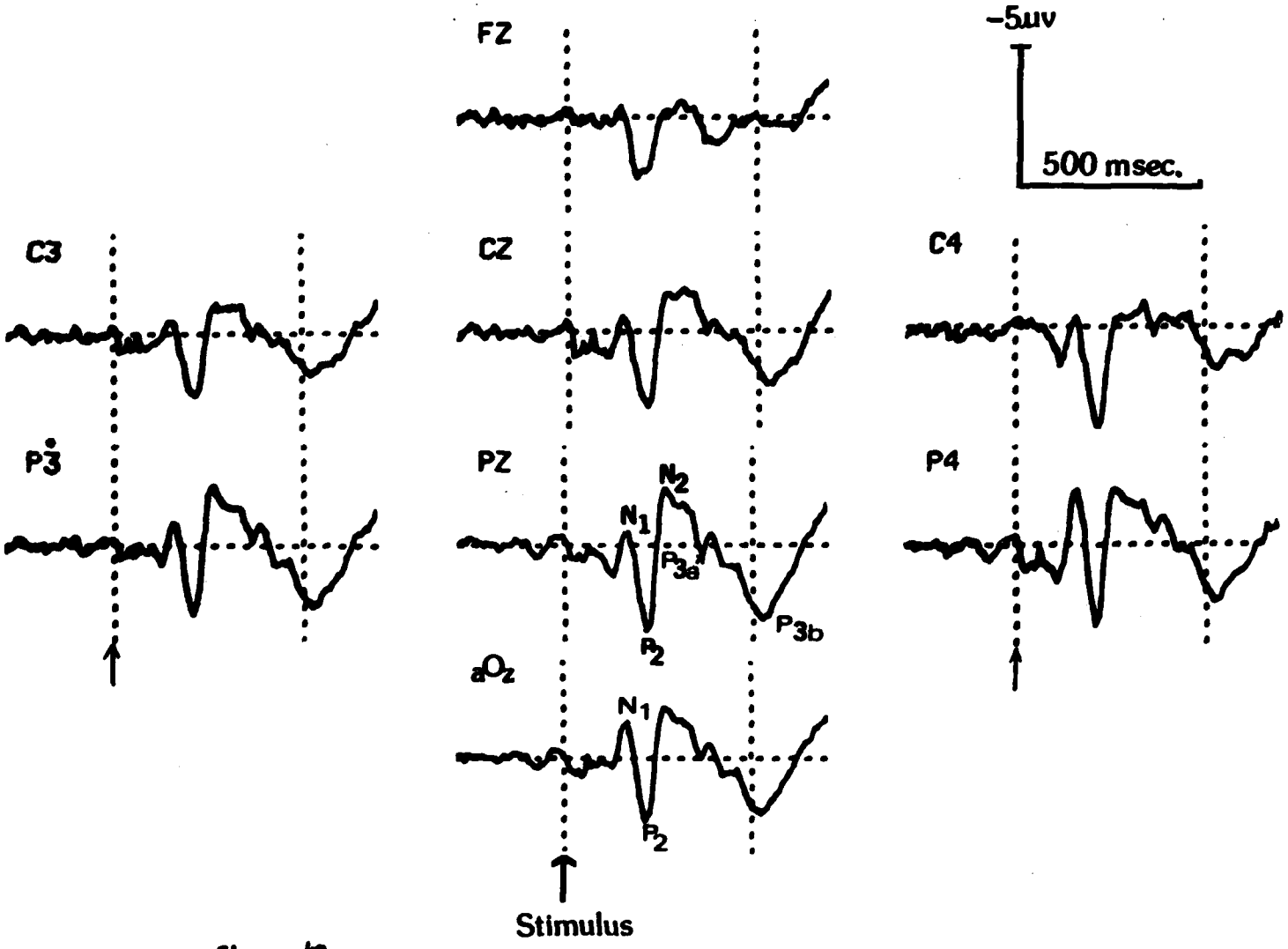
NO-MOVE
(604 Trials)
-5μv
500 msec.
FZ
C3
CZ
C4
P3
PZ
P4
N2
N1
P3a
P3b
P2
aO2
N1
P2
Stimulus

Figure 48

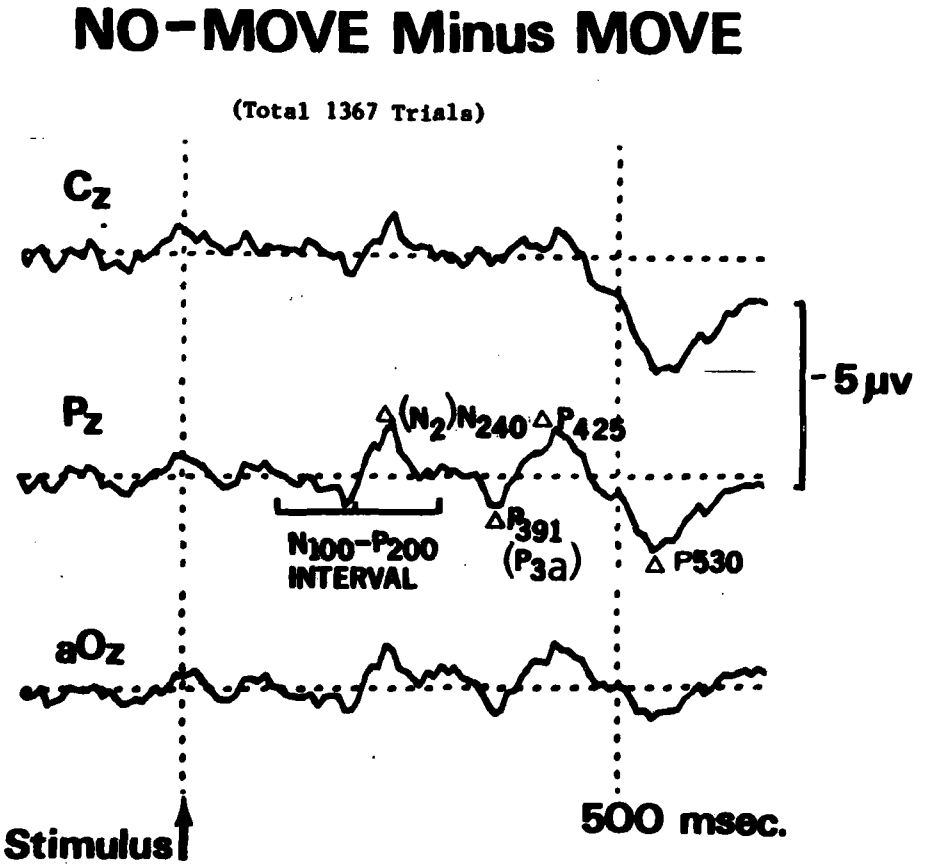
NO-MOVE Minus MOVE
(Total 1367 Trials)
Cz
Pz
aOz
-5 µv
Δ(N2)N240
ΔP425
ΔP391
(P3a)
N100-P200
INTERVAL
ΔP530
Stimulus
500 msec.

Figure 5

MOVE vs. NO-MOVE
(NCP Analysis)

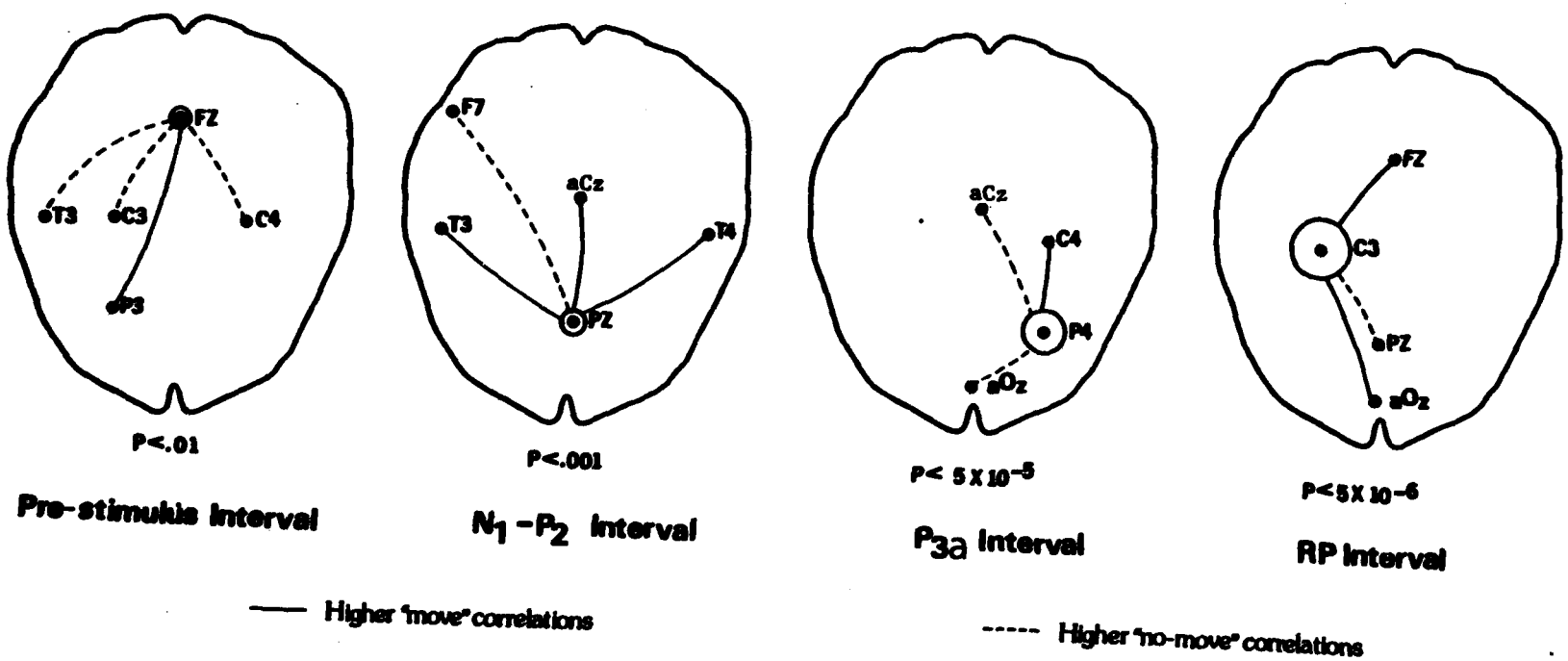

Figure 6

V. SIGNAL PROCESSING STUDIES (Also Sponsored by the Office of Naval Research and the USAF School of Aerospace Medicine)

A. Introduction

In order to further understand the signals extracted in the move/no-move visuospatial experiment (Sections III and IV), we are attempting to determine which type of measurements and frequency bands have the most specific task-related information. Preliminary results of these ongoing studies are presented in this section. We began by digitally filtering the single-trial brain potential timeseries into five passbands determined from Fourier analysis of each person's average ERPs. This was based on the strategy that mass brain potentials of different frequency bands might have different types of information. This resulted in separate 'delta', 'theta', and low and high 'alpha', and 'beta' frequency band timeseries for each person. Then, using brief analysis intervals centered at latencies determined from the peaks of each person's average ERPs, four types of measurement were made on the timeseries of each frequency band: 1) maximum covariance between a pair of channels, 2) lag-time to maximum covariance, 3) shape of the lagged covariance function, and 4) single channel power. These measurements were then used as features in a between-task pattern recognition analysis, and the relative classification accuracy obtained with each measure was used as an index of its usefulness.

B. Methods

The analysis was confined to the data of the last four of the original nine people (see Table I in Section IV). Three of the four were Air Force fighter test pilots, while the fourth was formerly a transport pilot. All were highly-trained individuals who demonstrated a professional motivation towards the experiment and produced data of superior quality. The analysis was confined to the time windows and channel pairs in which highly significant between-task differences in results had been obtained using the zero lag correlation measure: the three right parietal (P4) electrode-pairs in the P3a interval and the three left central (C3) electrode-pairs in the response preparation (RP) interval (see Fig. 6 in Section IV).

For the NCP analysis each of 3 training sets contained 804 trials and each of 3 testing sets contained 402 trials (total trials = 1206). Optimal feature subsets were selected by exhaustive search. Pattern classification accuracy was the average of the performance of the equations on the 3 testing data sets. The classification accuracy for each significance level is shown in Table 4. For each significant result, terms of the equation having weights exceeding a threshold of 15% of the maximum weight of the largest term were selected for display.

1. Measures

Zero-lag correlation was replaced by several covariance-derived measures to determine whether useful information was discarded in the normalization involved in the correlation measure. The entire covariance function, rather than just the zero-lag value, was considered to test for information in the timing of the ERPs (Figures 4 to 6). Each covariance function was formed by lagging the signals ±6 time points (48 msec). Lag values were computed from extended real data points, rather than from an increasing number of zeros as done in the noncyclic fast convolution (FFT) method.

As a preliminary step, spectral analysis and bandpass filtering were performed on the averaged ERP for each person. Three non-overlapping FFT's were performed for the 0.5 second prestimulus and two 0.5 second post-stimulus windows for each averaged ERP channel for each person. A histogram was formed from spectral frequencies over each channel (Figure 7) and used to determine passband widths for each person. Unfiltered average ERPs for one person are shown in Figure 8a. Filtered ERPs, with passbands selected from Figure 7, are shown in Figures 8b-h.

Covariance was computed between two filtered single trials , X(t) and Y(t), using the raw score method:

$$C_{XY}(\tau) = \left[N \sum^{N} X(t)Y(t) - \sum^{N} X(t) \sum^{N} Y(t)\right] / N^2$$

where N is the number of points in the time window. Three features were derived from the covariance function. The first was the maximum (absolute) value of the covariance function. The second was the lag time at the peak of the covariance function, employed to measure the relative timing of signals between channels. Since this peak lag measure was likely to be unstable, a third measure was used to assess inter-electrode timing. This was a lagged covariance function 'shape measure,' computed as the similarity of the lagged covariance function to a cosine function. Since the cosine is an even function, this measure would indicate the tendency of one channel in a pair to lead or lag the other. The frequency of the cosine used was the center frequency of the passband used to filter the ERP forming the covariance function. The 'shape measure' was computed as the sum of cross-products between the points of the covariance function and the cosine function. The sum was divided by the maximum absolute cross-product to equalize the range across frequency bands. This measure was expected to be more stable than the lag-to-peak measure since it is derived from all points in the covariance function rather than just one. The fourth measure was single channel power, computed as the mean square value of the filtered timeseries over the points of the time window.

2. Channels

In the between-task results of the earlier analysis (Sections III and IV) correlations of the right parietal (P4) electrode distinguished the move vs no-move tasks in the P3a interval with greatest accuracy.

The three correlations which contributed most to this discrimination were P4-aOz, P4-C4, and P4-aCz. Likewise in the RP interval, C3-aOz, C3-Pz, and C3-Fz were most effective in distinguishing the tasks. Consequently these six channel pairs were used in the present study. In the P3a interval, the C3 pairs were used as controls, and in the RP interval the P4 pairs were controls.

Single channel power was computed for the seven channels which formed these pairs, as well as for the P3 electrode to preserve symmetry in the eight-channel power analysis.

3. Time intervals

The P3a interval was determined individually for each of the four people so that it straddled the P3a component of each individual's averaged ERP. The RP interval was centered at the time of onset of the response, as measured by the average EMG onset for each person.

The width of the analysis intervals varied with the frequency band in order to accommodate at least one full cycle of the highest frequency component in a given band. For reasons of stability of the measures, 100 msec was the shortest window width. For the delta band the windows were 200 msec wide, for the theta band they were 175 msec, and for the three higher bands they were 100 msec.

Each single-trial timeseries was separately filtered into five frequency bands before other computations were performed. The average bandpass settings were 0-4 Hz (delta), 4-8 Hz (theta), 8-11 Hz (low alpha), 11-15 (high alpha), and 15-22 Hz (beta). Exact settings were individually set for each person based on Fourier analysis of their averaged ERPs. Linear phase, Hamming FIR filters were employed. They were convolved with the timeseries by a fast convolution (via FFT) using the overlap-save method.

C. Results

1. Crosscovariance Measures

Using the maximum covariance measure, the pattern classification analysis was able to differentiate the two tasks in the P3a interval using the P4 electrode-pair covariances ($p<5 \times 10^{-4}$) (Figure 9), but was unable to do so using the C3 electrode-pair (control) covariances. The algorithm was allowed to combine frequency bands to achieve optimum classification. The major features which it used were from the delta and theta bands. In Figures 9 and 10, a solid line connecting two electrode sites indicates that the value for the move task was greater, a dashed line that it was greater for the no-move task. A previous analysis in this interval, using the .1-12 Hz band, zero-lag correlation for the same three P4 electrode pairs, discriminated the tasks with significance of only 1×10^{-3}. Therefore greater discrimination was achieved by definition of the frequency range, by using covariance rather than correlation, and by shifting the time series in time to find their maximum covariance.

In the RP interval, the two tasks were successfully classified by the C3 electrode-pair covariances ($p<5 \times 10^{-5}$) (Figure 9), but not the control (P4) electrode-pair covariances. Again the major features were from the delta and theta bands. Although this classification significance was high, it was below that of the previous zero-lag correlation study.

The lag-to-maximum covariance was not successful in significantly discriminating tasks, presumably because of the instability of this measure without thresholding.

Using the shape lagged covariance measure in the P3a interval, the P4 pairs classified the trials ($p<1 \times 10^{-4}$) (Figure 10), whereas the control pairs did not. Shape measures from the delta and beta band were the major ones used. In the RP interval, the shape measure of the C3 pairs classified the trials ($p<10^{-4}$), but the controls did not. The major features were in the theta band.

2. Single-Channel Power Measures

For the power measures, P4, C4 and a0z were used for the P3a interval, P3, C3 and a0z for the RP interval. In the P3a interval the algorithm was unable to discriminate the tasks with these channels. In the RP interval, the delta band was used to discriminate at $p<.001$ (Figure 11) compared to $p<.05$ for controls. In Figures 11 and 12, an upward arrow indicates that the move task power was greater, a downward arrow that no-move power was greater.

Another analysis was performed with the power measure from eight channels. Separate analyses were performed for each of the five frequency bands (Figure 12).

In the RP interval discrimination was achieved in the delta band at ($p<1 \times 10^{-4}$), using channels C3, Pz, a0z and aCz most strongly. For the theta band, discrimination was achieved in both the P3a ($p<5 \times 10^{-4}$) and RP ($p<1 \times 10^{-2}$) intervals. In the P3a interval, a0z, aCz, C3, C4 and Fz were the main channels used; and in the RP interval it was P4, Pz and Fz. For the low alpha band, discrimination was achieved in the RP interval at $p<5 \times 10^{-2}$, using Pz, C3 and P4. For the high alpha band discrimination in the RP interval was at $p<5 \times 10^{-4}$ using aCz and Fz. Discrimination was not achieved for beta band power in either interval. In general, the direction of the between-task difference in power was not the same for a given channel in the different frequency bands.

D. Conclusions

These preliminary results suggest somewhat that the between-tasks differences in inter-electrode correlations and covariances may not be due solely to volume conduction of potentials from a single distant generator. First, there was discriminatory information in the maximum covariance measure, which was often found at non-zero lags. Second, there was information in the shape of the lagged covariance function

which was sensitive to the phase relation between two signals. Third, when the power measure of a channel was greater for one task, power on a highly correlated channel was seen to be lower for that task. For example, the C3-a0z covariance was greater for move than no-move task in the delta band (Figure 9). In this case, a0z delta power was greater for the move task, but C3 delta power was lower (Figure 12). If correlation was due solely to volume conduction from a single generator, power for both correlated channels would show the same between-task variation. Of course, the suggestion that separate generators contribute to the reported between-task differences in scalp correlation patterns is mere speculation. Further studies will be required to determine if this is actually so and if pairwise interchannel measures are the best way to characterize the activity of such generators.

Significant differences between tasks were found to be specific to certain frequency bands. In particular, all covariance-derived measures were significant only in the delta, theta and beta bands. In some cases (e.g. the shape measure in the RP interval) a measure differentiated the tasks in only one band. Only for the power measure was there any discrimination in the alpha bands.

Specificity was also achieved in the type of measure which distinguished the tasks. Zero-lag correlation depends on the timing of two signals as well as their similarity. These two aspects were separated in the lag and shape measures on the one hand, and the maximum covariance on the other. These measures were found to have different abilities to discriminate in the different frequency bands. Since the between-channel covariance measures differentiated tasks differently than the power measures, such measures may provide information about the brain which complements that obtained from power measures.

Further investigation is proceeding in several ways. An improved shape measure which carries information as to lead or lag between channel pairs has been developed. An improved single channel power analysis will make more explicit the similarities and differences between single and multichannel measures. Additional studies will fill in the gaps in the present study from non-lagged correlations to lagged covariances.

significance ($p \leq$)	% accuracy
5×10^{-2}	52.4
1×10^{-2}	53.4
5×10^{-3}	53.8
1×10^{-3}	54.5
5×10^{-4}	54.8
1×10^{-4}	55.4
5×10^{-5}	55.6
1×10^{-5}	56.2
5×10^{-6}	56.4
1×10^{-6}	56.9

Table 4 - Classification accuracy at different significance levels. (1206 trials from 4 persons)

DELTA BAND COVARIANCE - MOVE

SSS 1-4, 260 TRIALS, 1-4 HZ, P3a INTERVAL

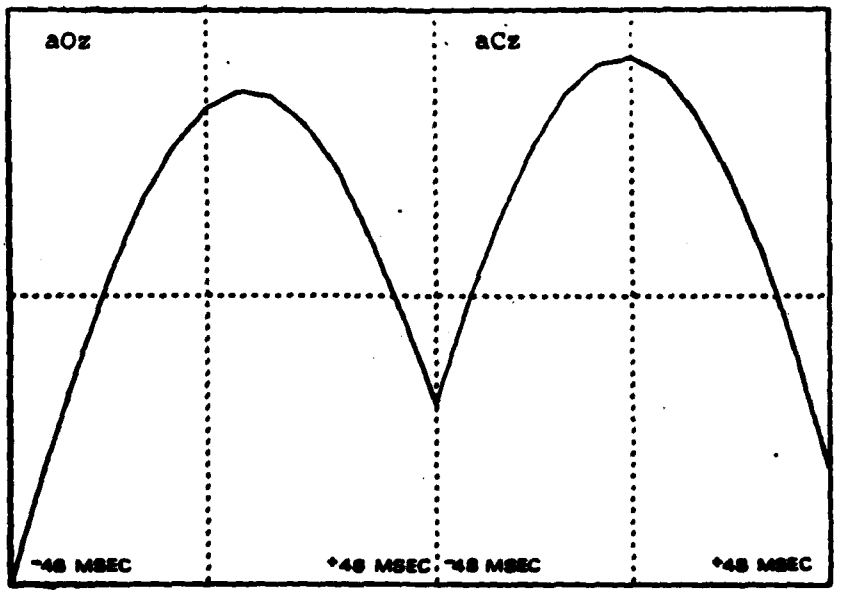

DELTA BAND COVARIANCE - NO MOVE

SSS 1-4, 260 TRIALS, 1-4 HZ, P3a INTERVAL

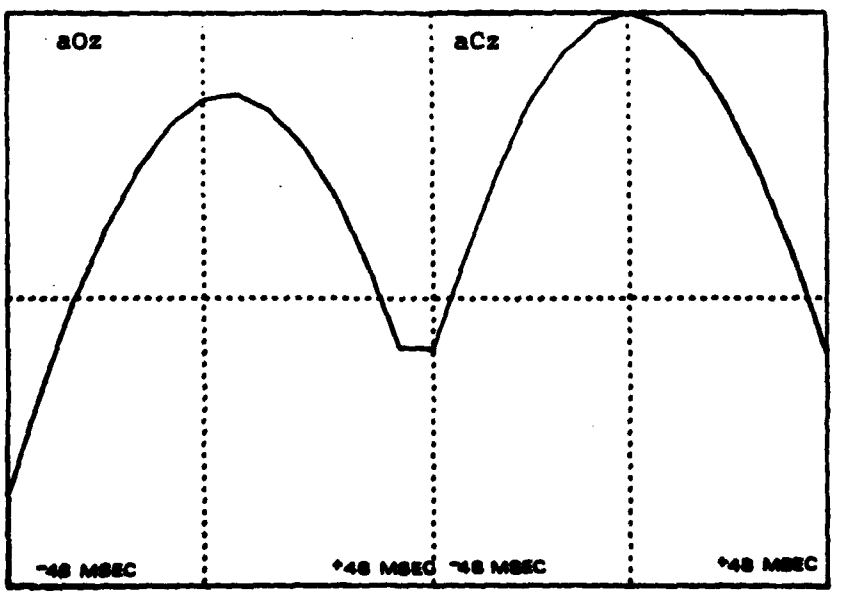

Figure 4

THETA BAND COVARIANCE- MOVE

SSS 1-4, 260 TRIALS, 4-8 HZ, P3a INTERVAL

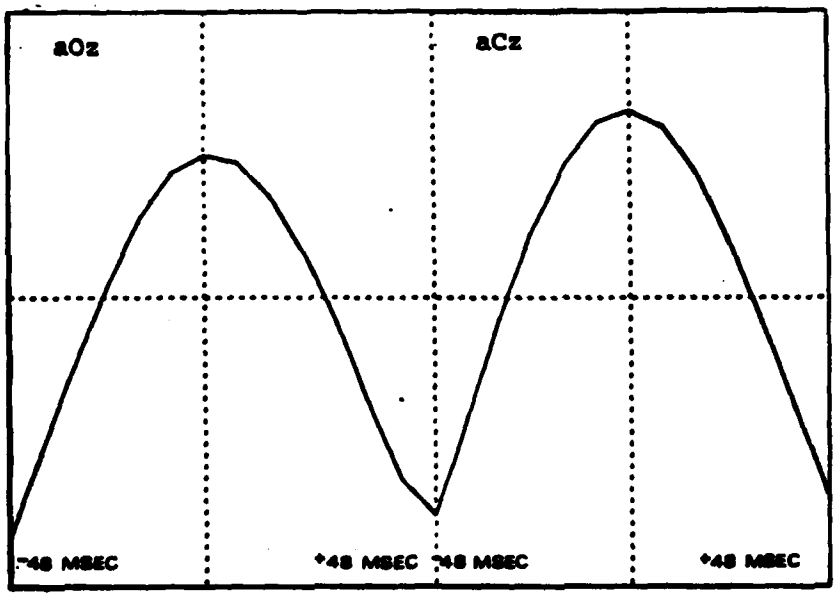

THETA BAND COVARIANCE- NO MOVE

SSS 1-4, 260 TRIALS, 4-8 HZ, P3a INTERVAL

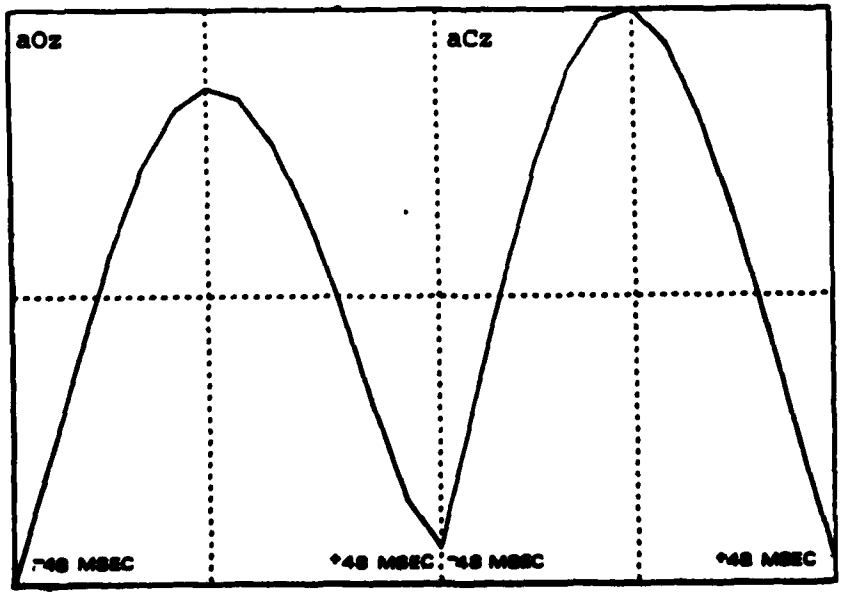

Figure 5

BETA BAND COVARIANCE- MOVE

SSS 1-4, 260 TRIALS, 16-23 HZ, P3a INTERVAL

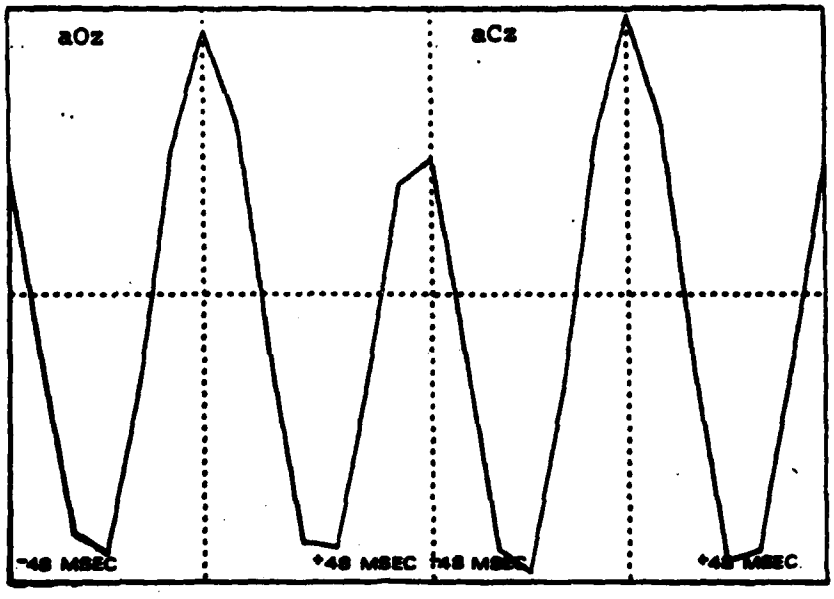

BETA BAND COVARIANCE- NO MOVE

SSS 1-4, 260 TRIALS, 16-23 HZ, P3a INTERVAL

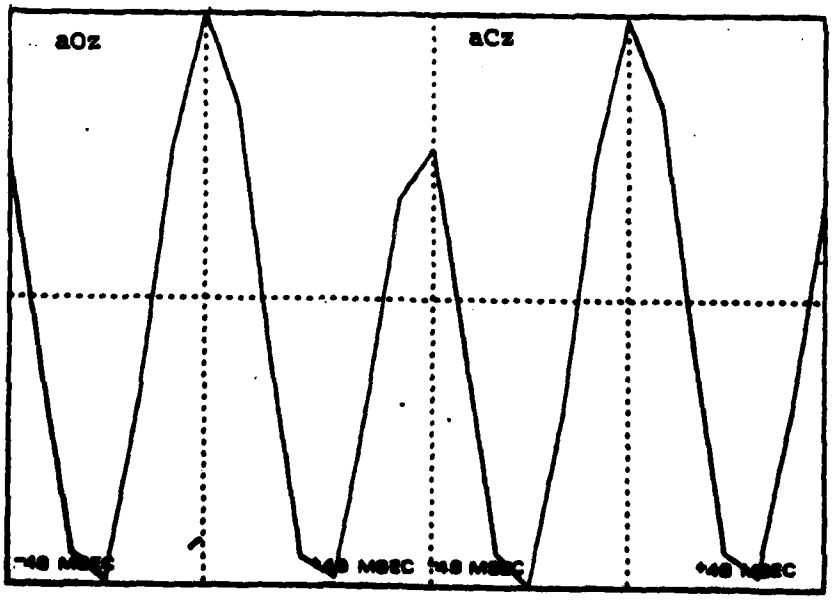

Figure 6

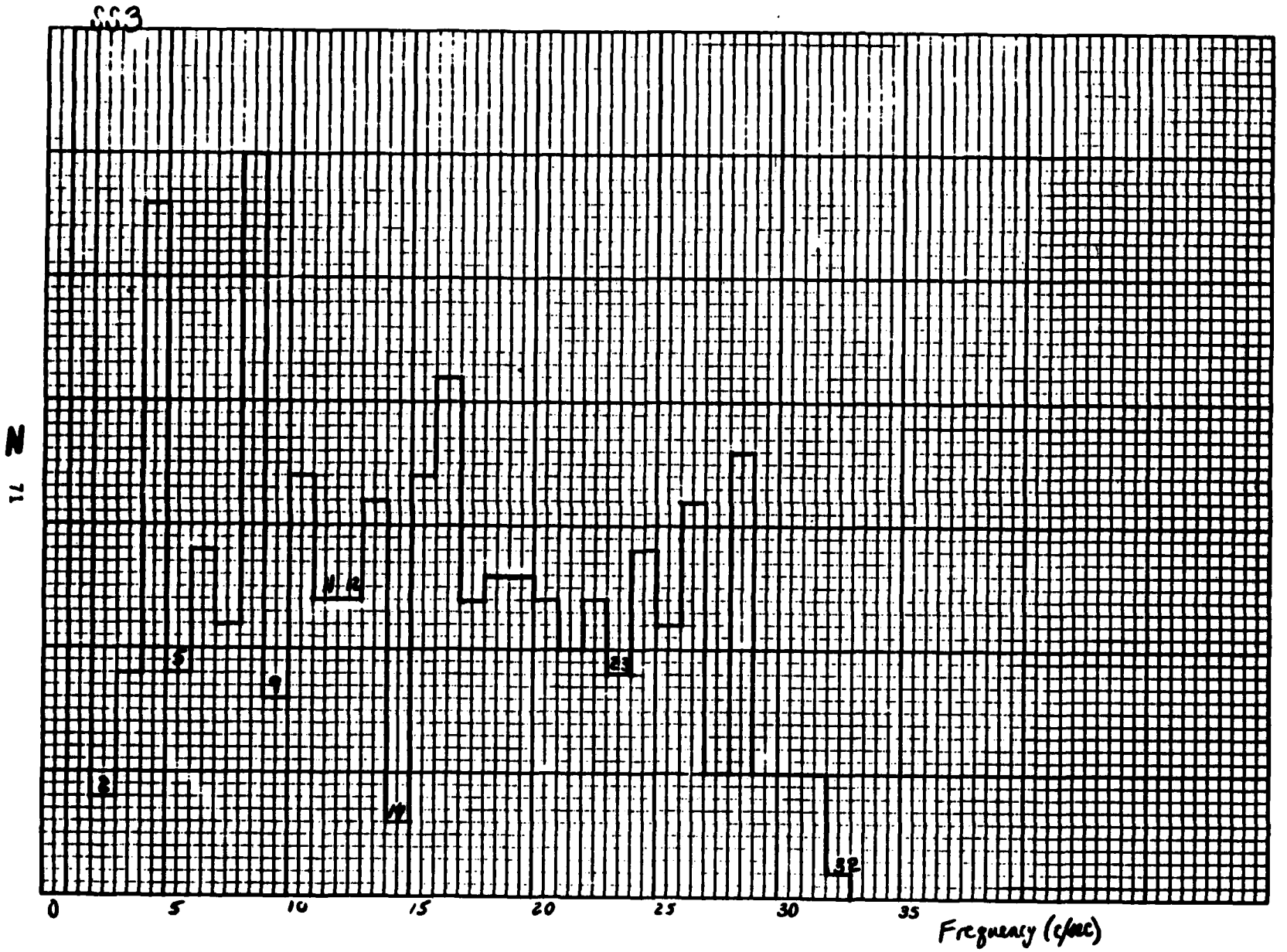

Figure 7 - Spectral component histogram (participant #3).

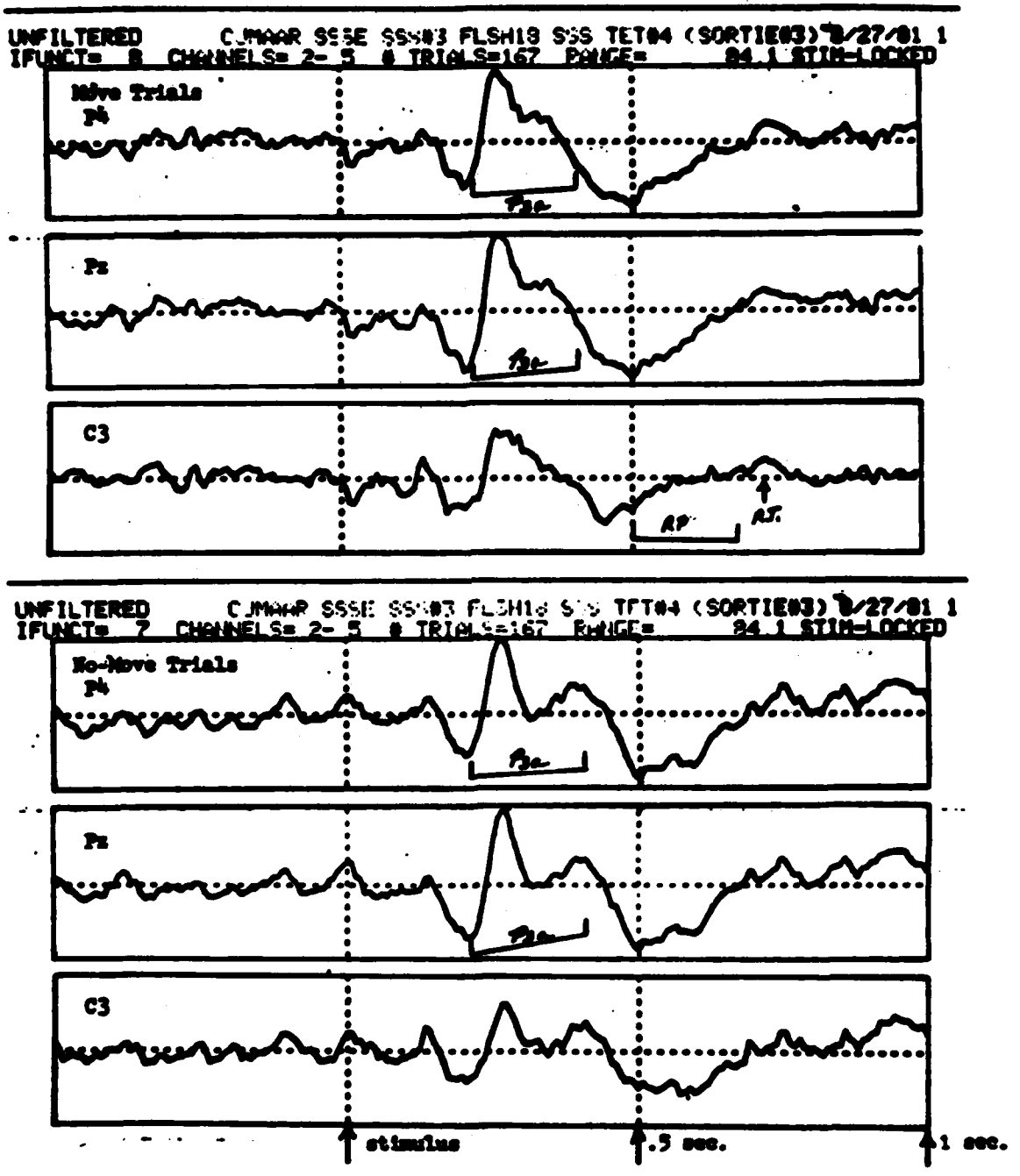

Figure 8a Unfiltered averaged evoked potentials for three channels (P4, Pz, C3) for one participant prior to bandpass filtering; "move" trials (top) and "no-move" trials (bottom) of the spatial estimation visuomotor task. The P_{3a} and RP intervals for this person, and his average reaction time (R.T.), are indicated on the appropriate channels.

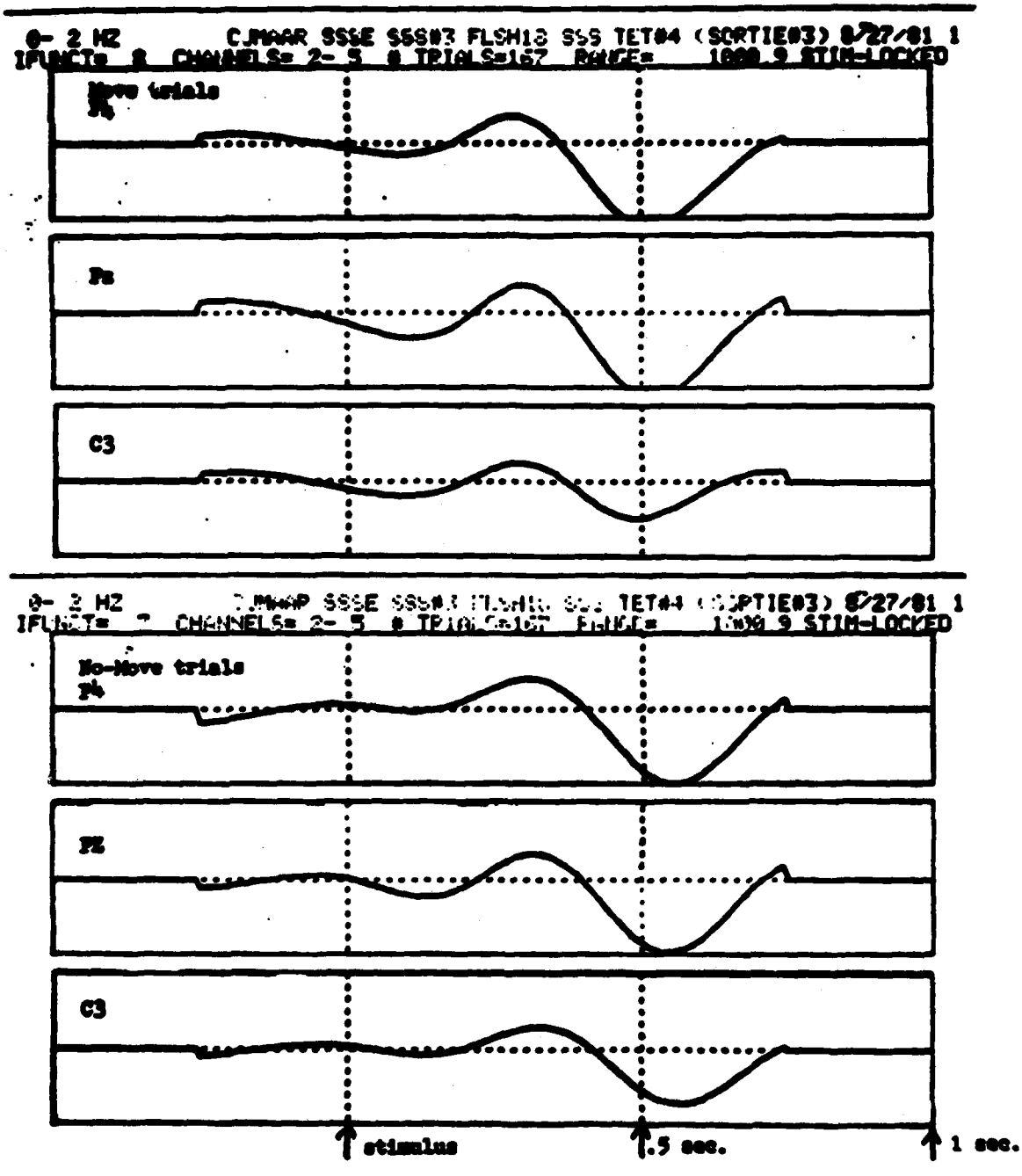

Figure 8b .Delta frequency band (0-2 Hz.) averages from the same person.

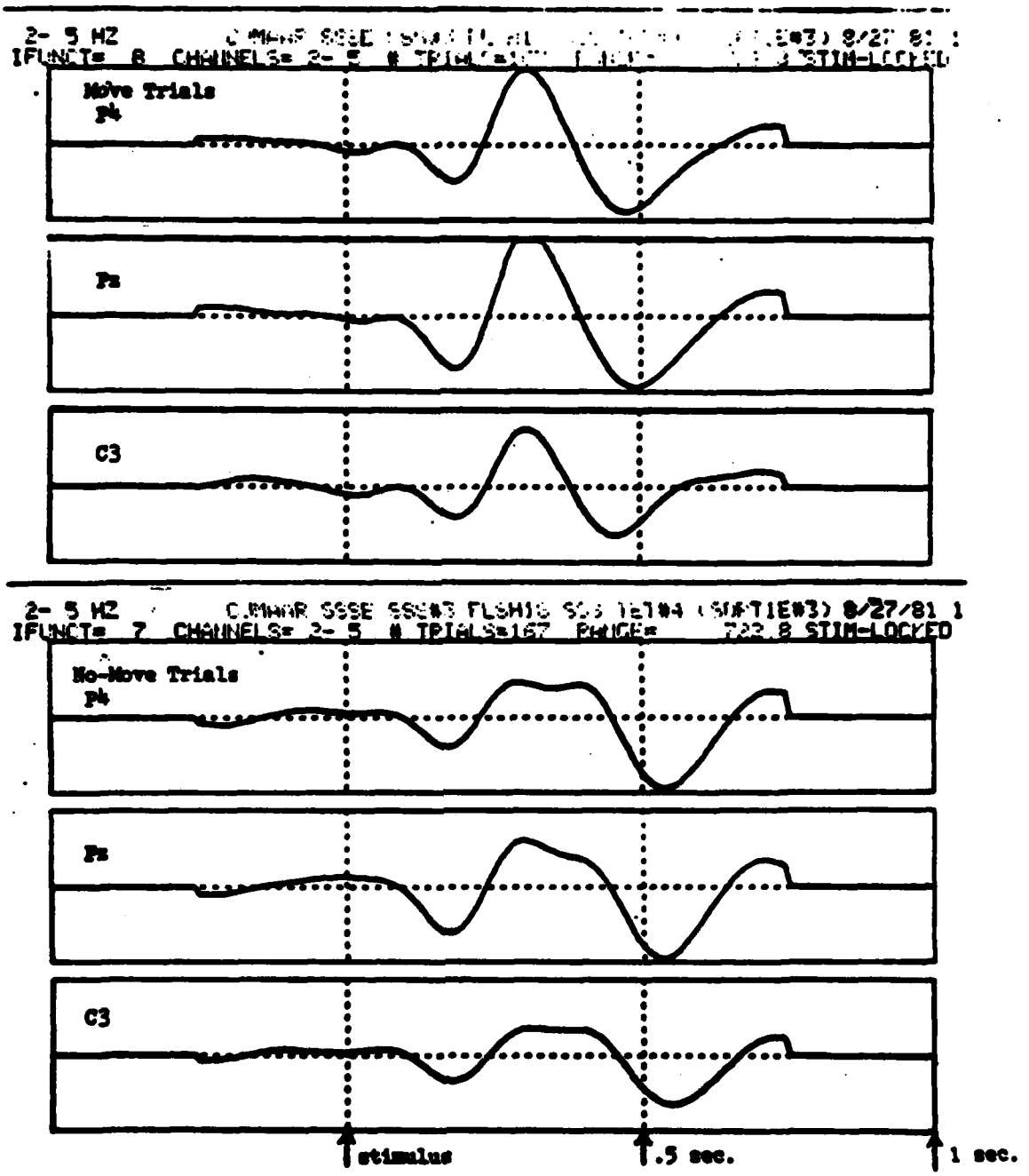

Figure 8C. Low theta frequency band (2-5 Hz.). In this person the theta frequency band spanned two spectral peaks (see fig. 5d).

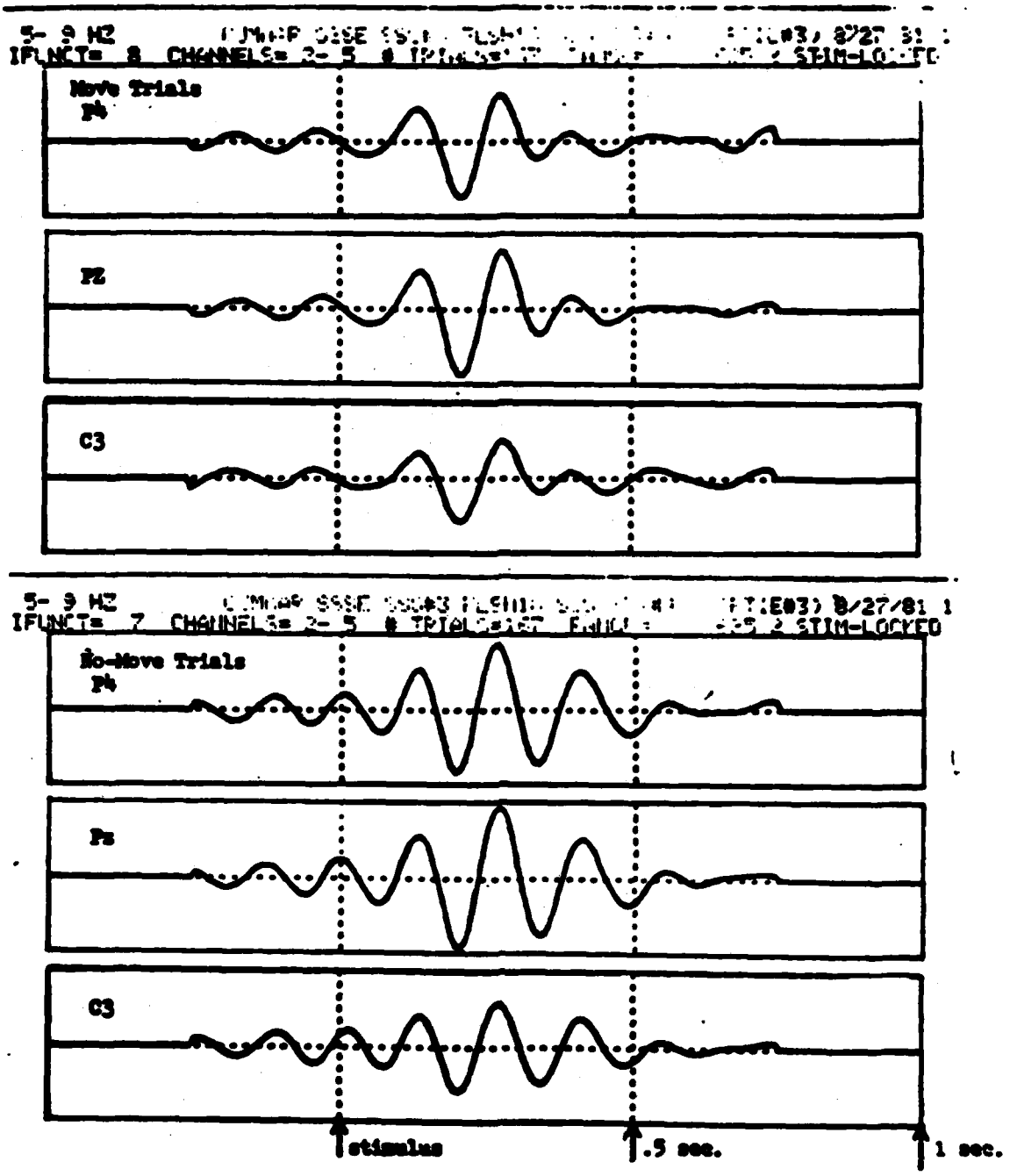

Figure 8D. High theta frequency band.(5-9 Hz).

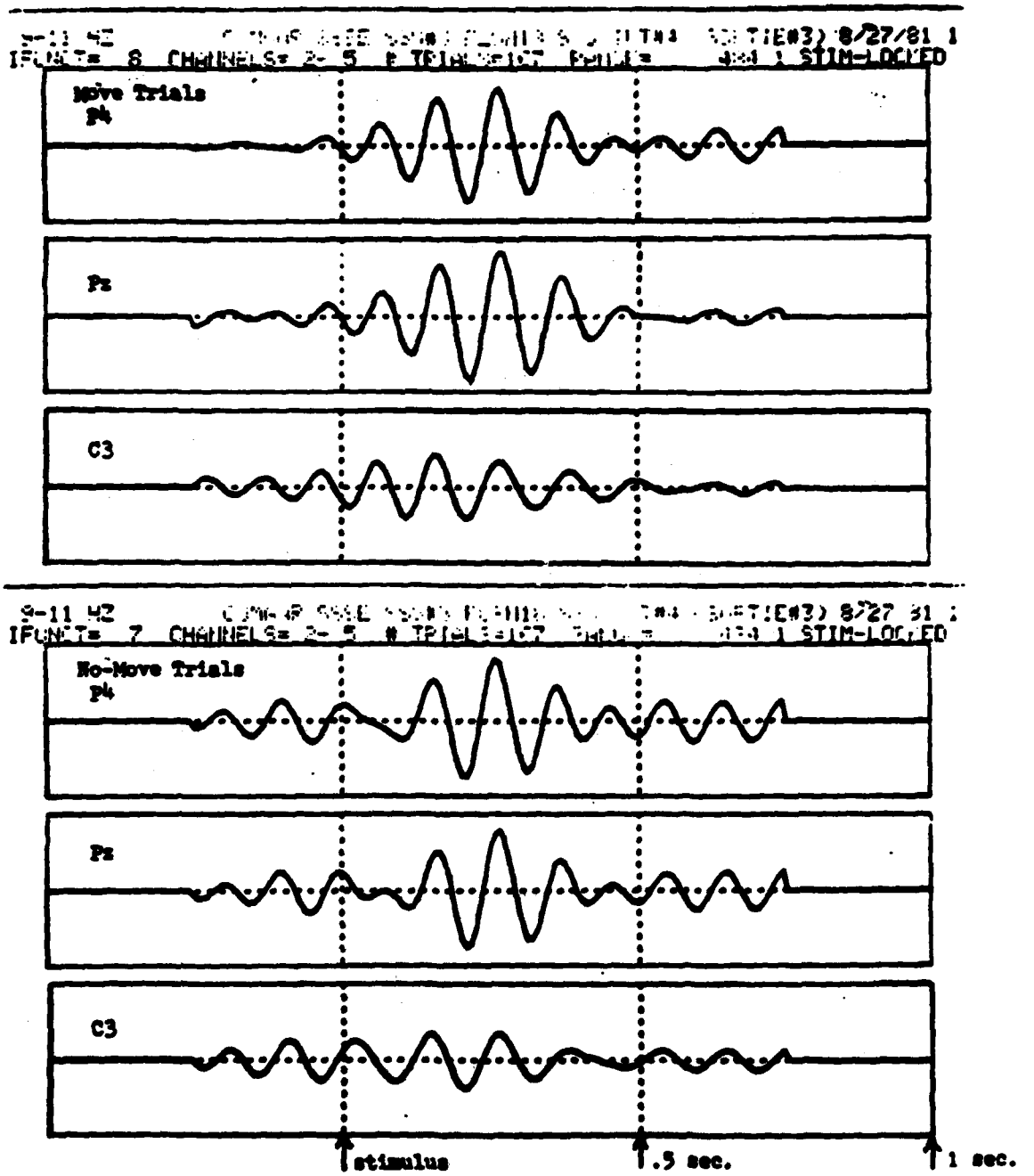

Figure 8E Alpha frequency band (9-11 Hz).

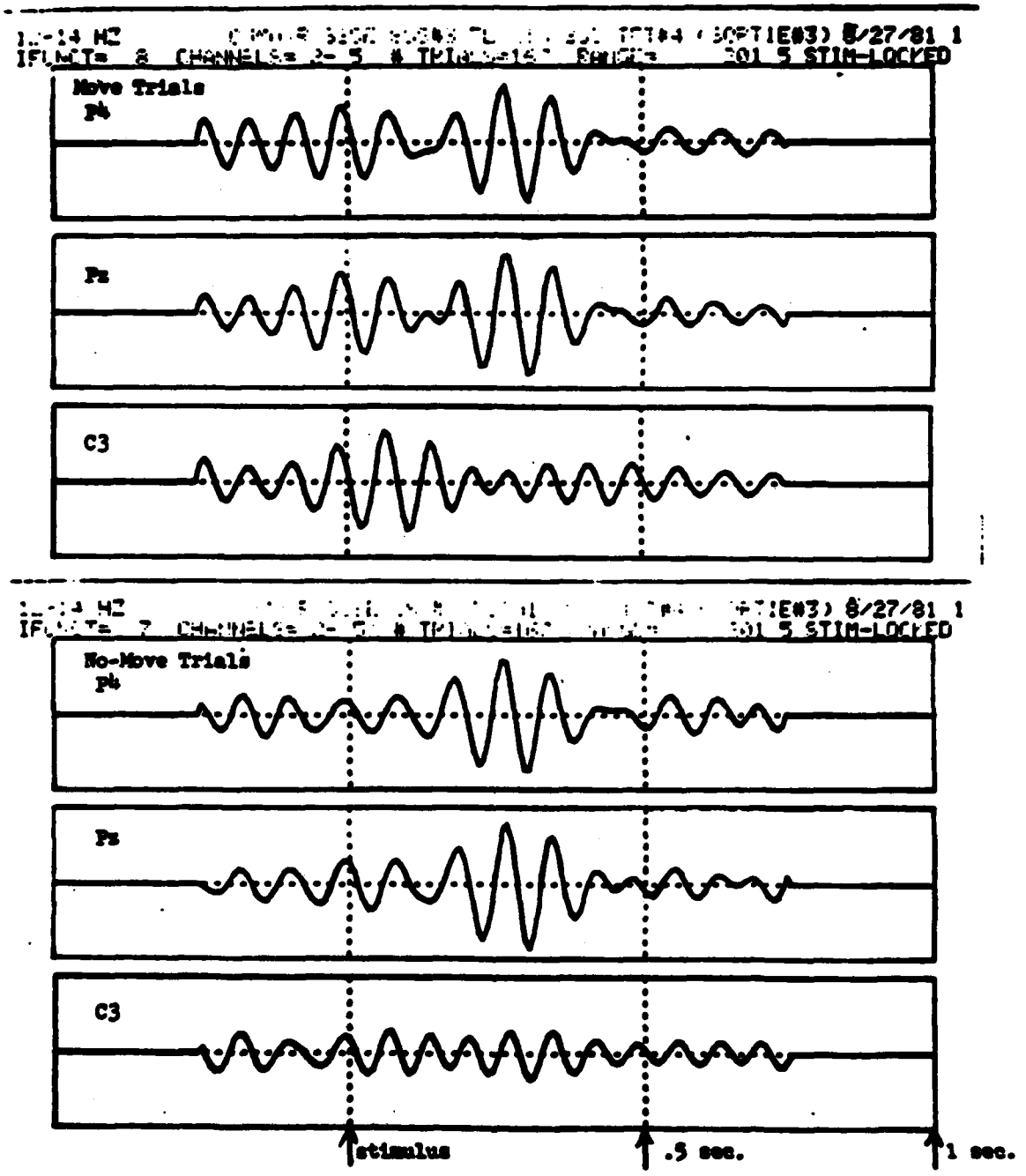

Figure 8F Low beta frequency band (11-14 Hz.).

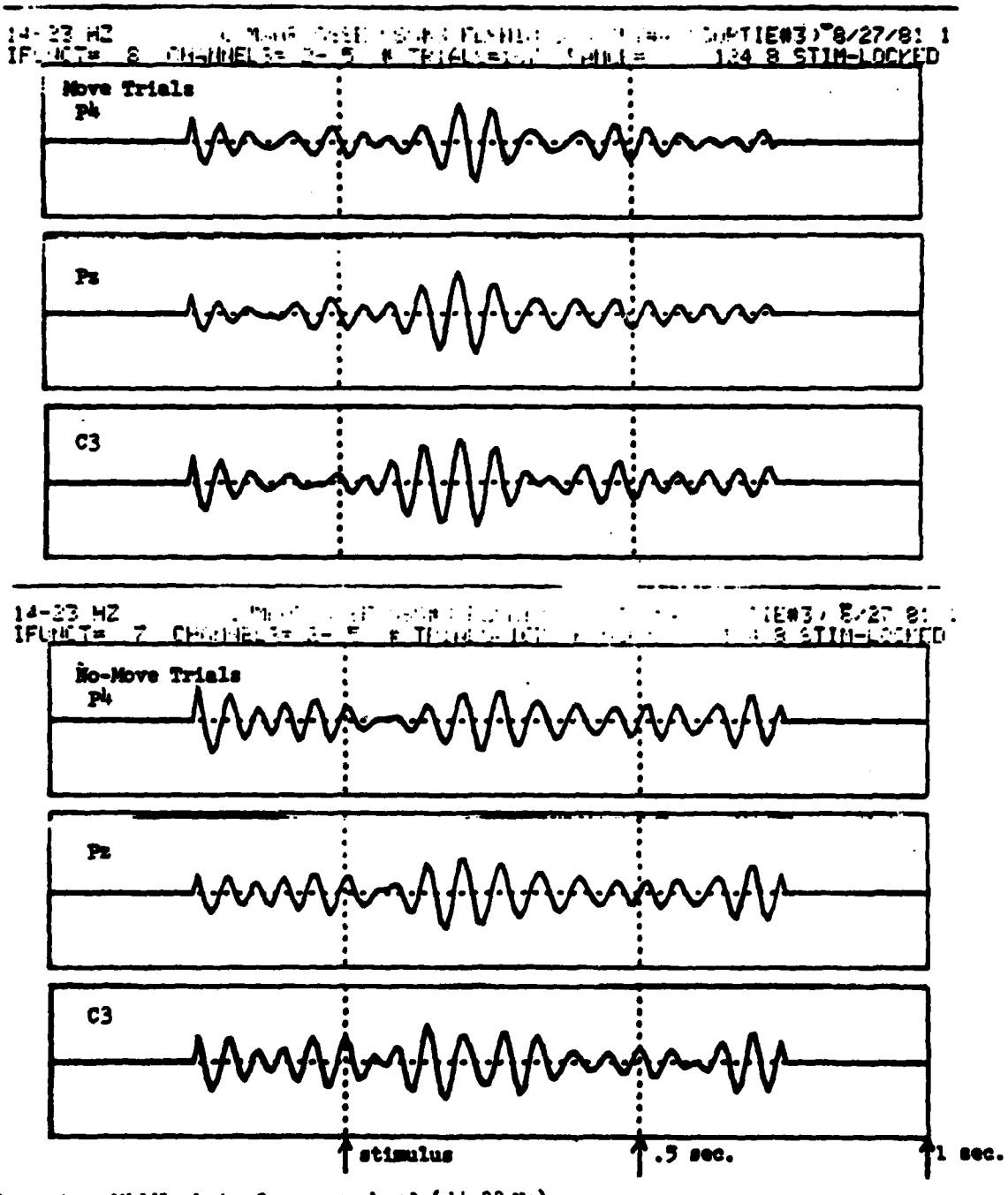

Figure 8G ,Middle beta frequency band (14-23 Hz).

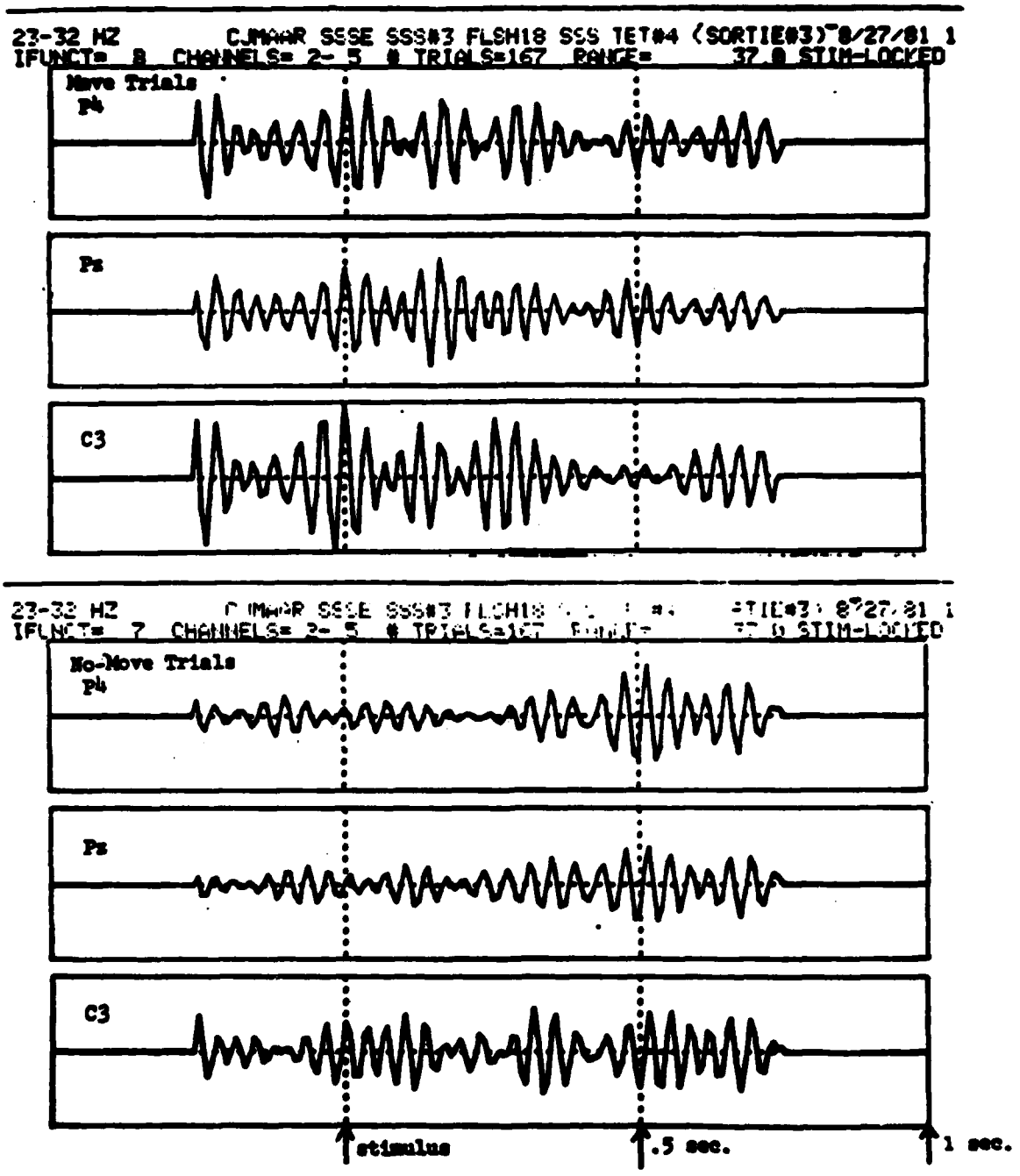

Figure 8E High beta frequency band (22-32 Hz).

MAX. COVARIANCE

(Δ, θ, α_1, α_2, B BANDS)

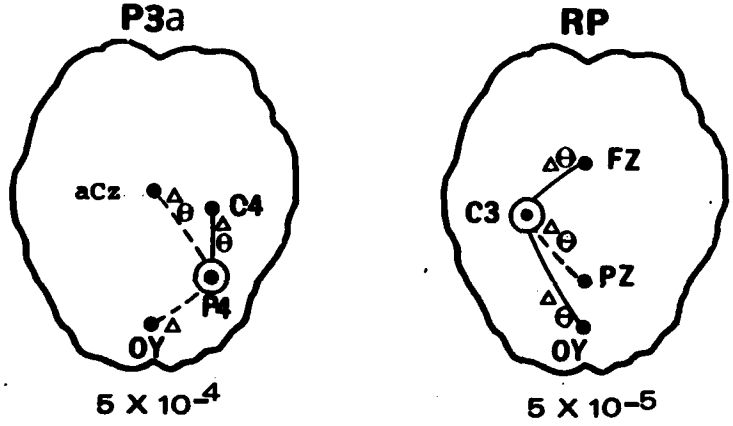

FEA > .15 MAX

FIgure 9

SHAPE LAGGED COVARIANCE FUNCTION

(Δ, θ, α_1, α_2, B BANDS)

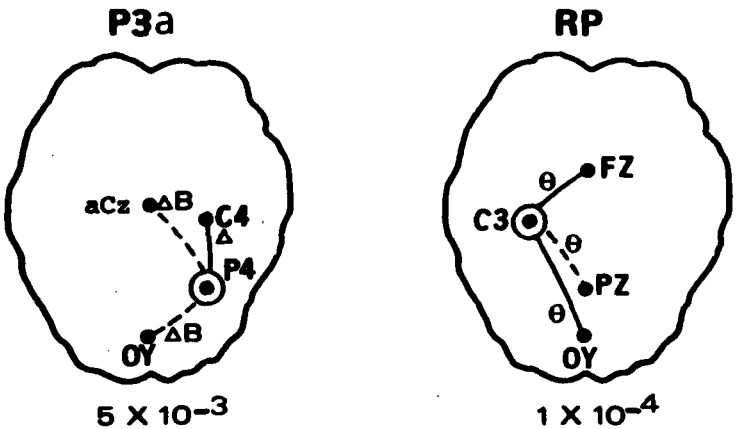

FEA > J5 MAX

Figure 10

POWER

(Δ, θ, α_1, α_2, B BANDS)

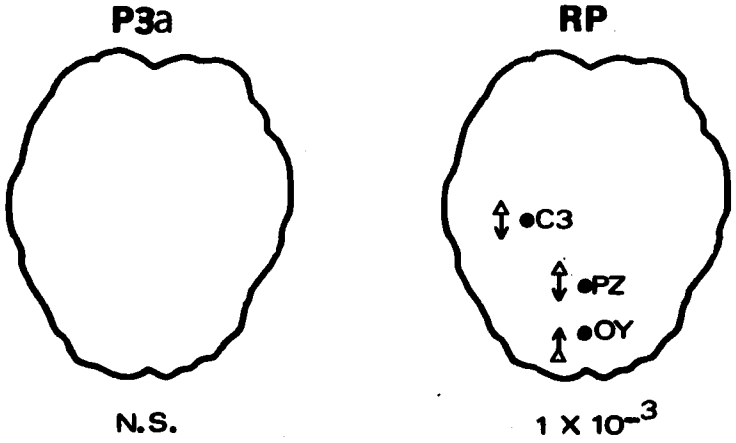

Figure 11

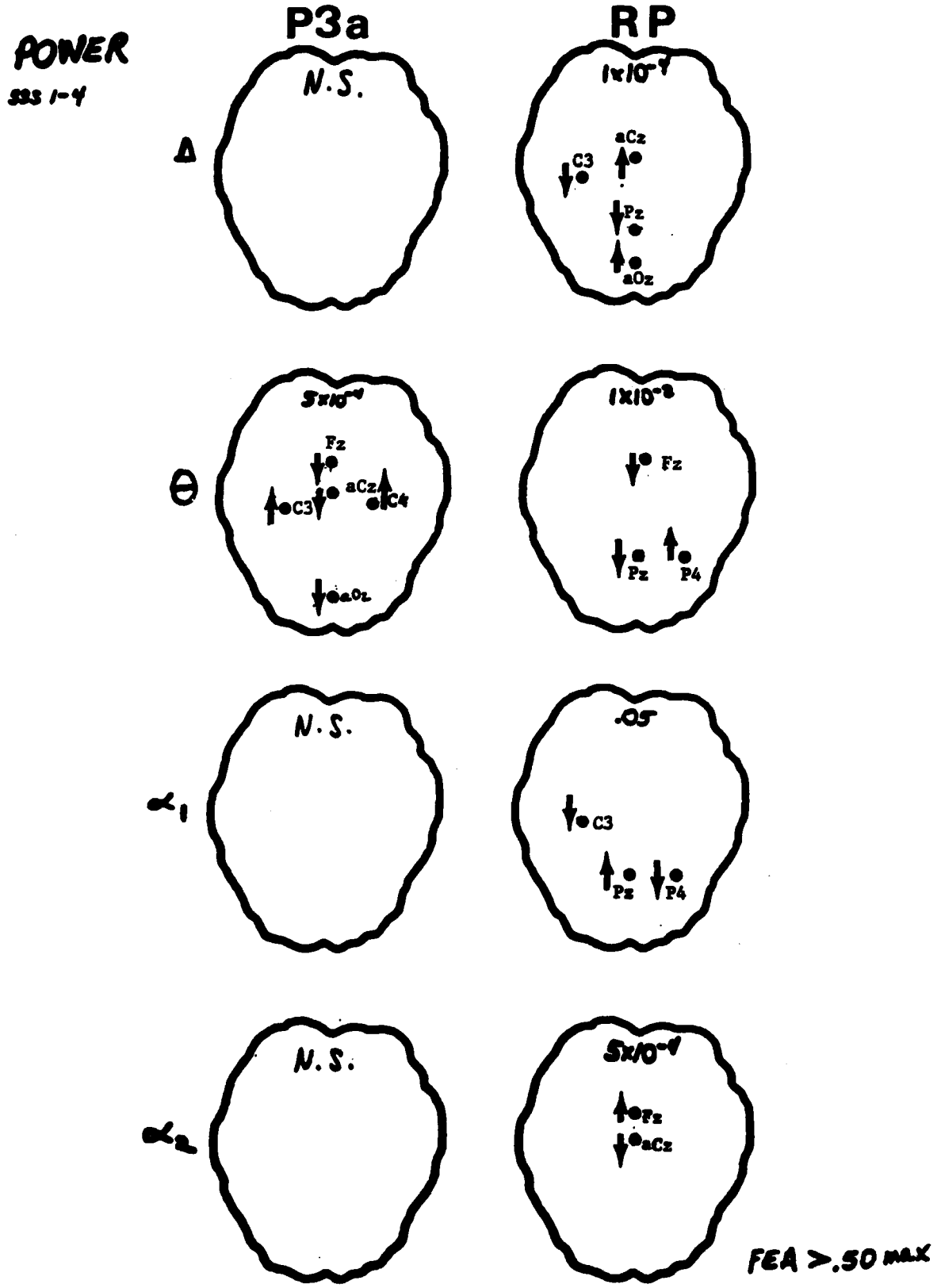

Figure 12 - Results of analysis of 8 channel power measures in P3a and RP intervals.

VI. DISTINCT BRAIN-POTENTIAL PATTERNS ACCOMPANYING BEHAVIORALLY IDENTICAL TRIALS (Also sponsored by the Office of Naval Research)

In order to examine patterns used by the pattern recognition algorithm to define the move and no-move trials, the classification assigned by the algorithm to each trial of the testing data was noted. In all cases, the data were behaviorally correct. Trials for which classification was correct for both P3a and RP intervals were called correct; those with incorrect classification for both intervals were called incorrect. This was done for both move and no-move conditions, resulting in four classes: (a) correct move, (b) correct no-move, (c) incorrect no-move, and (d) incorrect move. Unfiltered ERPs were formed for each class for the data of the last 4 people in the study (Figure 13).

The main difference between correctly classified move and no-move ERPs was the positive P3a and P3b peaks at approximately 365 and 530 msec post-stimulus, respectively. Comparing Figure 13c with Figure 13b, the incorrect no-move ERP is seen to lack a P3a peak and have a smaller P3b peak, thus resembling the correct move ERP. The incorrectly classified move trials (Figure 13d) have a more distinct P3b peak than the correctly classified move trials (Figure 13a), thus resembling the correctly classified no-move ERP.

Another obvious difference between correctly and incorrectly classified ERP's, both move and no-move, was the strong pre-stimulus alpha 'train' in incorrectly classified ERPs. This dissimilarity is clearly seen in alpha band-pass filtered averages (Figure 14). In both the correct and incorrect move conditions there are alpha band ERPs which occur at the same post-stimulus time (in phase). In the incorrectly classified waveform the pre-stimulus alpha is much larger than in the correct, and is phase reversed. The incorrect ERP appears to undergo a phase adjustment prior to the zero-crossing at approximately 90 msec post-stimulus, which occurs at the same time in the correctly classified trials, and is followed by a negative peak at 160 msec in both. This peak corresponds to the N163 peak in the unfiltered ERP. This could reflect a timing process which regulates the activity of sensory cortex in preparation for incoming stimuli (the old idea of the 'neuronic shutter'). These alpha-band filtered ERP's are also clearly different in the P3a and RP intervals where the classification was made. The high prestimulus alpha in the incorrectly classified trials may be related to cognitive state, so that incorrectly classified trials are qualitatively different, perhaps due to automatic processing. Alternatively, incorrectly classified trials may be those with a particular alpha phase at stimulus onset, resulting in enhanced summation of pre-stimulus waves, and difference in post stimulus activity. These possibilities are being further investigated since the results show that different neural patterns may accompany the same behavior.

a)Correctly classified move trials

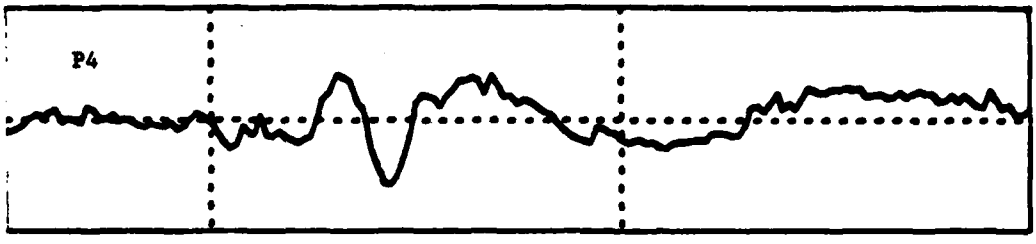

b) Correctly classified no-move trials

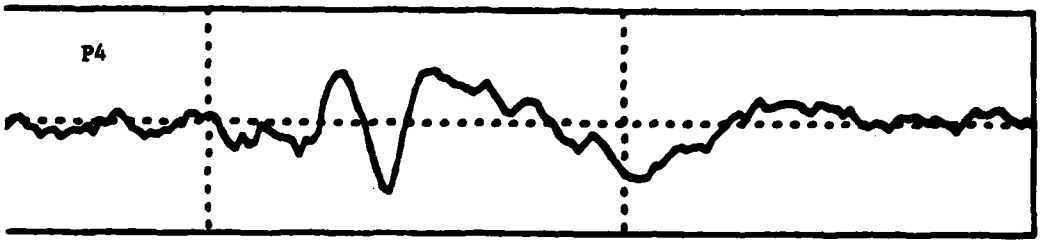

c) Incorrectly classified no-move trials

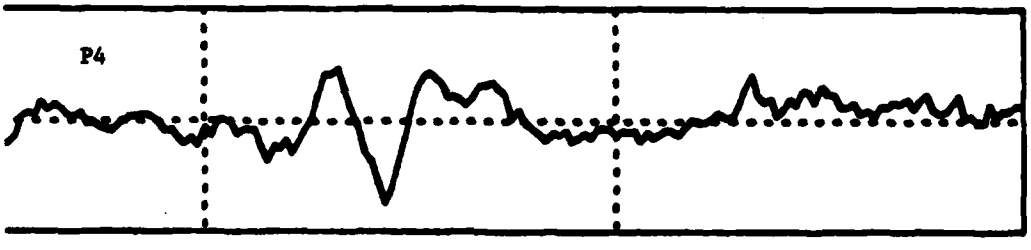

d) Incorrectly classified move trials

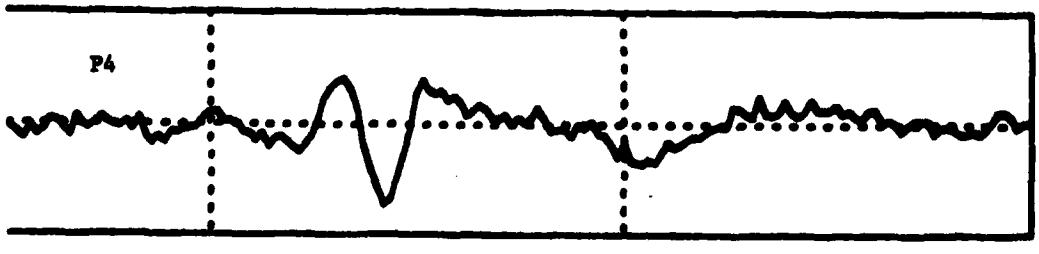

Figure 13 - Average ERPs for trials which were correctly and incorrectly classified by the NCP analysis.

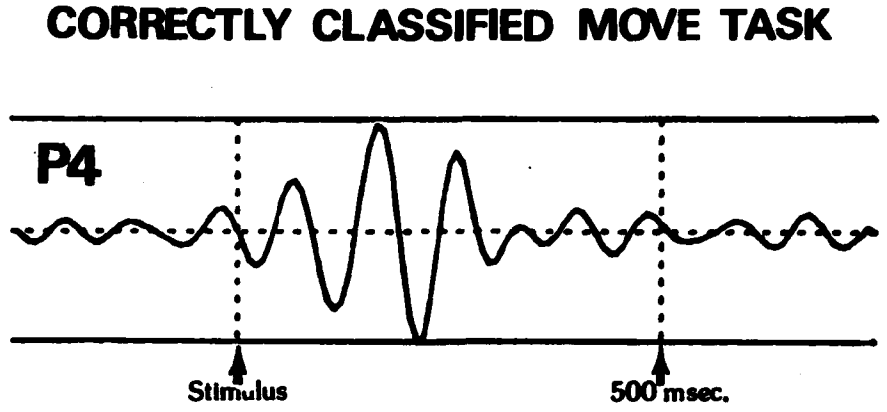

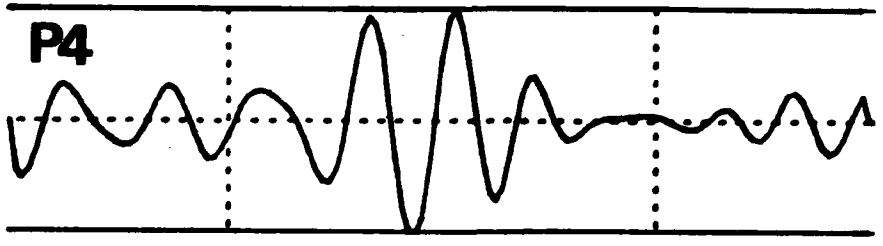

(317 Trials Total, 8-15 Hz)

Figure 14.

END

DATE
FILMED

1 84

DTIC